

Flexible Electronics for High-Density EMG Based Signal Acquisition for Upper Limb Myoelectric Prosthesis Control

by
Damini Agarwal

A thesis submitted to Johns Hopkins University in conformity with the requirements for the degree of Master of Science.

Baltimore, Maryland
May, 2017

© 2017 Damini Agarwal
All Rights Reserved

ABSTRACT

The research detailed in this thesis is aimed at developing flexible electrodes for high-density control of an upper limb myoelectric prosthesis. Different flexible dry electrode materials (made from doped traditionally non-conductive substrates) were used and compared to titanium (which is the industry standard for EMG electrodes). We determined that conductivity measurements alone, (the current industry standard for characterizing electrical properties of materials), are not sufficient due to their complex impedance. We measured the skin electrode complex impedance and relationship with signal to noise ratio (SNR) and settling time. We show that complex skin electrode impedance is linearly related to the SNR of signals and that complex skin electrode impedance better characterizes the electrical properties of doped, traditionally non-conductive materials for physiological signal acquisition.

Next we constructed a flexible high-density array with 128- contact points arranged in an 8 x 16 configuration to cover the entire residual limb. Myoelectric signals, and its relationship to derived time domain features of all 128 channels were extracted and represented as spatio-temporal values as 8 x 16 images to represent the muscle activity map of the residual limb. Thus, a traditional signal-processing problem is converted into an image processing problem. Obtaining High Density (HD) (128 channel) spatio-temporal information has significant merits which include: ability to easily identify the optimum myoelectric recording sites on a residual limb, ability to temporally study the onset and decline of a contraction, predicting the stage of contraction and, finally, ability to implement proportional control and fine motor myoelectric control.

Thesis Committee Chair: Dr. Kevin Yarema

Thesis Project Adviser and Thesis Committee Member: Dr. Nitish Thakor

Thesis Committee Member: Dr. Sridevi Sarma

PREFACE

ACKNOWLEDGEMENTS

I would like to thank my adviser, Dr. Nitish Thakor, for his mentorship, support and advice that has enabled me to successfully pursue this research. I would also like to thank him for always encouraging me to become a better version of myself and for supporting all my academic and non-academic endeavors that allowed me to receive numerous accolades. In addition, I would like to thank Dr. Rahul Kaliki for his regular assistance and insights in this research as well as for being a key mentor in all facets of my graduate school experience. Thank you also to Dr. Ananth Natarajan for his guidance in both my research and entrepreneurial interests. I would also like to thank Dr. Sridevi Sarma and Dr. Kevin Yarema for taking the time out to review and discuss my work with me. I would like to extend a big thank you to my colleagues at Infinite Biomedical Technologies, particularly Michelle Zwernemann for her help and advice in all the development and testing associated with this research. I am also grateful to all my colleagues in the lab, George Levay, Luke Osborn, Joseph Betthausen, Ryan Smith, Guy Hotson, Juhi Baskar, Sapna Kumar and Geoffrey Newman for their willingness to offer advice by drawing from their own research experiences. I am honored to have had a chance to work alongside such great minds. Finally, a warm thank you to all the undergraduate research volunteers, students, prosthetists and patients with amputations who willingly offered their time, ideas and feedback throughout this research project.

DEDICATION

This thesis is dedicated to my family, my wonderfully creative sister, my loving and supportive parents, my encouraging uncle and my kind grandparents. Thank you for being the strongest pillars of support that a person could wish for.

I would also like to dedicate this thesis to my teachers and my professors who have always believed in me and have molded me into who I am today. Thank you for teaching me that I am always more capable than what the world will let me believe.

TABLE OF CONTENTS

CHAPTER 1	1-13
1. Chapter 1: Electrode Design for EMG Acquisition in Prosthesis	1
1.1. Types of Electrodes	1
1.2. Rigid Electrode Design and EMG for Myoelectric Control	7
1.3. Rigid Socket Design and its Effect on Electrodes	8
1.4. Use of Silicone Liners in Body-Powered Prosthesis	10
1.5. Location Specificity of Electronics in a Socket Affects EMG Signal Quality	11
1.6. Potential Use of Silicone Liners in Myoelectric Prosthesis	13
CHAPTER 2	14-25
2. Chapter 2: Advances in Technology for Flexible Electronics: Application to a Prosthetic Liner	14
2.1. Advances in Flexible Electronics	14
2.2. Materials for Flexible Electronics for EMG Acquisition	15
2.3. Flexible Electronics for Myoelectric Prosthesis	23
2.4. Summary	25
CHAPTER 3	26-51
3. Chapter 3: Developing Flexible Electronics and Methods to Characterize Their Electrical Properties	26
3.1. Introduction to Skin Electrode Complex Impedance	26
3.2. Principle Behind Skin Electrode Impedance Measurement	27
3.3. Methods for Measuring Skin Impedance in Existing Electronics:	

Lead off Detection for Skin Impedance Measurement	28
3.5. Complex Skin Electrode Impedance Better Characterizes the Electrical Properties of Doped, Traditionally Non-Conductive Materials for Physiological Signal Acquisition	30
3.6. Summary	51
CHAPTER 4	52-87
4. Chapter 4: HD EMG for Myoelectric Control	52
4.1. Relevance of HD EMG to Myoelectric Control	52
4.2. Hardware Setup for HD EMG	55
4.3. HD EMG Muscle Activity Maps	59
4.4. Use of HD EMG in Myoelectric Prosthesis	71
4.5. Summary	87
CHAPTER 5	88-93
5. Chapter 5: Conclusion and Future Directions	88
5.1. Flexible Contacts	88
5.2. High Density EMG	90
6. APPENDIX	94-98
7. REFERENCES	99-120
8. BIOGRPAHICAL SKETCH	121

LIST OF FIGURES

CHAPTER 1

1.1. Overview of current classification of electrodes for EMG signals measurement	2
1.2. Wet Gel Electrode	3
1.3. Dry EMG electrodes	4
1.4. Comparison of initial electrode types	5
1.5. Intramuscular Needle Electrodes	6
1.6. Electrodes and Processor Attachment to Myoelectric Prosthesis Socket	7
1.7. Silicone liners used in Upper Limb Prosthesis	10
1.8. Prosthesis Fitting Session	11

CHAPTER 2

2.1. Textile Electrodes	16
2.2. Textile Electrode with Conductive Traces	16
2.3. Spring Loaded Polymer Electrodes	18
2.4. Polymer based Electronic Tattoo	18
2.5. Conductive Silicone Electrode Contacts	19
2.6. Conductive Foam EEG Electrodes	20
2.7. Conductive Ink Printed Circuit	21
2.8. Conductive Yarn	22

CHAPTER 3

3.1. Flexible Contacts	33
-------------------------------	-----------

3.2. Electrical Modeling of Skin Electrode Interface	35
3.3.a. The apparatus for conductivity measurements	37
3.3.b. The contact material attachment to the IBT electrodes	37
3.3.c. The attachment of the electrode to the forearm	37
3.4.a. Conductivity of Materials vs. Time	43
3.4.b. SNR vs. Time	43
3.5.a: Signal from Titanium contact	44
3.5.b: Signal from Silicone (Doped with CNT) Contact	44
3.6.a: Complex Impedance vs. Time	46
3.6.b. Complex Impedance vs. Signal to Noise Ratio	46
3.7. Skin Electrode Complex Impedance vs. Signal to Noise Ratio	48
3.8.a. Signal to Noise Ratio vs. Time	50
3.8.b. Skin Electrode Complex Impedance vs. Time	50
CHAPTER 4	
4.1. Vision of the HD EMG System with Flexible Silicone Electrode Contacts	54
4.2. Hardware for HD EMG	56
4.3. FFT on Monopolar Signals	58
4.4. RMS and MAV Activity Maps	61
4.5. Muscle Activity Maps for Wrist Flexion and Wrist Extension	62
4.6. Different Finger Flexion Patterns	63
4.6. 32 Channel HD EMG Maps	66
4.7. 128 Channel HD EMG Maps	67
4.8. Muscle Activity Maps and Forearm Anatomy	69

4.9. KL curves for rest and thumb flexion.	73
4.10. KL curves for index flexion and middle flexion.	74
4.11. Onset of Contraction	77
4.12. Peak Contraction	78
4.13. Decline of Contraction	79
4.14. Liner detection algorithm	82
4.15. HD EMG maps for Myosite Location	86
6. APPENDIX	
6.1. EMG pattern recognition performance based on feature relevancy	95

LIST OF TABLES

CHAPTER 3

3.1. Epidermal and Sub-Epidermal Resistance, Capacitance and Impedance	39
---	-----------

CHAPTER 4

4.1. Mean Squared Error between 5 Wrist Flexion Muscle Activity Maps	68
---	-----------

CHAPTER 1

1. Electrode Design for EMG Acquisition in Prosthesis

Electromyography is the process by which signals generated by muscle activation are acquired by electrodes placed above muscle groups on both upper and lower limbs. It is a powerful tool in myoelectric prostheses because the acquired muscle signals or EMG from the residual limb of the patient are used for control of the artificial limb [1 - 3]. Electrode design, processing circuitry, algorithms as well as their integration are all essential for robust control of a myoelectric prosthesis. This chapter provides an overview of the electrodes that are used for EMG acquisition, their shortcomings and potential improvements in their design.

Figure 1 illustrates an overview of the chapter. Study of electrodes involves experimental methods as well as design approaches. Experimental approaches reviewed include noninvasive as well as invasive methods, configurations used include monopolar and bipolar, and designs include dry, wet, insulating, and both rigid and flexible. This research makes case for HD electrodes for EMG recordings for upper limb prosthesis.

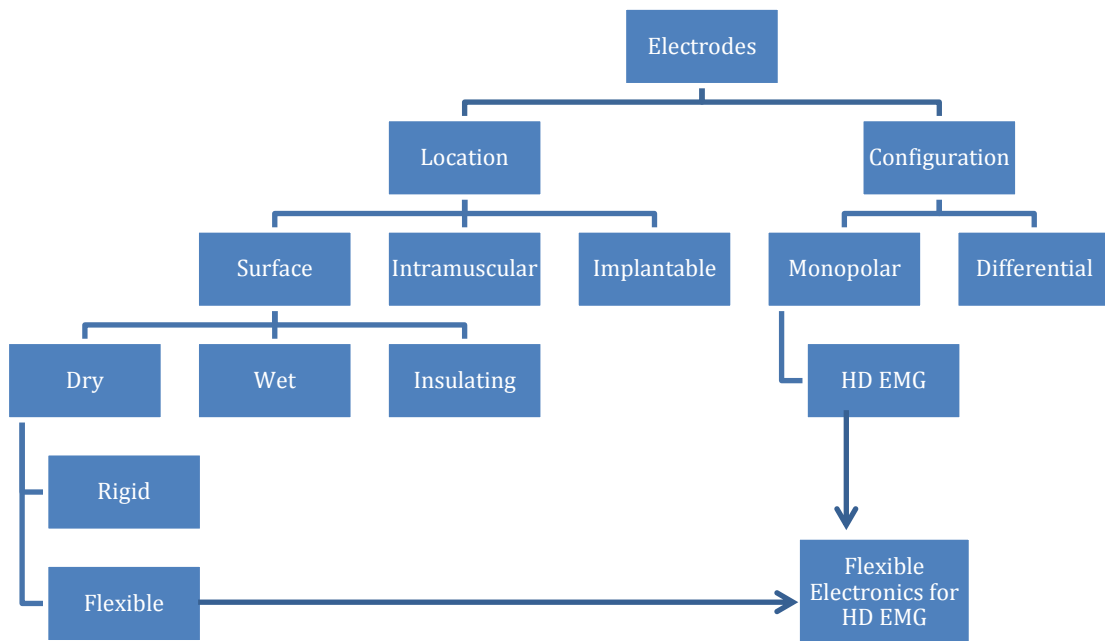


Figure 1.1: Overview of current classification of electrodes for EMG signals measurement. Over the years, electrodes have undergone several significant changes all aimed at improving the quality of physiological signal acquisition, to provide a more reliable insight into the functioning of the various parts of the human body.

1.1. Types of Electrodes:

One of the biggest factors that determine the quality of the biosignal acquired is the type of electrode used. As a result, a large fraction of the work in biosignal/biopotential acquisition field has been to develop more robust, reliable electrodes, which give good signal fidelity as measured by SNR, especially for ECG (Electrocardiogram), EMG (Electromyogram) and EEG (Electroencephalogram) signal acquisition. An overview of the classification of electrodes is given in Figure 1.1.

1.1.1. Surface Electrodes

There are different kinds of electrodes for EMG and the technology has evolved significantly over the years. Based on how they are placed, they are classified into three types: surface electrodes for global EMG acquisition from the surface of the

skin, intramuscular electrodes for localized EMG

acquisition using thin needle electrodes from the interior of muscles and implantable electrodes for action potential recordings from nerves. Of

the above, surface electrodes are the industrial standard for EMG electrodes for prosthetic control. There are various types of surface

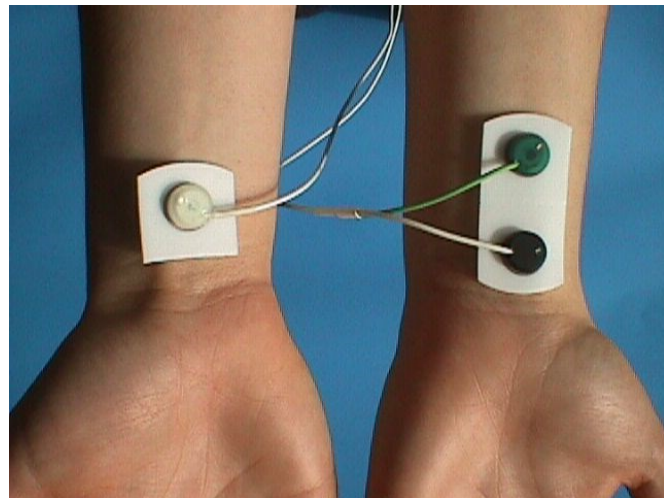


Figure 1.2: Wet Gel Electrode [5]: Traditional Ag/AgCl electrodes have been successfully used for EMG acquisition. The gel provides a stable conductive path for signals to flow across the skin electrode interface. However, they cannot be used for long term measurement due to the drying up of the gel. There is thus a need for gel-less, dry electrodes.

electrodes such as wet, dry and insulating [4]. Wet electrodes, as shown in Figure 1.2, use a layer of electrolyte to form a conductive path between the skin and the electrode. Dry electrodes, as in Figure 1.3, use a metal such as platinum or stainless steel and are attached to the skin. Insulating electrodes consist of a metal or semiconductor with a thin dielectric surface layer to form capacitive coupling between the skin and the electrode [4].

The most commonly used bioelectrode is the silver/silver chloride (Ag/AgCl) type, which is more often found in a disposable form. While Ag/AgCl electrodes have excellent properties such as low resistance and polarization potentials, they are also more expensive and need gel and good adhesive for attachment to the skin. Other problems, as that of greater powerline interference, use of electrolyte [6,7] amongst others lead to the design of other electrode types.



Figure 1.3: Dry EMG electrodes [8]. Dry EMG electrodes are currently the industry standard for myoelectric prosthesis, EMG acquisition. Numerous companies like Ottobock, LTI, and CoAPT commercialize different dry electrode technologies such as analog electrodes, digital electrodes and remote electrodes.

Similarly, dry and insulating/active electrodes have the advantage that they do not need any electrolytic gel, they come with their own host

of problems. Some of them are summarized in Figure 1.4 given below ***I don't see Fig. 1.4.*** Dry active electrodes are currently the industry standard for EMG acquisition for prosthetic control. While myoelectric control of prosthesis is constantly evolving from an algorithmic point of view, there has been very little change in the actual rigid differential electrode design of the electrode itself. As a result, the drawbacks associated with the same continue to be what they were over the last several decades. This is evident from the following table. The instability of the acquired signal, more specifically the quality of SNR resulting from motion

artifacts and interference, presents the biggest challenge to reliable use of prosthesis and some ways of overcoming it are mentioned in the next few sections.

Year	Reference	Dry	Ins.	Construction	Findings
1995	Taheri		•	Si ₃ N ₄	High signal-to-noise ratio (SNR). Uses four redundant sites
1994	McLaughlin	•		Screenprinted Ag/AgCl (no gel)	
1994	Taheri <i>et al</i>		•	Si ₃ N ₄ on steel	High SNR. Low frequency signal present due to electrode movement
1992	Nishimura <i>et al</i>	•		Stainless steel	
1990	Padmadinata <i>et al</i>	•		Silver, stainless steel	
1989	Geddes and Baker	•	•		Effective dielectric thickness changes with dry skin layer and perspiration
1979	Griffith <i>et al</i>		•	Tantalum pentoxide	Films robust until heavily scratched
1979	De Luca <i>et al</i>	•		Stainless steel	
1974	Ko and Hyncecek		•	SiO ₂ on Si	Electric field problems. Motion artefact a problem due to long settling time from RC constant
1973	Matsuo <i>et al</i>		•	Barium titanate	Material is piezoelectric
1973	Geddes <i>et al</i>	•		Silver	
1972	David and Portnoy		•	BaTiO ₃ , TiO ₂ , Ta ₂ O ₅ , SiO ₂	Insulated electrode less affected by movement artefact. Some loss of low frequency information
1971	Bergey <i>et al</i>	•	•	Ag, Au, brass, stainless steel, anodized Al	Charge sensitive, Al ₂ O ₃ erratic. Movement artefact least with stainless steel, most with Al ₂ O ₃
1971	Lagow <i>et al</i>		•	Anodized Ta and Al	Careful shielding arrangement required
1970	Potter and Menke		•	Pyre varnish	
1969	Wolfson and Neuman		•	Silicon oxide	
1969	Lopez and Richardson		•	Anodized aluminium	
1968	Richardson <i>et al</i>		•	Anodized aluminium	Movement artefacts
1967	Richardson		•	Anodized aluminium	

Figure 1.4. Comparison of initial electrode types [4]. This table summarizes different materials that have been used for creating electrodes over the years and highlights their advantages and disadvantages. It is interesting to note that while most of these findings are several decades old, they remain relevant even today due to the widespread use of some of these materials for signal acquisition. Research efforts are now focused at developing alternate materials that overcome the limitations of traditional dry electrode materials.

1.1.2. Intramuscular and Implantable Electrodes

One way of addressing the problem of unstable signals is to use intramuscular and implantable electrodes. While surface electrodes are an easy way of acquiring global muscular activation, they are not as useful when trying to understand the detailed

activation patterns of individual muscle groups. Intramuscular EMG was developed as a solution for the same, using thin needle like electrodes as shown in Figure 1.5 that are inserted into the muscle, so that localized muscle activation information can be easily acquired [9]. Moreover, direct contact with the muscle ensures that motion artifacts and other problems with surface EMG, does not affect this method as much.

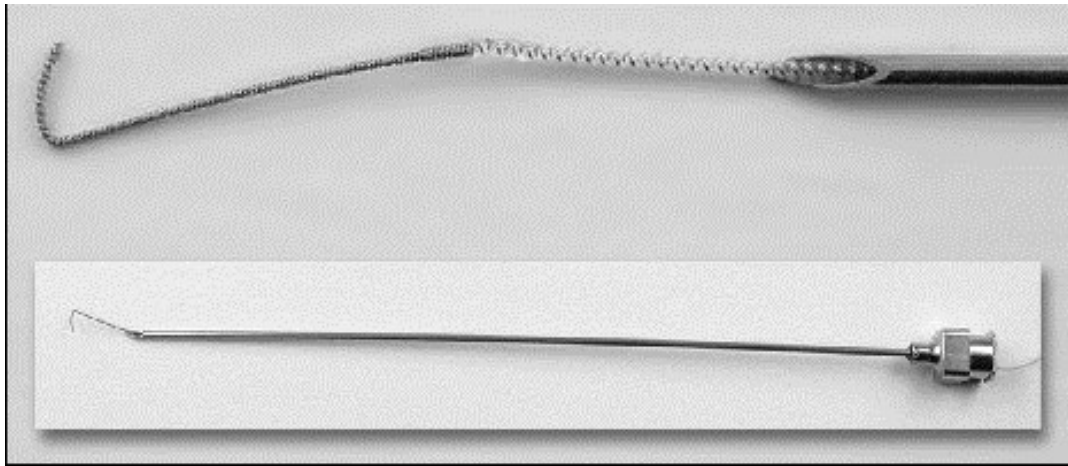


Figure 1.5. Intramuscular Needle Electrodes [10]. Given above is picture of two different kinds of needle electrodes used for intramuscular EMG acquisition. The area of insertion is usually numbed with a local anesthetic before the needles are inserted into the muscle groups. Sometimes, multiple tries are needed to get the electrodes in the correct spot. The hook at the end of the electrodes attaches to the muscle fiber.

While an intramuscular EMG can be more specific for capturing local muscle activity than a surface EMG, it has numerous disadvantages for long-term recording. Besides needing an invasive procedure, needle electrodes need to be placed at the exact same location every single time and their insertion is a painful process. Inflammation, infection movement and other problems also arise over time.

To overcome the disadvantages associated with intramuscular EMG, numerous research efforts have focused on developing implantable electrodes that can be surgically inserted under the skin, over a desired muscle group and anchored for long

term EMG measurement [11]. The biggest challenges that need to be overcome include biocompatibility of the materials, their flexibility, as well as wireless data and power transfer to and from the implanted electrode [12-14].

1.2. Rigid Electrode Design and EMG for Myoelectric Control

While location of the electrodes is one of the reasons for signal instability, the bigger contributor is the rigid electrode design. It is responsible in numerous ways for biosignal infidelity. EMG electrodes are mounted on the inner surface of the rigid prosthetic socket, good socket fit on the residual limb determines good skin-electrode contact. See Figure 1.6 for the same.

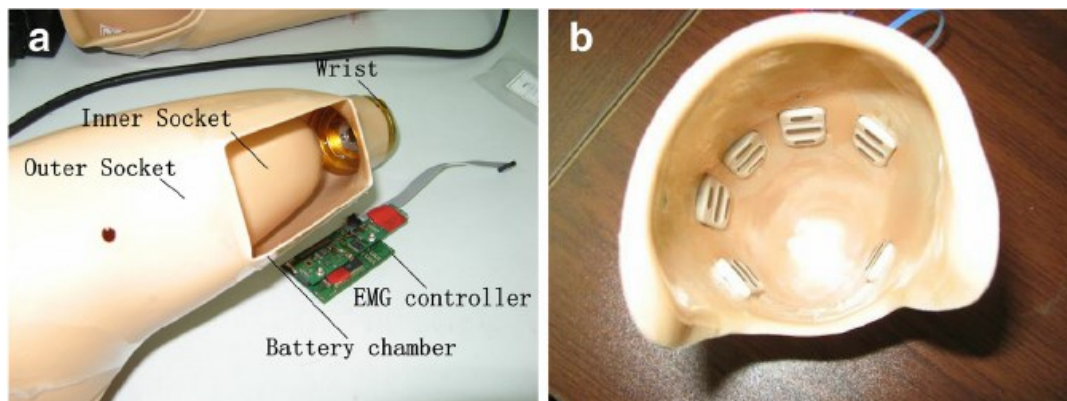


Figure 1.6. Electrodes and Processor Attachment to Myoelectric Prosthesis Socket [15]. The electrodes are fabricated into the socket at myosite locations that give good EMG signal. They connect into a processor that is usually mounted at the distal end of the prosthesis.

This dependency on the socket gives rise to a large number of problems. Firstly, rigid electrodes have a tendency to migrate under force and loading, and bad or irregular contact with the skin degrades system performance [16]. This is further exacerbated by the time required for skin-electrode chemical equilibrium, also called settling time, to be established again before a stabilized signal can be obtained [17]. Moreover,

under excessive loading, electrode lift-off from the skin further leads to acquisition of degraded EMG signals.

All of the above lead to two major disadvantages, not just from a signal acquisition point of view but also from the perspective of signal use. With particular reference to myoelectrically controlled upper limb prosthetics, bad EMG signal quality can seriously undermine the efficacy of the algorithm used for limb control [18]. This leads to longer limb response times, greater instability of hand and limb positions and lack of dependency on the limb for everyday tasks.

Thus, there is an inherent need for redesigning electrodes for EMG acquisition in prosthetics that affords signal fidelity across a variety of conditions. Most of the major concerns include, motion artifact due to absence of electrolyte layer and greater electrical interference [13]. In order to overcome these drawbacks, research is currently focused on redesigning the electrode material substrate to make it more flexible, conformal and less susceptible to rigidity induced motion artifact [14]. Moreover, advances in wireless data/power transfer in electrode design are also making mounting easier [15] and eliminating the need for long cables, rigid supports and other accessory components. The next generation of electrodes can pave the way for use of implantable electrodes in myoelectric prosthesis control.

1.3. Rigid Socket Design and its Effect on Electrodes

Rigidity of electrodes is one of the reasons that contributes to bad signal acquisition, particularly as a result of electrode lift off or motion. A rigid electrode is actually a

part of the much larger rigid socket design. Socket design for prosthesis has undergone very little change since its conception in the early nineteenth century, and a rigid socket can be attributed to many problems associated with current prosthetic limbs [19]. These include bad fit leading to non-conformity to residual limb, bad ventilation within the socket leading to sweating, and friction with the skin leading to raw and damaged skin surface [20].

All of these issues directly or indirectly affect the functioning of electrodes as well. Lack of ventilation leads to sweating and release of other bodily secretions, which not only disturb the skin-electrode chemical equilibrium but also affect the path of conductivity between the skin and electrode [21]. Moreover, changes in the environment of the electrode skin interface due to the socket are not easy to predict and thus lead to instability in final prosthetic limb control. Non-conformity of the socket leads to electrode migration, lift off under loading and other associated problems as mentioned earlier.

A rigid socket design also dampens the advantages of flexible electrodes if used in conjunction with them. The conformity, which the flexible electrode could otherwise provide is decreased and it is still susceptible to movement under loading and lack of ventilation leading to conduction abnormalities.

Thus, one of the most comprehensive solutions to the current EMG signal acquisition problem as well as for providing better fit and comfort to the user is the re-design of the rigid socket to better interface with conformal electrodes and better fit the residual human limb. One way of ensuring better attachment of electrodes is to integrate them

within silicone liners used with some prosthesis systems as mentioned in the next section.

1.5. Use of Silicone Liners in Body-Powered Prosthesis

An alternative suspension technology developed over the last 20 years is the roll-on gel liner which comfortably interfaces between the skin and the socket [36 – 39]. Gel liners are typically formed from soft silicone gel or thermoplastic elastomer and are usually cylindrical in shape with a rounded cap at the distal end. Images of a silicone liner are given below in Figure 1.7.

These liners form a suction fit onto the limb and are even strong enough to suspend the rest of the prosthesis through the use of a distal pin attachment which mates with a lock in the prosthesis. While liners offer better suspension, comfort, and ease-of-fabrication than traditional sockets, they are not routinely used with myoelectric



Figure 1.7. Silicone liners used in Upper Limb Prosthesis [40]. A silicone liner is silicone sleeve that is worn prior to donning a body powered prosthesis. It maintains compression on the residual limb, is soft, and prevents abrasions on the limb due to socket movement. Moreover, use of a liner allows for the socket to be fabricated with a tighter fit on the residual limb without hurting the limb itself.

prostheses due to the difficulty of accommodating electrodes in the liner and aligning the electrodes within the liner with the target EMG sites on the limb.

1.4. Location Specificity of Electronics Affects EMG Signal Quality

As per current industry protocol, for direct control systems and above-elbow pattern recognition systems, prosthetists must accurately locate sites to place electrodes within the socket such that there is minimal activity or “crosstalk” measured during the contraction of the antagonist muscle [22]. If channels have too much crosstalk during use, the prosthesis can become unresponsive and lead to abandonment. This problem is compounded by the fact that clinicians do not have the necessary tools to locate EMG sites. Currently, prosthetists palpate the patient’s residual limb with their hands during prompted contractions to locate EMG sites [23]. Some may also



Figure 1.8 Prosthesis Fitting Session [25]. The image above shows a prosthesis fitting session for a Targeted Nerve Reinnervation (TNR) patient. The fitting for a regular transradial or transhumeral amputee is also similar. Myosites that give good EMG are located either by manual palpation or by attaching numerous electrodes over the residual limb and asking the patient to contract.

manually move EMG sensors from place to place over residual limb to find areas of maximal contraction [24] as shown in Figure 1.7.

However, both methods are not always accurate and can lead to poor site selection, which can propagate through to the final construction of the prosthesis. Once a final prosthesis is fabricated, moving electrodes to another site becomes very expensive and time consuming, leading to frustration for the patient. This makes myoelectric prosthesis a heavily specialized procedure as clinicians need to be experts in site location. In fact, despite clinicians' best-efforts, it is estimated [26] that one out of five upper limb amputees eventually abandon their prostheses altogether, most commonly citing a lack of functionality and difficulty of use [27].

In addition, the most significant challenges limiting pattern recognition algorithms from achieving significant clinical utility are that they require exceedingly noise-free EMG signals [27]–[30]. Signal noise can be attributed to a variety of sources including displacement of the electrodes from their originally calibrated location [32] and poor electrode-skin contact [33]. With regards to electrode displacement, one study has shown that movement of 10 mm decreases decoding performance by an average of 30% [34]. Such small displacements can happen every time a patient dons (puts on) their prosthesis at the start of the day, thus requiring a minimum of daily recalibration. However, shifts can also take place through the course of a day requiring more frequent recalibration sessions, which can lead to user frustration.

1.6. Potential Use of Silicone Liners in Myoelectric Prosthesis

One way of solving the problem associated with rigid electrodes is to change the material properties of the electrode itself and to embed it in a silicone liner in order to make it pliable and conformal to the skin surface. This would have several advantages including: It would provide better skin-electrode contact, prevent lift off under loading conditions thus giving relatively stable signals, increase user comfort, allow use of liners with myoelectric prosthesis. Flexible electrodes are being developed using a variety of materials such as polymers [32], silicone with embedded microelectronics [42], and textiles like conductive silk [43]. Moreover, development in liquid gallium interconnects or meanders for creation of flexible circuits interconnects could further support work in conformal electrode design [44] that could ultimately be embedded in a silicone liner.

While use of flexible materials would make it possible to integrate electronics within a liner, it still does not address the problem of location specificity. A possible way to eliminate the need for location specificity is to replace the tradition 2-8 channel electrode system with an HD array (greater than 8 contact sites) that covers the entire limb of the patient. Algorithmic selection of the desired contacts for prosthesis control could make flexible electronics in an HD configuration in a liner, an ideal solution for the current drawbacks with myoelectric prosthesis.

CHAPTER 2

2. Chapter 2: Advances in Technology for Flexible Electronics: Application to a Prosthetic Liner

Due to the limitations of traditional rigid electronics, numerous research groups and companies are now focusing on developing flexible materials that can be used for creation of electronics. The definition of electronics is evolving significantly from PCBs (Printed Circuit Boards) and solid components to use of unconventional materials and innovative technologies. This chapter highlights the different advances in flexible electronics and how they may be used within a silicone liner for EMG acquisition for myoelectric prosthesis control.

2.1. Advances in Flexible Electronics

2.1.1. Background

Health monitoring using wearable electronic sensors has recently come to the forefront with its usefulness in applications for EMG based device control, rehabilitation studies, cardiopulmonary monitoring and neurological studies. With most biomedical industries moving closer to developing wearable devices, the rigidity and bulkiness of current electronic hardware is proving to be a major disadvantage in conformity to the human body as well as for fidelity of acquired biosignals [45]. As a result, the need for flexible electronics has led to the development of numerous materials that could potentially be used to form the contacts with the skin, convert

conventionally rigid electronic boards to innovative pliable ones, thereby enabling the development of devices that are truly wearable in nature.

Based on current research in flexible electronics, we could classify the different types of conformal electrodes based on the material and processes used to produce the conductivity. Typically, based on material some broad classifications include textile based, polymer based, silicone based, foam based and composite based flexible electronics [52] for use in the passive parts of the circuit. Apart from developments in conductive materials themselves, numerous research attempts are also focused on creating flexible conductive interfaces using conductive inks and conductive tattoos. This section provides an insight into different innovative conductive materials and how they could be used for physiological signal acquisition. With a special reference to prosthesis, all the above mentioned materials and processes could be potentially used to integrate electronics with prosthetic liners made out of textile, silicone, polymers as well as conductive tattoos.

2.2. Materials for Flexible Electronics for EMG Acquisition

2.2.1. Textile Based

Textile based electrodes are typically passive (do not require an active power supply) in nature, and form the interface for signal acquisition from the body and for input to the processing circuitry. They can be formed through numerous techniques and one such method is the inclusion of the conductive fibers in the weave itself to form a uniformly conductive textile patch [53]. While this method is useful in some ways, it

is particularly complex to interface such an electrode with further processing circuitry on account of having to mechanically strip the fibers to expose the conductive interconnects.

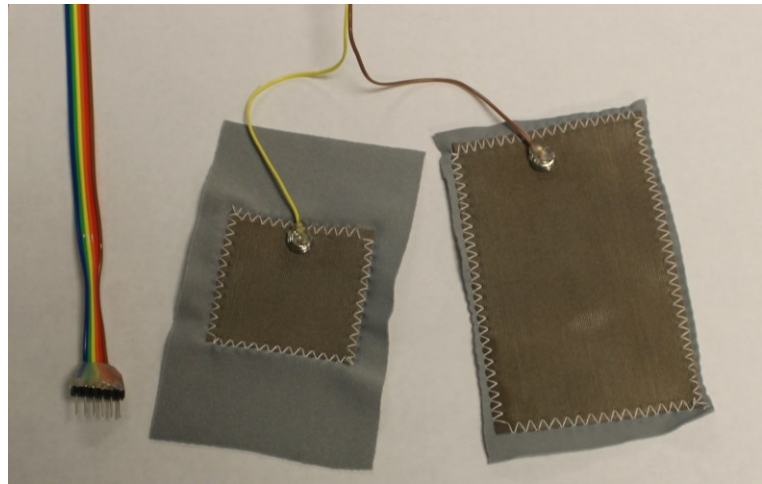


Figure 2.1. Textile Electrodes [54]. Textiles are being used in numerous wearable physiological signal acquisition electronics. The most basic of them is used as a pliable interface for signal acquisition from the human body.

Another mechanism of creating conductive textiles is to coat the same with conductive inks and solvents which

post absorption by the textile and drying, lead to the formation of significantly conductive textiles that can be interfaced with the next stage of hardware with flexible interconnects as described in section 2.2.6. Most textiles require a prior curing stage in order to eliminate the roughness induced by the weave and to create a smooth

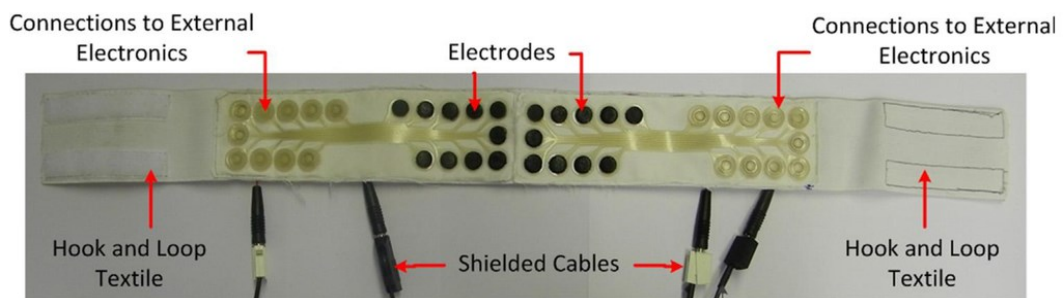


Figure 2.2. Textile Electrode with Conductive Traces [45]. A more advanced application of textile-based electrodes includes screen printing of traces on the material itself to form a compliant, conformal electrode assembly that interfaces with subsequent processing electronics.

surface for fine deposition of the conductive inks and substrates [55].

The unevenness of the surface as well as the porosity contributes to a bigger problem of cracking and degradation of the conductive ink interface over time which is not very conducive for most long term wearable devices [56]. Moreover, most textiles tend to absorb moisture and thus sweating can lead to a change in the physical, chemical and electrical properties of the conductive fabric.

In order to overcome the drawbacks of the previous two methods, efforts are being made to deposit metallic layers through screen-printing onto the textile directly after it has been cured for ensuring smoothness [57]. This allows the formation of a contact lead with sufficient thickness to be formed over the fabric and can be interfaced with subsequent circuitry using the aforementioned method. Depending on the nature of fabric used, it may still undergo cracking and flaking in prolonged use and is also susceptible to changes in environmental conditions.

Due to the flexibility of textiles and fabrics, they conform well to the body. In order to hold them in place well, the conductive patches are sewn onto elastic material else are held in place using straps and Velcro strips [58].

2.2.2. Silicone and Polymers

Traditionally, polymers have been used for physiological signal acquisition since the compressibility and softness of the polymer often decides its suitability for its use in a conductive environment. One example of polymer based electrodes are the wearable dry EEG electrodes that use soft villi like protuberances on the contact side to cover a

larger surface area of a person's scalp through hair and at the same time provide a little compressibility as well [63].



More recently, efforts have been made to use these substrates to make thin electronic patches. A key advantage of polymer and

Figure 2.3. Spring Loaded Polymer Electrodes [62]. These electrodes are particularly useful for EEG acquisition as they allow for good contact with the scalp, are compliant and water/oil resistant.

silicone based substrates over all other materials is their high conformity to bodily



Figure 2.4. Polymer based Electronic Tattoo [60]. The concept of tattoo based wearable electronics is becoming sought after technology due to the stability it provides to the skin electrode interface. However, long term use of these circuits is not feasible currently and remains the biggest hurdle towards their commercial adoption.

surfaces on account of low Young's Modulus. This makes them extremely useful for forming the base substrate for flexible electrodes [59].

With regards to application of metallic layers to silicones, the tattoo technique is extremely popular. This involves creation of a metalized layer of contact material and then it's transfer onto PDMS using an elastomeric stamp. A water soluble substrate is used to help apply the PDMS with the metallic coating onto the skin [61]. The biggest advantage of using silicone as a potential material is its hydrophobicity and relative inertness in a salty environment thus making it invaluable for use within the socket/liner where a humid, sweaty environment is a fairly common occurrence.

2.2.3. Conductive Silicone

Developed as a modification of the traditional silicone material, conductive silicone is new state of the art material and extremely useful. It is formed by creating a solution of the conductive material with silicone to disperse the conductive particles through the bulk of the base material. Curing brings about the necessary stability in the structure. With recent advancements, curing can be performed at room temperature as well, making this material compatible for application on other



Figure 2.5. Conductive Silicone Electrode Contacts. The electrode contacts in this picture are made of conductive silicone so that they are pliable, conformal and provide a more stable interface to the skin.

heat sensitive materials. Some conductive particles include silver, gold, copper, aluminum and graphite.

2.2.4. Conductive Foam

While the materials mentioned previously are extremely conformal in nature, they are unable to provide a wide range of compressibility. This is especially important in the creation of contacts for electrodes that require a certain degree of automatic adjustments to changes in external pressure so that the electrode skin contact is well maintained.

As a result, conductive foam that consists of conductive particles distributed across its bulk provides excellent compressibility across a wide range from 25x to more. Moreover, compressibility also ensures that the force that is applied to the user in order to hold the electrode in place does not lead to injury.

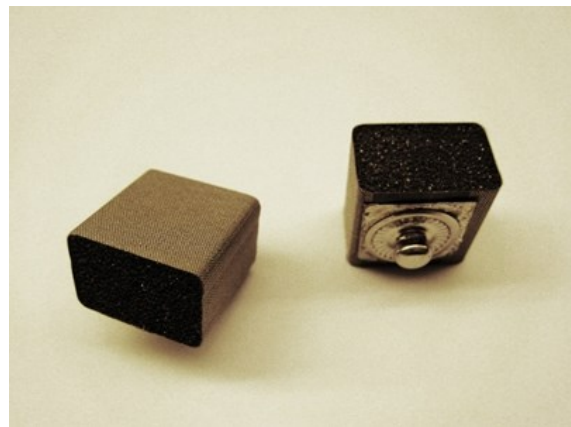


Figure 2.6. Conductive Foam EEG Electrodes [63 - 64]. These conductive foam electrodes are super compliant and compressive thus eliminating the problems that occur due to electrode liftoff. In case of a lift off, the electrode simply decompressed and a conductive path between the skin and electrode is maintained.

Conductive foam is usually used in conjunction with conductive textiles to form the even interface with the surface for surface physiological signal acquisition. An example is the MINDO textile covered conductive

foam electrodes for EEG acquisition. With minimal motion artefact and good conductivity, the electrodes are suitable for any surface signal acquisition [64].

Conductive foam can be made out of different materials, such as copper, aluminum and graphene. While electrical properties are similar, their use depends majorly on the level of compression that can be achieved as well as compatibility with skin.

2.2.5. Creation of Conductive Interface using Conductive Inks

Apart from using the aforementioned materials for forming the base material for creating the conductive interface, sometimes, additional metallic or conductive ink layers are added to these materials to form a better interface with the skin.

With metal being the top choice for creating the passive components of a circuit such as the contact leads and interconnects, a lot of effort is currently focused at developing an easy and cost effective mechanism for metal deposition on a variety of

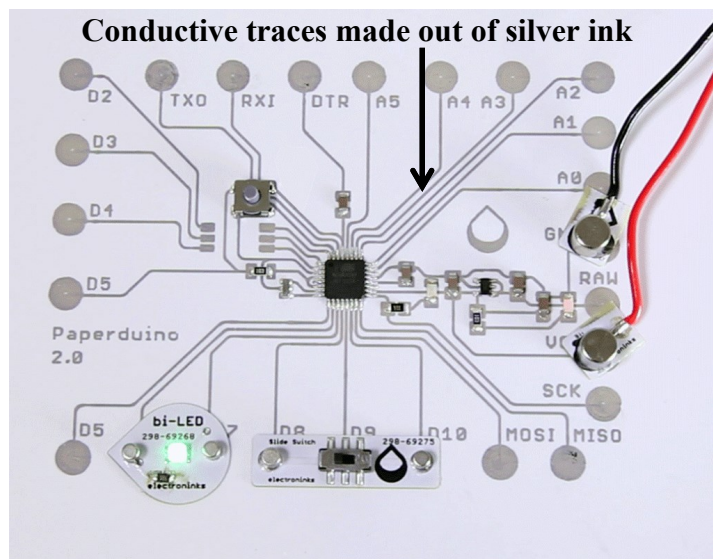


Figure 2.7. Conductive Ink Printed Circuit [65]. Conductive inks are becoming extremely popular in creating flexible circuits on materials that are pliable but cannot be doped.

substrates like plastics, elastomers, papers and textiles. Innovative technologies like PAMD (Polymer-Assisted Metal Deposition) allow fabrication of foldable, flexible, stretchable and compressible wearable metal with high conductivity [67].

While metal deposition techniques can often be cumbersome, conductive inks can be applied much more easily through various methods such as screen printing, syringe dispensing, dipping and spraying. The technique used is often dependent on the nature of the base material as well as the nature of the contact that needs to be formed.

While most of the different techniques are extremely useful in application of inks for short-term use, longer usage tends to cause cracks because of mechanical wear. This makes the post processing methods used extremely important. Creation of a nanoporous microstructure by post heat treatment after ink jet printing tends to create more stable metallic layers than that of traditional evaporated films [66].

2.2.6. Flexible Conductive Interconnects

Innovative use of technologies ranging from development of conductive yarn as






	Verstraeten	Dhawan	Cottet	Post	Watson
Conductive Part (# of Strand)	Copper (1)	Copper (28)	Copper (1)	Steel (spun 20%)	Steel (4)
	d=148 μm	d=70 μm	d=40 μm	Not Known	d= 35 μm
Non-conductive Part (# of Strand)	Steel (3)	-	Polyester	Polyester (80%)	Polyester (1)
	d=12 μm \times 275		150.3 denier	4.5 denier	600 denier
Structure (Location of conductive material is described in darker colors)					
Twist Density (tpm)	Z100	Not Known	Not Known	Not Known	S350 & Z350
Resistance (Ω/m)	1.2	0.2441	15.7 – 17.2	~5,000	180

Figure 2.8. *Conductive Yarn [46]. This figure gives a detailed overview of the different fabrication techniques and composition of conductive yarns. They form the basis for conductive textile development, as well as are essential for creation of flexible electronic traces in textiles.*

shown in Figure 2.1, [46] that is interwoven with metallic wires and connects to novel methods of using liquid metal for interconnects in circuits is paving the way for development of flexible device interfaces with the human body.

A key idea is to separate the fabrication of the electrode leads from interconnects between the leads and subsequent parts of the circuitry. Thus, fabrication of a thin conductive layer on a flexible substrate and specialized development of the stretchable interconnects can help combine elements of conductivity and stretchability which are otherwise difficult to incorporate together [50, 51].

2.3. Flexible Electronics for Myoelectric Prosthesis

One way of creating a robust EMG acquisition system that is compliant with the upper limb, is to integrate a EMG acquisition flexible circuit within a silicone liner.

This flexible circuit would have 2 parts:

1. The electrode contacts that interface with the skin
2. The amplifier and processing circuitry

The design of this hardware will determine how it can be integrated within a liner. Traditionally, EMG electrodes are used in a differential configuration with the processing circuitry mounted as close to the contacts as possible to prevent contamination by interfering signals. However, with appropriate shielding, the contacts can be used in a remote configuration in which the electrode contacts are located differently than the processing circuitry.

For a flexible circuit design that can be easily integrated into a liner, it would be technically more feasible to integrate remote flexible contacts within the liner and have them connected to processing circuitry at the distal end of the same. The same is elaborated upon in the next few sections and chapters.

2.3.1. Electrode Contact Design

An ideal electrode contact would result in signals with high SNR, be compressible to ensure contact even when the electrode shifts as well as have minimal settling time when used with a prosthetic hand. Moreover, it would have to be such that it can be easily integrated into a silicone liner. As a result, the most appropriate base material for creating the electrode contacts would be conductive silicone. It has similar material properties as non-conductive silicone due to which the two can be integrated well. As a result, the electronics created can be integrated within existing silicone liners with the electronics mounted at the distal end so that a remote electrode system can be implemented.

This system could be supported further by the use of high-density electrode arrays for EMG acquisition with flexible contacts for skin-electrode contact based channel selection for use of EMG for prosthetic limb control.

The amplifier and processing circuitry design is strongly dependent on the configuration of electrode contacts. While traditionally, a differential configuration is used in electrodes for EMG acquisition, that may not be the best method when integrating within in a liner due to the need for location specificity with respect to the

limb. It is nearly impossible to wear the liner the exact same way every single time thus an arrangement of contacts in a HD location independent configuration may be useful. Thus, use of HD of EMG electrodes on a flexible substrate may prove to be beneficial in this regard.

2.4. Summary

This chapter provides an overview of the advances in flexible electronics. It also describes how these advances could be relevant to redesigning electronics in a prosthesis system. These include:

1. Flexible electronics are being created from several different base substrates such as textiles, polymers, silicones and foams. Moreover, methods such as screen-printing with conductive inks are allowing the creation of tattoo like circuits.
2. Of the above materials, conductive silicone is very pertinent for use in prosthesis systems.
3. Traditional rigid electrodes mounted within the socket could be replaced by flexible electronics created out of conductive silicone and integrated with a silicone liner.
4. Doing so in a HD configuration will allow for the creation of a flexible location independent interface to the residual limb for signal acquisition.

The next few chapters discuss the creation of high-density flexible electrodes for EMG signal acquisition.

CHAPTER 3

3. Chapter 3: Developing Flexible Electronics and Methods to Characterize Their Electrical Properties

Working with flexible materials for electronics development introduces numerous challenges. These include establishing parameters for comparisons of electrical properties of these new materials in a repeatable and universally replicable manner to ensure that a standard is followed. Thus, the development of flexible electrodes using doped traditionally non-conductive materials requires the design of new methods not only for the creation of new materials, but also for the characterization of these materials. This chapter highlights the ineffectiveness of traditional parameters used to characterize conductive materials and establishes skin electrode complex impedance as the better universal standard for characterizing new flexible materials for physiological signal acquisition.

3.1. Introduction to Skin Electrode Complex Impedance

Skin-electrode impedance is the impedance of the skin and the electrode between the electrode inputs. When the electrode is properly attached, the measured impedance is low, and the input signal or injection current for measuring the skin electrode impedance is extremely attenuated. When the electrode is not attached properly to the skin (loosely contacting the skin or partially lifted off from the skin), the impedance is very high and is reflected as such in the output signal [68].

Real time continuous monitoring of skin-electrode impedance measurement can provide information about the nature of contact between the skin and the electrode. This data can be used to determine whether the EMG signal acquired at a given instance of time is of high fidelity or not and whether it should contribute to the prosthetic limb control algorithm or not for greater stability and control. Impedance measurements can help monitor bad contact between skin and electrode as well as can be used to eliminate bad quality signals from inclusion in the algorithm for limb control. While impedance monitoring for electrode lift off is not a permanent solution to acquiring high quality signals, use of impedance to determine electrode lift off conditions can limit the extent of instability in limb control.

3.2. Principle Behind Skin Electrode Impedance Measurement

Generally, the concept of measuring skin electrode impedance is accomplished by inputting a known excitation current signal at a high frequency through one lead and acquiring the signal after it has traversed through layers of electrode and skin at the other lead [69].

The strength of the conductive pathway between the electrode and patient (or in other words, skin electrode impedance) causes a proportional voltage drop across the two leads, which after processing by the analog front end can be viewed digitally.

The measured output voltage when divided by the known injection current gives us the skin electrode impedance at a given instance of time, real time.

Typical values while measuring skin electrode impedance [70]:

- Impedance : $1\text{k}\Omega$ to $1\text{M}\Omega$
- Frequency of stimulation: 0 - 5 kHz (Depends on the AFE (Analog Front End))
- Injected current: Few nA (Depends on the AFE used)

Skin electrode impedance is assumed to have dependency on numerous factors such as:

- Skin properties of the user
- Contact area of the electrode
- Pressure on the electrode [71]
- Sweat/Bodily secretions of the user

3.3. Methods for Measuring Skin Impedance in Existing Electronics: Lead off Detection for Skin Impedance Measurement

Most AFE systems have built in current injectors for measurement of skin-electrode impedance to detect Lead Off. This can be done in multiple ways as listed below [72].

- Analog DC Lead Off - Using a simple dc current source or passive components in a pull-up or pull-down resistor configuration are common methods for DC lead-off detection. This method has multiple drawbacks. Firstly, it does not give us an output with physical impedance values since the AFE has built in comparators against which the measured value is compared. The output is in terms of Lead On or Lead Off which is not useful for studying the intermediary

stages of bad contact. In addition, by virtue of most EMG electrodes being dry and capacitive in nature, DC give a very high offset and cannot be used successfully.

- Analog AC Lead Off – This method uses a mechanism by which it monitors the magnitude of AC excitation signal frequency. Like in the previous method, comparison takes place by inbuilt comparators in the chip and the output is of the form of Lead Off or Lead On. While it is more accurate than DC Lead off since it eliminates effects due to DC offset, it still does not give us an output with physical impedance values.
- Digital AC Lead Off – This method overcomes the drawback of the previous two allowing the measured signal to be viewed digitally at the output superimposed over the biopotential signal. The impedance signal can be isolated using filtering and the amplitude when divided by the injection current provides a real time reading of the skin electrode impedance. This method can only be used when there are connected electrodes and cannot be used for individual electrodes.

Thus, for real time EMG signal acquisition and skin-electrode impedance measurement, the most appropriate method is to use Digital AC Lead Off, which allows an injection current in the frequency of 10KHz with a few nA magnitude to be inserted into the body. Since this frequency is out of the range of the useful EMG bandwidth, this signal can be filtered out at the digital output and can be used for calculating the skin electrode impedance by dividing the amplitude of the output signal at 10KHz by the injection current value.

3.5. Complex Skin Electrode Impedance Better Characterizes the Electrical Properties of Doped, Traditionally Non-Conductive Materials for Physiological Signal Acquisition

Conventionally, for long term recording of EMG signals, such as in a prosthesis, dry electrodes having bar or dome contacts made of titanium or stainless steel [73 - 74] are used because their high conductivity as well as due to the usability of the EMG signal acquired through them. Skin preparation [75] using alcohol swabs or CalStat Skin preparation solution [127] is preferred to quickly establish equilibrium at the electrode skin interface and to reduce the settling time.

Moreover, for acquiring usable EMG signals from the residual limb for long periods of time and in order to ensure a tight fit, the electrodes are attached to the inside of a prosthesis socket that is custom - designed for each user [76 – 77]. Often due to the anatomy of the residual limb, the socket can move under loading conditions of the arm which causes electrode migration and electrode lift off, thereby affecting signal fidelity [28 - 78].

In order to overcome the limitations of current rigid electronic systems in prosthetics, research is focused on developing flexible electronic solutions to the same. Electrode contacts made out of compressible, flexible and doped polymers, silicones and textiles as given in references [79 - 81] conform to the shape of the residual limb and form a stable interface to the socket. However, the biggest problem in the comparison of these new materials in their ability to be used for signal acquisition is that there is no uniform metric that can be used to objectively quantify or predict the quality of signal that can be acquired through the material by measuring a known electrical parameter.

Traditionally, conductivity was assumed to be the best measure of approximating the quality of signal acquired through a material, since a high conductivity indicates a good ability of the material to conduct signals and correlates to a high quality of signal through a material [82 - 83]. Even today, most datasheets for materials (both metals and doped substances) from commercial manufacturers have conductivity or resistivity values as the metric to define electrical properties [84 – 87].

While this relationship works very well with purely resistive materials like metals that have conventionally been used to develop electrode contacts, it becomes invalid when working with materials that are primarily non-conductive and are made conductive only through doping. This is because doped materials have a capacitive component in addition to the resistive component that contributes to the nature of signal acquired through that material which conductivity does not account for. Since conductivity measurements do not provide an accurate representation of electrical properties of all kinds of materials, many researchers use SNR or Signal to Noise Ratio [13– 88] of the signal acquired as a means of quantifying and comparing the conductive properties of different materials. The higher the SNR of the signal acquired through a given material, the better the electrical properties of the material for signal acquisition.

However, the mechanism of SNR measurement is not always uniform and results from different research groups cannot always be compared against each other. There is thus a need for a more uniform and generic parameter for quantification of the electrical properties of all kinds of electrode contact materials such as metals, polymers, silicones and foams amongst others. Instead of looking purely at the conductivity values, complex impedance is a better metric to quantify the electrical

properties of a material. Moreover, including the skin electrode impedance may be an even better metric for comparison when studying materials used for making electrode contacts since the composite measure provides the most accurate representation of how the material interacts with the skin which subsequently governs the physiological signal quality [89 - 91].

Therefore, apart from a need for flexible electrode contacts that match the electrical properties of the skin better, there is also a need for a uniform parameter to characterize the electrical properties of all kinds of materials used for making these electrode contacts.

3.5.1. Methods

For this study, we created electrode contacts from a wide range of materials in order to understand their interaction with the skin, determine the quality of signal through them and find a universal way to electrically characterize them. The different materials include: Anodized Titanium (industry standard for EMG electrodes for prosthesis), conductive silicone doped with three different kinds of dopants in to induce conductivity namely Carbon Nanotube (in three different concentrations – WW46, WW45, WW44), Silver [87] (CSC), and Copper Nickel [84 – 85] (in two different concentrations) (CSA and CSB), electrically conductive polyurethane foam coated with copper and nickel [86], and conductive foam coated with a layer of conductive silicone [86, 87]. The conductive silicones with silver and copper-nickel dopants were commercially obtained from Silicone Solutions in uncured form and were cured in-house.

The conductive foam was obtained from Holland Shielding Systems, BV, Netherlands. Our team collaborators fabricated the silicones with Carbon Nanotube (CNT) doping.

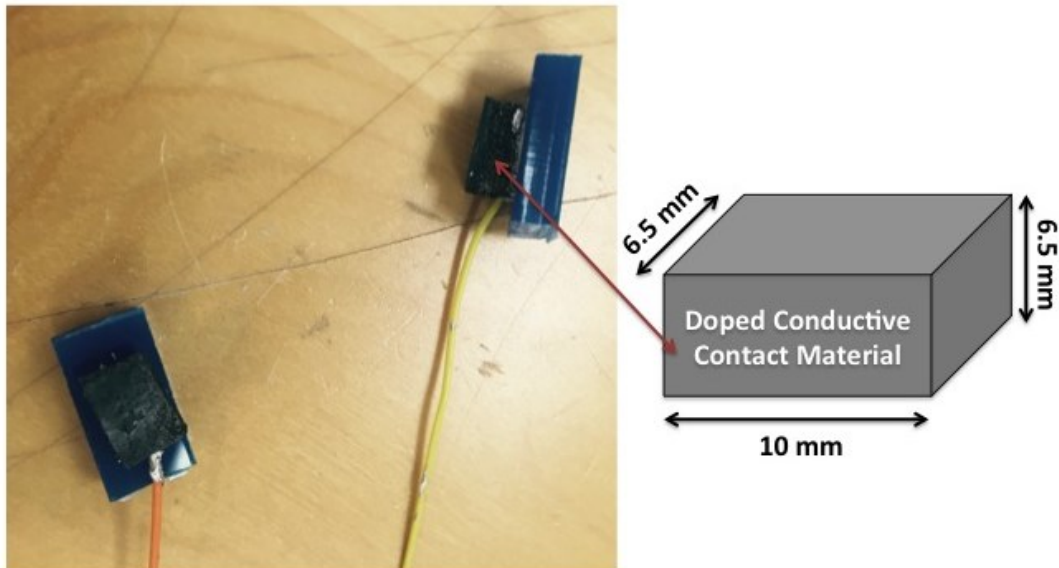


Figure 3.1, Flexible Contacts. It represents the layout of each contact made out of metal, doped silicone, conductive foam or a combination of foam and silicone. The electrode contacts were developed in two sizes: 10mm (L) x 6.5mm (B) x 6.5mm (H) and 10mm (L) x 3.5mm (B) x 6.5mm(H) for attachment to the reference input and differential signal inputs of the custom made active differential EMG Element electrodes from Infinite Biomedical Technologies LLC. In addition, one contact of each type of material was also mounted on a plastic base with conductive epoxy to allow easy attachment to subject forearms for impedance measurements.

The electrode contacts were developed in two sizes: 10mm (L) x 6.5mm (B) x 6.5mm (H) and 10mm (L) x 3.5mm (B) x 6.5mm(H) for attachment to the reference input and differential signal inputs of the custom made active differential EMG Element electrodes from Infinite Biomedical Technologies LLC. A sample of the contact is shown in Figure 3.1

In addition, the electrical equivalent diagram of the dry electrode combination was determined to model the skin electrode interface through passive components [64 -

92]. Unlike gel electrodes where the gel is purely resistive in nature, the dry materials used in this study have a layer of air present between the skin and electrode interface and they are comprised of a non-conductive matrix, which contributes to a capacitive component in addition to a resistive component. It is modeled as CC and RC respectively. The surface potential of the skin electrode interface is present as a DC voltage. As per literature, its standard value is -39.6mV [70]. The epidermis and sub-epidermal layers are also both resistive and capacitive due to the presence of the Extracellular Fluid (ECF), cell membrane of cells and the Intracellular Fluid (ICF). They are modeled as RE+SE and CE+SE, The deep tissue layers are modeled as purely resistive in Nature and have a value of about 200 Ohms at frequencies below 10 kHz and a value of 120 Ohms at frequencies in the MHz range [70].

In order to determine a stable frequency for studying the skin electrode impedance behavior of different materials, skin electrode impedance values were measured from three sets of different materials placed in contact with the forearm of a single subject at 1000 Hz (industry standard for impedance measurement for electrode lift off detection) [72] and at 5000Hz (higher frequencies between 5KHz and 1 MHz ensure that the impedance measured is independent of the shape and size of the material used) [28]. The gathered data along with complex impedance values of the material itself as well as the known constants of the skin electrode interface modeling (two resistance in parallel with capacitance all in series with a resistance, as given in Fig. 3.2) [70] was then used to calculate the impedance values of the sub-dermal tissue layers alone. Mathematically,

$$Z_{\text{Epidermal+Sub-Epidermal}} =$$

$$Z_{\text{Skin Electrode Interface}} = Z_{\text{Contact Material}} + R_{\text{Deep Tissue}} \quad (\text{Eq.2.1})$$

Where $Z_{\text{Skin Electrode Interface}}$ is the Skin Electrode Complex Impedance measured by placing the material on the skin and taking impedance reading of the entire interface at both 5000Hz and 1000Hz

$Z_{\text{Contact Material}}$ is the Complex Impedance measured by taking impedance readings of the material alone at 5000Hz and 1000Hz

$R_{\text{Deep Tissue}}$ is 200 Ohms based on prior literature [70].

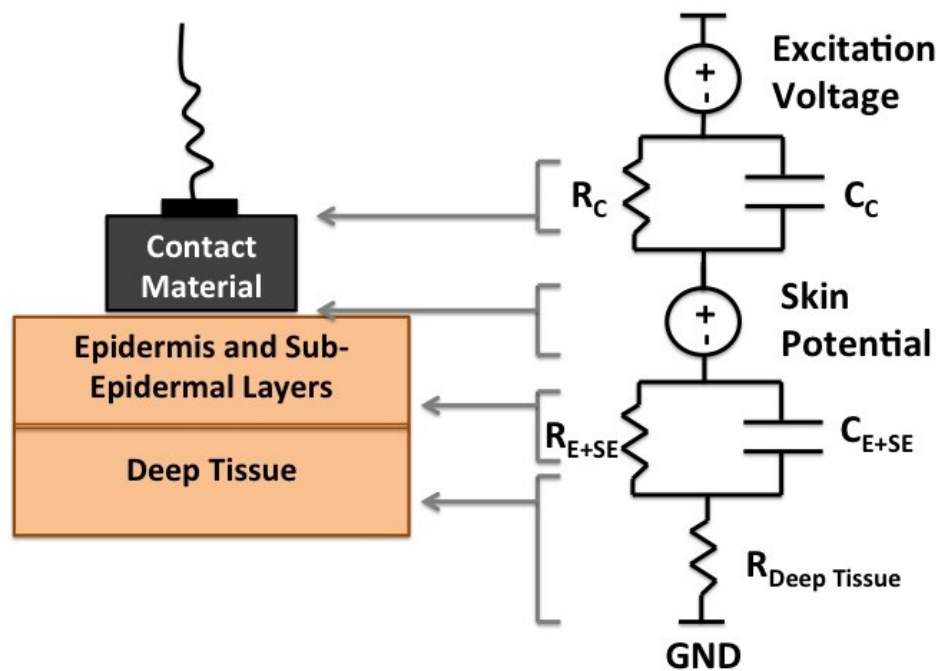


Figure 3.2. Electrical Modeling of Skin Electrode Interface. The diagram represents the electrical equivalent diagram of the dry electrode skin combination. The dry materials used in this study have layer of air present between the skin and electrode interface, which contributes to a capacitive component in addition to a resistive component. The materials themselves have a resistive and capacitive component. The surface potential of the skin electrode interface is present as a DC voltage. The epidermis is also both resistive and capacitive due to the presence of conductive fluids like sweat and non-conductive dry skin. The sub - dermal layers are modeled as purely resistive in nature.

Four different measurements were made for each of the eight different materials for five different healthy subjects (18 - 30 years) over 20-minute recording sessions for each material, with data points gathered each minute. The study was conducted over a 20 minute interval since all the materials used in this study stabilized in their signal quality within a 20 minute interval. This is consistent with literature on titanium and stainless steel (industry standard), which stabilize within 10-15 minutes of being attached to the skin [74]. If a material takes more than 20 minutes to reach electrical stability, it is unsuitable for instantaneous electrophysiological measurements [134]. The different datasets gathered were: Conductivity, Complex Impedance, Skin Electrode Complex Impedance and Signal to Noise Ratio (SNR) [93]. Conductivity measurements were made by placing the electrode contact within a mechanical contraption for maintaining good surface contact. Wires from the two plates of the contraption in contact with the material were connected to a Fluke 15B F15B+ Professional Auto Range Digital Multimeter Tester and the DC resistance was recorded. Each contact was measured with a pair of calipers and the dimensions were recorded.

The resistivity of the material was calculated by:

$$\rho=R \cdot l / A \quad (\text{Eq.2.2})$$

where ρ is the resistivity of the material, R is the resistance measured from the multimeter, A is the area of cross section of the material touching the plates and l is the height of the material between the two plates.

The conductivity values were determined through:

$$\kappa=1 / \rho \quad (\text{Eq. 2.3})$$

where κ is the conductivity and ρ is the resistivity calculated in Equation 2.2.

Similarly, the Complex Impedance (CI) values were calculated by placing the electrode contact within a mechanical contraption for maintaining good surface contact. However, wires from the two plates were connected to a different system. The Intan RHD2000 system by Intan Technologies LLC [128] was used to make electrode impedance measurements. This processor and amplifier board system injects a known current of 5 nA into the contact and measures the voltage developed across the material. The known current magnitude and the measured voltage is then used to mathematically compute the complex impedance.

One of the wires from the mechanical contraption was connected to an amplifier input channel and the other was connected to ground to make this measurement.



Figure 3.3.a. The apparatus for conductivity measurements. The material is placed between the metal plates of the mechanical contraption, which is held at a constant spacing using spacers. The wires leading out of the measurement rig are connected to the digital multimeter and DC resistance is measured. The same is used with the Intan system for complex impedance measurements.

Figure 3.3.b. The contact material attachment to the IBT electrodes is shown. The metal, conductive silicone or foam material is mounted on the outer enclosure such that when the electrode board is encased within the enclosure, a continuous path of conduction is formed between the material to be tested and the spring contacts on the electrode board.

Figure. 3.3.c. The attachment of the electrode to the forearm is demonstrated. The electrode is placed about 2 inches distal to the elbow at the point of maximum muscle activity for a hand flexion.

Skin electrode complex impedance measurements were made by attaching each contact to the subject's forearm, 2 inches distal to the elbow and connecting it to an amplifier channel in the Intan system [128] with a separate ground electrode connected to the epicondyle on the elbow of each individual.

For SNR measurements, the contact material was used in conjunction with an Infinite Biomedical Technologies Element electrode [129] used in commercial prosthesis for EMG measurements. The electrode is a dry differential electrode with titanium contacts that uses the Texas Instruments ADS1291 as the amplifier with a programmable gain. The experimental construction of SNR measurements is described in Figure 3.3. The electrode was placed over the flexor muscle, approximately 5 centimeters distal from the elbow and secured with an elastic cuff. The subject was asked to contract the flexor muscle every minute and the SNR ratio of each EMG contraction signal was calculated using a custom MATLAB function and noted. The acquired signal was analyzed for SNR in MATLAB using a custom written function calculates the ratio of the RMS of signal to the RMS of noise in a specific window period.

Mathematically:

$$\text{SNR} = (\text{RMS of desired signal}) / (\text{RMS of baseline noise}) \quad (\text{Eq 2.4})$$

In addition, for all SNR measurements, the location with the highest signal amplitude was located using a traditional dry EMG electrode and the same location was used for all subsequent electrode placements for different contact materials. All the data

acquisition from the subjects was performed without any skin preparation in order to study the natural behavior of the material when put in contact with skin.

3.5.2. Results and Discussion

3.5.2.1. Stability of Impedance Data at 5000 Hz as compared to 1000 Hz

At a frequency of 1000 Hz, the standard deviation in the resistance of the sub-dermal layers was in the range of 160 kOhms and the standard deviation in capacitance was in the order of 8 nF for all materials. However, at a frequency of 5000 Hz, the standard deviation in the resistance of the sub-dermal layers was in the range of 2 kOhms and the standard deviation in capacitance was ~5 nF for all materials. Overall, the impedance measured at 1000 Hz varies very highly by almost 75 kOhms, however, the impedance at 5000 Hz follows a very stable trend with limited variation and has a standard deviation of only 0.6 kOhms. The reason for the stark difference between impedance measurements at 1000 Hz vs 5000 Hz could be attributed to how the current and frequency interact with the biological tissue layers. At low frequencies, <5 KHz, the current cannot penetrate through the cell membrane and hence most of the current travels through Extracellular Fluid (ECF). At high frequencies, since the current is able to penetrate through the cell membrane, it travels through Intracellular Fluid (ICF) in addition to the ECF [121].

As per our data, the average capacitance at 5000 Hz is ~18 nF while that at 1000 Hz is ~8 nF. Measuring a higher capacitance indicates that part of the current is flowing through the ICF after penetrating the cell membrane which contributes to the

capacitance value. Part of the current also flows through the ECF. Thus resistance values at 5000 Hz are representative of the current flowing through both the ECF and ICF.

Table 3.1: Epidermal and Sub-Epidermal Resistance, Capacitance and Impedance

		5000 Hz				1000 Hz			
		WW46	WW45	WW44	AVERAGE	WW46	WW45	WW44	AVERAGE
R_{E+SE} (kOhms)	MIN	3.659	3.282	3.719		1.846	2.935	4.756	
	MAX	11.478	5.495	10.539		397.891	419.953	481.97	
	AVERAGE	5.604	4.191	5.625	5.140	101.127	142.198	140.095	127.807
	STD	1.861	0.621	1.711	1.398	146.874	162.527	166.788	158.73
C_{E+SE} (nF)	MIN	6.203	12.111	10.115		0.639	0.641	0.7	
	MAX	28.955	31.161	27.142		31.24	32.511	42.379	
	AVERAGE	16.067	19.64	18.13	17.946	8.728	7.565	8.293	8.195
	STD	6.354	4.906	5.108	5.456	7.557	7.611	9.389	8.186
$ Z_{E+SE} $ (kOhms)	MIN	1.061	1.001	1.12		1.795	2.838	3.756	
	MAX	4.546	2.315	3.016		211.033	203.163	196.849	
	AVERAGE	2.142	1.576	1.789	1.836	52.983	62.601	60.164	58.583
	STD	0.944	0.36	0.52	0.608	75.669	71.975	73.258	73.634

Table 3.1: The table summarizes the resistance, capacitance and impedance of the epidermal and sub-epidermal layers for three different contact materials CNT doped silicone materials with different doping concentrations at 1000 Hz and 5000 Hz. We can see that at 5000 Hz, the average capacitance is $\sim 18\text{nF}$ and is higher than $\sim 8\text{nF}$ at 1000 Hz. This indicates that more current flows through the Intracellular Fluid at 5000 Hz and that the average resistance of $\sim 5\text{ kOhm}$ is representative of current flowing through both ICF and ECF. At 1000 Hz, the current flow is majorly through the ECF and the average resistance of $\sim 130\text{ kOhms}$ depicts the same. We know that the path of least resistance to current flow can vary significantly within the ECF even for the same person at two different times and this variability is evident by the high standard deviation of $\sim 160\text{ kOhms}$ in the resistance values and high standard deviation of $\sim 70\text{ kOhms}$ in the net impedance values at 1000 Hz. This is in contrast to the much lower standard deviation of $\sim 2\text{ kOhms}$ in the resistance values and very low standard deviation of $\sim 0.6\text{ kOhms}$ in the net impedance values at 5000Hz. Thus, 5000Hz is used as the frequency for all subsequent data analysis on account of greater stability of impedance values at the same.

However, smaller capacitance indicates that lesser current flows through the ICF and it indicates that majority of the current is not able to penetrate through the cell and hence travels through the ECF. The resistance thus measured at 1000 Hz is indicative of the current flowing through the ECF alone.

The path of current when travelling through the ECF can vary significantly since the path of least resistance can be affected by the variation in the composition of the ECF

as well as arrangement of the cells inside it, as a result of which, every measurement of resistance as well as capacitance, which is also dependent of the path length varies more at lower frequencies [122, 123, 124, 125].

This makes measurements at 1000 Hz highly variable and unsuitable for studying the relationship of impedance with other parameters. Thus due to the stability of impedance values at 5000 Hz, it was used as the frequency to study the relationship of impedance with respect to parameters such as time and SNR in the following sections.

Using 5000 Hz has other advantages which include minimal interference from motion artefact, lack of dependence on shape and size of contact [94] as well as minimal effect of stray muscle contractions (EMG signals lie in the 10 – 500 Hz range) [74] which ensures that the measurements quantify the electrical properties of the skin electrode interface alone.

3.5.2.2. Conductivity Variation for Long Term Measurement and Comparison with SNR

A standard parameter for characterizing the electrical properties of a material, specially its ability to conduct, is conductivity. The inverse of resistivity, conductivity is a constant for a given material and for purely resistive materials like metals, and is the best parameter for characterizing the nature of signal one may acquire out of purely resistive materials.

Three resistance readings for each sample of material were made and were averaged to calculate the resistivity and conductivity of the material. Data from four samples of the same material were averaged to determine the bulk conductivity of the material.

However, based on the tests with samples of materials like conductive silicone, which are primarily non-conductive and capacitive and are made conductive through doping, it was seen that the conductivity measurements do not account for the capacitive components.

The graph given in Figure 3.4, demonstrates the order of materials based on their conductivities. As seen, Titanium has conductivity in the order of $[10]^6$ Siemens/cm whereas other materials such as WW46 and WW45 are much lower at a few 100 Siemens/cm. Based on these measurements, one would traditionally assume that WW46 and WW45 would give significantly poor EMG signals if used as electrode contacts. However, if we study the SNR of these materials over time as in Figure 3.5, not only do we see that WW46 and WW45 give a signal with SNR that is definitely usable for prosthesis control, they are almost identical to Titanium in terms of baseline noise and amplitude of contractions if not better than Titanium at times. The same was observed across all subjects, thus indicating, that conductivity may not be the most comprehensive method for characterizing materials for physiological signal control.

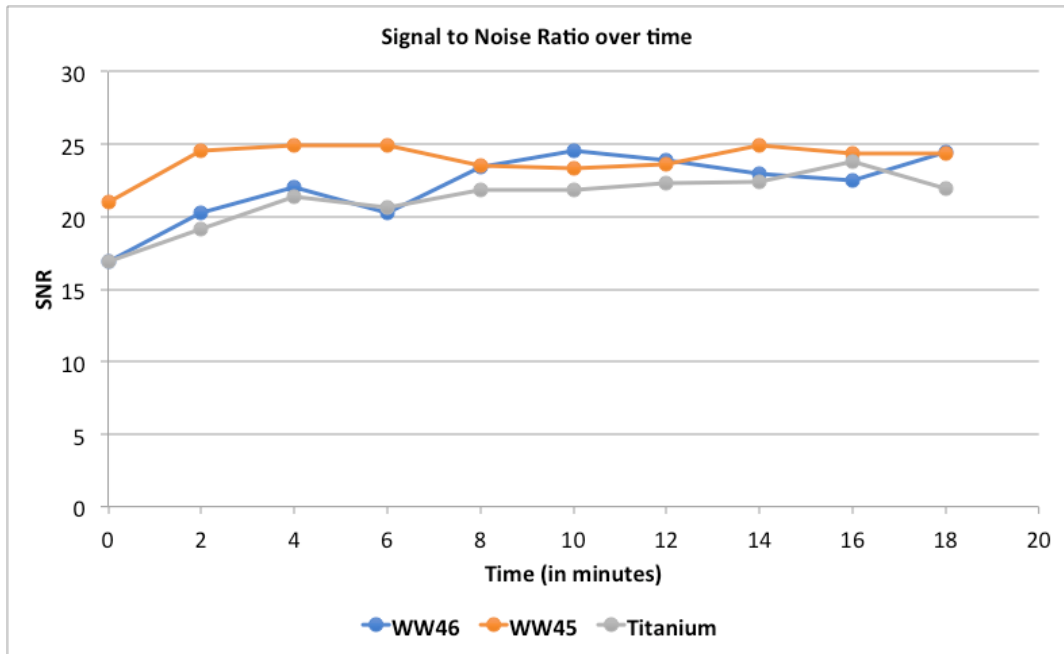
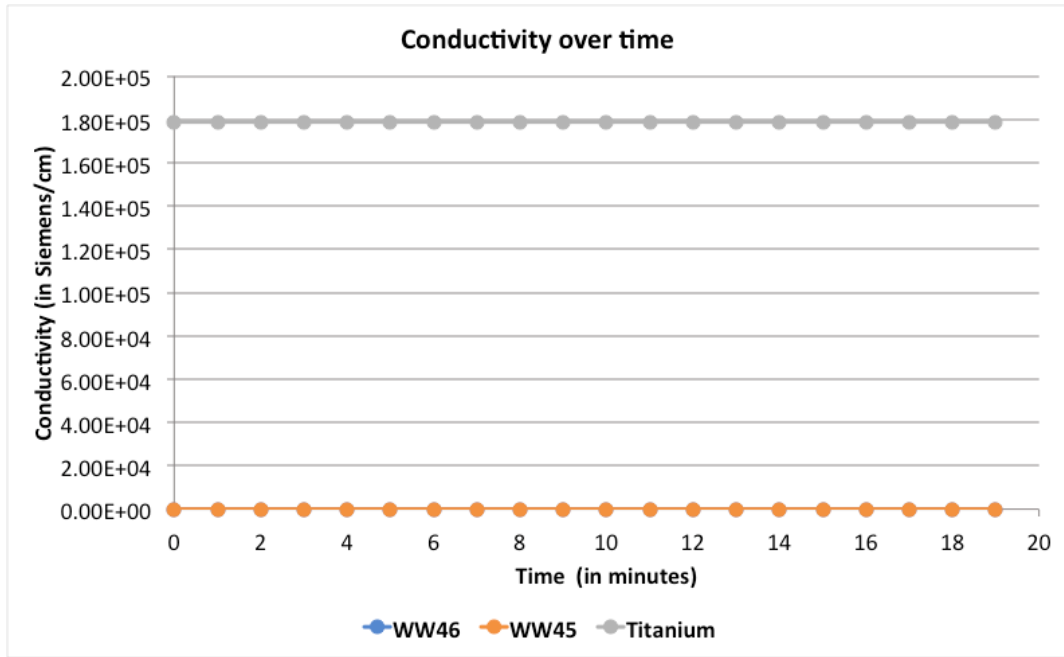


Figure 3.4.a: Conductivity of Materials vs Time. The graph shows the average conductivity of 5 measurements every minute of three materials namely, WW45, WW46 and Titanium, over a 20 minute interval. The three materials lie on opposite sides of the conductivity range. However, in Figure 3.4.b. SNR vs Time, we can see the SNR of the same three materials over time, and the SNR of all three is very similar. Thus, for metals, while a high conductivity correlates to a high SNR, we see that the relationship falls off for traditionally non-conductive materials that were made conductive through doping with conductive fillers.

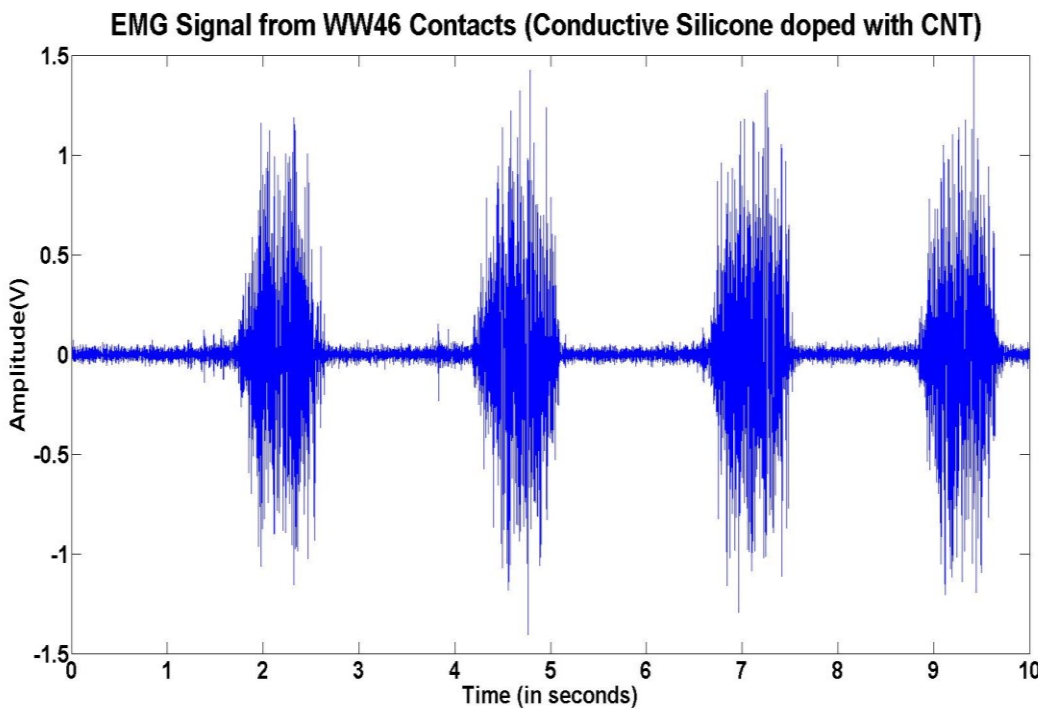
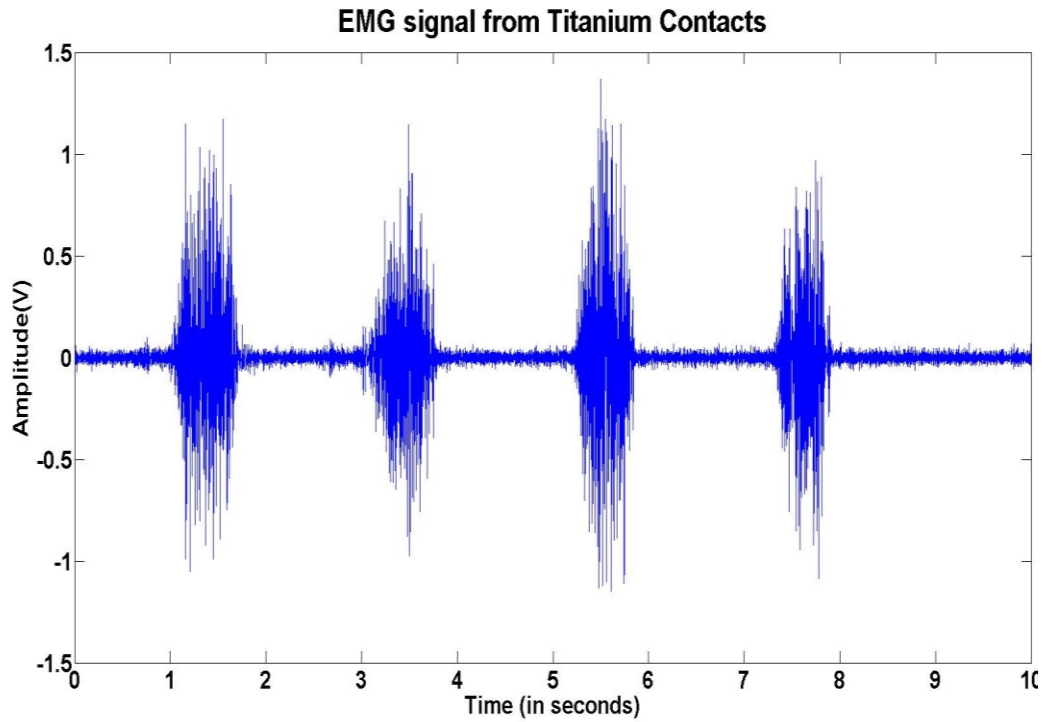


Figure 3.5.a: Signal from Titanium contact, Figure 3.5.b: Signal from Silicone (Doped with CNT) Contact. Comparison of both signals shows that they are comparable both visually and computationally using SNR as a metric. The peak amplitude of the EMG signal during a contraction is almost identical, if not better in the silicone sample. If the signal quality was estimated based purely on the conductivity values, the two materials would not have been identified as equally good for physiological signal acquisition.

3.5.2.3. Complex Impedance Variation for Long Term Measurement and Comparison with SNR

The complex impedance of each material was analyzed by using the electrode impedance measurement (Intan RHD2000 Evaluation System). A current at 50 nA ($\pm 10\%$) was injected at a high frequency of 5000 Hz through a pair of contacts placed on the forearm, approximately 2 inches distal from the elbow and the impedance of the skin-electrode interface was measured. A frequency at 5000 Hz was chosen to prevent small changes in the shape and size of the contact from affecting the complex impedance as per prior research in this area [94]. The forearm was kept at rest to prevent the action potentials from muscle contraction, from corrupting the impedance measurements. By looking at the complex impedance graph in Figure 3.6.a, we can see that the impedance properties of titanium, WW45 and WW46 are very similar to each other. This matches the similarity in SNR as well and shows that complex impedance provides a more accurate insight into the material's electrical properties. However, if we try to plot the complex impedance versus SNR, we can see that there isn't a very large resolution on the distribution of materials that conduct some form of EMG signals and they seem to be clumped together. However, the one material that did not give any EMG signal at all is starkly separated from the others. Thus, we could use complex impedance as an initial metric to determine whether a given material is capable of physiological signal conduction or not. It does not however, provide an insight into the quality of the signal acquired. Complex impedance measurement is extremely valuable when creating novel conductive materials for electronics, as complex impedance provides a simple metric for determining if the doping is sufficient for conducting physiological signals.

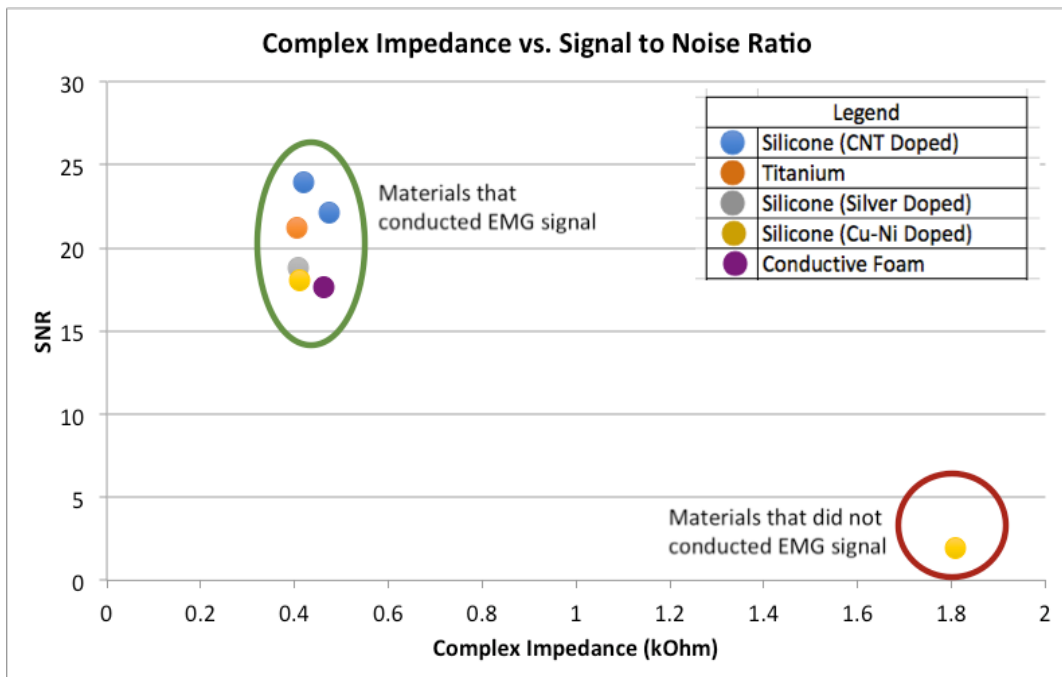
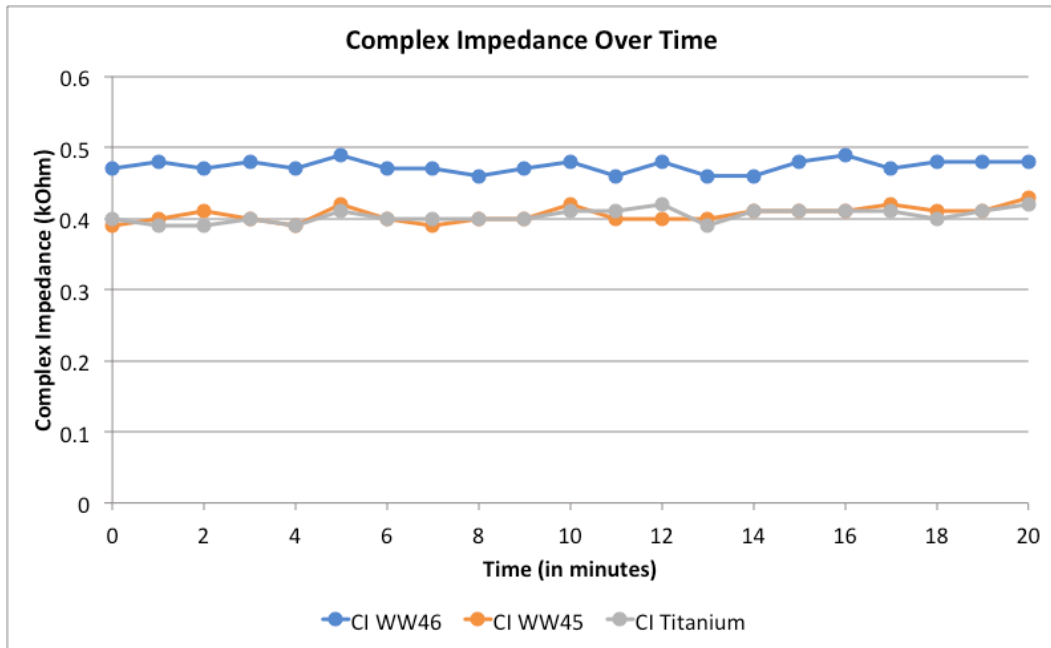


Figure 3.6.a: Complex Impedance over time, Figure 3.6.b. Complex Impedance versus Signal to Noise Ratio. As is evident from Fig. 3.6.a, the complex impedance curves of the three materials shows an increased similarity to the SNR graph in Fig 3.4.b. They separate out at levels in the complex impedance graph, proportionally inverse to their arrangement in the SNR graph. Thus, complex impedance may characterize these materials better. However, when the complex impedance of a diverse set of traditionally non-conductive materials was plotted against the SNR, the graph did not provide much information on the nature of relationship between the two apart from a stark clustering in materials that did conduct EMG signal in one part of the graph, with complete separation from materials that did not conduct EMG signal at all.

3.5.2.4. Skin Electrode Complex Impedance Variation for Long Term Measurement and Comparison with SNR

In order to quantify the quality of signal acquired through the electrode contacts by using electrical measurement, Skin Electrode Complex Impedance (SECI) measurements were made by placing the material on a human forearm and measuring the impedance of the interface. SECI thus allows us to quantify the behavior of the material when put in contact with skin. Measurements were again made at 5000 Hz to eliminate the effects of difference in shape and size of the contact and the interface.

Based on the graph given below in Figure 3.8, it was noted that the SNR variations were material dependent, while some had stable SNR values from the start of the data gathering session, other took time to stabilize and reach their peak value. This is similar to the SECI curves in which the materials that had stable SNR also had stable SECI values. For materials in which the SNR increased over time until the values reached stability, the SECI correspondingly decreased over time until it reached a stable value.

Intuitively, we can see a relationship between SECI and SNR such that when the SECI decreases, the SNR increases. A decrease in SECI results in lesser impedance to ionic current flow across the skin electrode interface thereby increasing the amplitude of the signal measured and thus improving the SNR. When SECI is plotted against SNR for all the different materials, we can see a linear relationship between the two. This linear relationship provides an insight into the nature of physiological signal obtained through a novel doped conductive material.

Based on our SNR calculations, we also saw that materials that provided SNR greater than 20 gave usable EMG signal with minimal baseline and distinct contractions. By identifying the SECI corresponding to an SNR of 20 on our SECI vs SNR graph in Figure 3.7, we can see that materials with a SECI lesser than 75kOhm gave EMG signals that were usable for myoelectric control.

Thus, by establishing this relationship between SNR and between SECI, we now have a universal electrical metric to determine not only if a traditionally non-conductive,

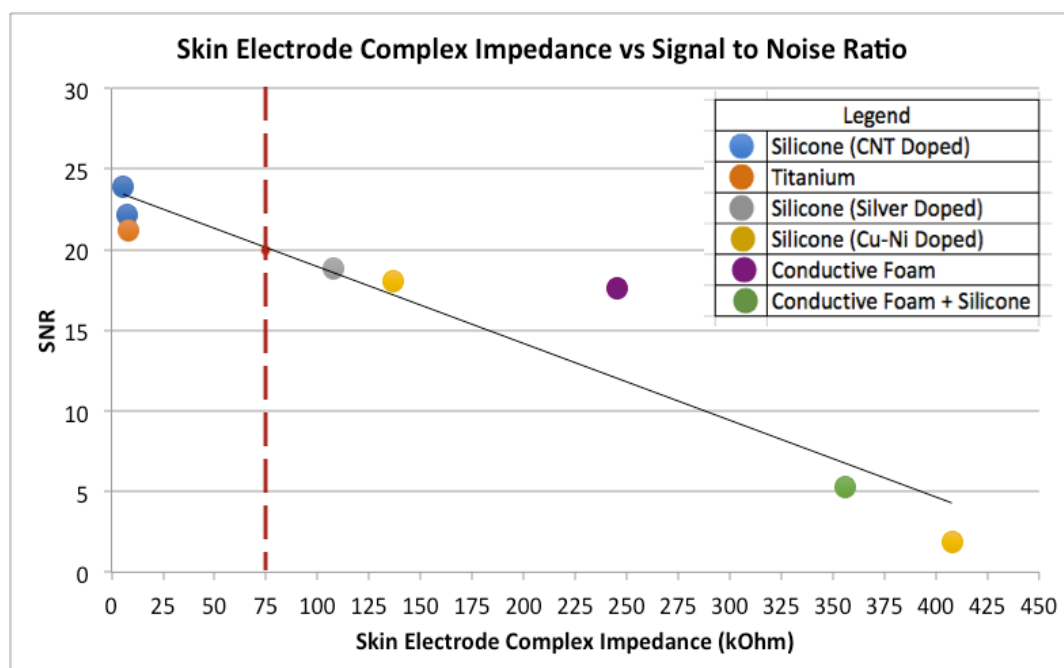


Figure 3.7: SECI versus Signal to Noise Ratio. In this graph, the mean values of the stable SECI for all 5 subjects were plotted against the mean of the stable SNR values for all 5 subjects. We can see a clear linear relationship between the two. This graph thus allows us predict the quality of the signal that could be obtained from a given contact material, based on a more universal, repeatable and stable metric i.e. SECI. In addition, a signal with an SNR of 20 is usable for myoelectric control of prosthesis. This corresponds to a SECI value of 75kOhms. Thus, if materials are designed such that their SECI is less than 75 kOhms, they should conduct high quality physiological signals.

doped material is suitable for physiological signal acquisition but also enables us to predict the quality of signal coming from it.

3.5.2.4. Comparison of Settling Time of Different Materials

Another interesting observation from this study is the effect of the skin electrode complex impedance of materials on their settling time. Typically, the human skin has complex impedance in the order of a few MOhms, while materials like metals have very low impedances in the order of a few Ohms. When metal contacts such as those made out of titanium are used for signal acquisition, it takes several minutes for the signal baseline to reduce to minimum and EMG amplitude to reach maxima. This could be attributed to the process of ionic equilibrium at the skin electrode interface, which takes time if the two materials have significantly different impedances.

When we look at the SECI and SNR graphs of the different materials over time (Fig. 3.8), we can see that materials like WW45 have very stable curves from the beginning of data gathering itself, i.e. they require almost no time to settle. The SNR values are high and the SECI values are intermediate to that of pure metal and skin, <75kOhms. Thus, if new materials are developed such that the SECI is intermediate to that of metal and skin, the material settles faster against the skin and will eliminate the need for skin preparation.

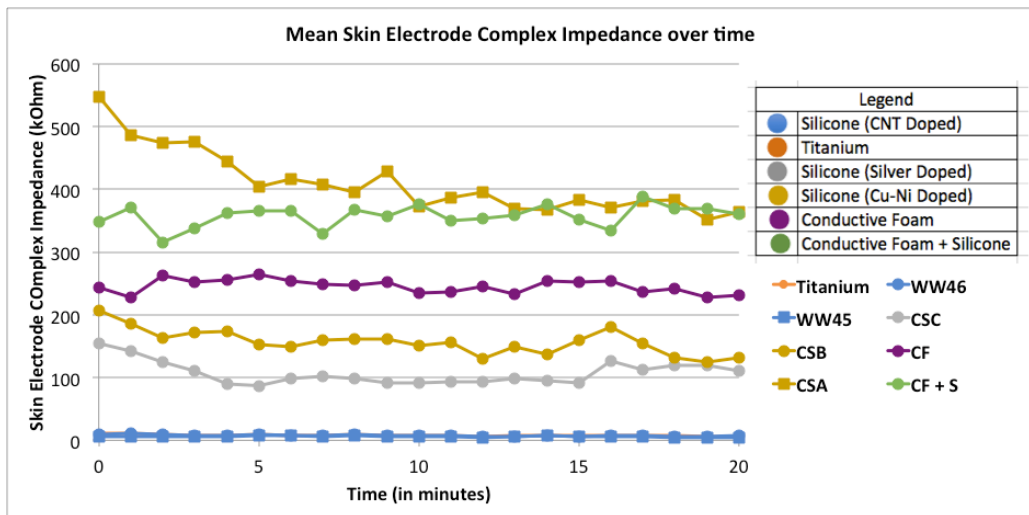
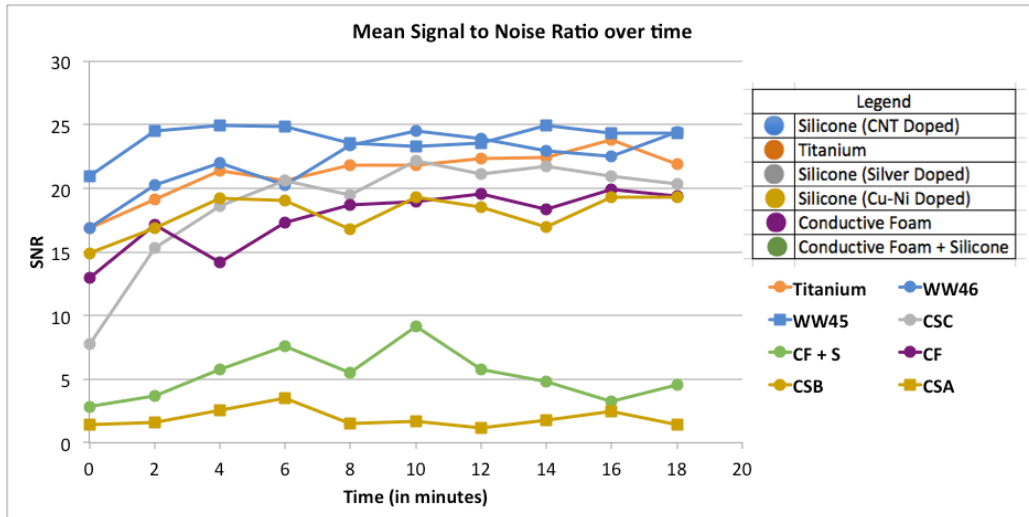


Figure 3.8.a: Signal to Noise Ratio over time, Figure 3.8.b. SECI over time, as we can see from the graphs, almost all the materials reach stable impedance and stable SNR values after a delay of few minutes. However, when we look at WW45, the material corresponding to the curve at the top of the SNR graph, we see that it “settles” very quickly, in under 2 minutes. Similarly, from the SECI graph, we can see that WW45 has a stable impedance value from the very beginning. This is very valuable in myoelectric control of prosthesis, since the faster a material reaches stability with minimal intervention, the easier it is for the user to generate EMG signals to control a prosthetic hand. If materials are designed keeping in mind impedance matching with the skin and the processing electronics, it will do away with the need for skin preparation and will make the electrode skin interface more stable.

3.6. Summary

1. Conductivity is not a good metric for characterizing doped traditionally non-conductive materials for physiological signal acquisition.
2. Complex impedance is a good metric for determining if a given material is capable of physiological signal conduction or not. However, it does not have a linear relationship to SNR.
3. SECI is inversely linearly related to SNR, thus providing a uniform measurement for comparing different materials and determining their ability to conduct physiological signals. Materials with SECI less than 75 kOhm will provide signals with high amplitude and low baseline noise.
4. There is a reduction in settling time by using materials with SECI intermediate to that of metal and skin.

CHAPTER 4

4. Chapter 4: HD EMG for Myoelectric Control

Developments in the field of flexible electronics have been both innovative and rapid. Flexible electronics, including sensors and circuits, offer many advantages outlined earlier. The possibility of incorporating such an electronics technology within a silicone liner for myoelectric signal acquisition use seems more appealing than rigid electronics. We previously outlined that location dependency of electronics within a liner as well the donning it in the exact way every single time is not practical. To solve this problem, we developed an electronic solution of incorporating flexible electronics within a liner. This is where HD EMG can provide a practical solution. The ability to gather data from 128 different spots ensures that no matter how the liner is worn, there will always be an electrode contact over the desired myoelectric signal source (muscle group) to acquire EMG data from it. This chapter describes how HD EMG can be used for more robust myoelectric signal acquisition as well as for the advancement of myoelectric prosthesis.

4.1. Relevance of HD EMG to Myoelectric Control

Traditionally, EMG acquired through specific locations on the residual limb are used for myoelectric prosthetic control. This requires the electrodes for EMG acquisition to be attached to the exact same spots every single time, which is done by embedding them in the custom designed rigid prosthetic socket that fits on the residual limb in a single specific way. However, this method often affects signal fidelity due to movement of the socket and electrodes under loading conditions as well as due to

electrode lift off. It can also cause abrasions and sores on the residual limb due to the rigid nature of both the socket and the electrode. Discomfort and unreliable prosthesis control is also one of the leading causes of prosthesis abandonment across the world.

Body powered prosthesis, face similar problems. In order to make the use of body powered prosthesis more comfortable, a silicone liner that fits snugly on the residual limb is worn prior to the socket and prosthetic arm. Not only does such a liner provide a cushioning effect, it also helps in attaching the prosthesis with greater stability to the residual limb.

Current myoelectric prosthesis system cannot use a silicone liner. This is because the liner is non-conductive and the electrodes are embedded in the socket, thus there is no path of conduction between the skin and the electrode. One way to overcome this problem is to incorporate the electronics within the silicone liner in a location independent manner.

The location specificity of EMG electronics can be overcome by the use of HD EMG in which more than 8 channels of EMG data are acquired simultaneously and are used to visualize muscle activity maps. HD EMG algorithms have been written to eliminate effects of electrode shift [95 - 97] as well as channel dropout to improve the skin electrode interface. Very recently, studies have focused at using HD EMG for myoelectric prosthesis control. Currently research attempts are focused at controlling robotic hands with greater than 2 Degrees Of Freedom (DOF) [130].

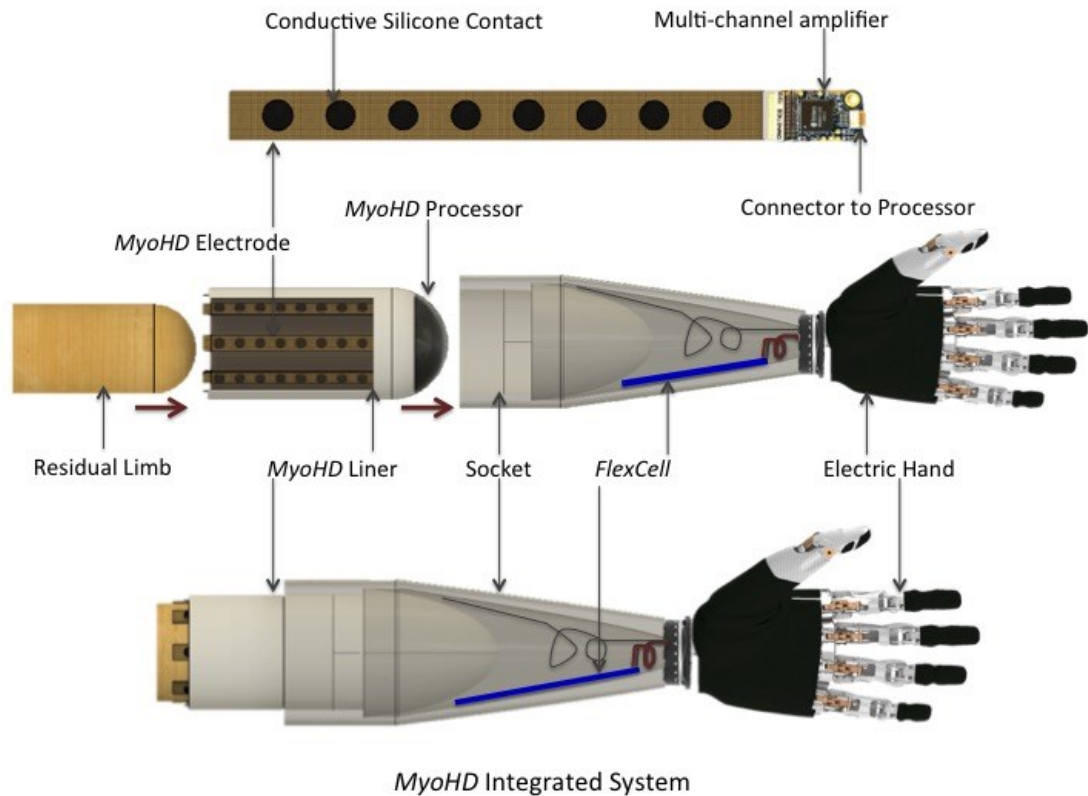


Figure 4.1. Vision of the HD EMG system with flexible silicone electrode contacts. The MyoHD system uses flexible silicone contacts arranged in a 128 channel HD configuration integrated within a silicone liner for generating muscle activity maps of the forearm using 128 channels of simultaneous EMG signals. This makes the signal acquisition hardware location independent, no matter how the conductive liner is worn; there is always an electrode at every point of the forearm.

There is thus an immense opportunity for HD EMG based muscle activity maps to be used for prosthesis control. Some of these areas include myosite localization for prosthesis fittings, proportional control, fine motor control and spatio-temporal study of onset and decline of a muscle contraction. Moreover, HD EMG electrode arrays can be incorporated within the liner itself, allowing a better skin electrode interface in a location independent manner. In order to make use of HD EMG liners a fool-proof solution, there also needs to be a way to detect the position of the liner on the upper

limb automatically, which also adds to the immense potential for myoelectric prosthesis research using HD EMG.

4.2. Hardware Setup for HD EMG

4.2.1 Design of the HD electrode arrays and processing hardware

The hardware setup for HD EMG acquisition (Figure 4.2) comprised of custom designed flexible electrode arrays comprising of 32 (4 rows and 8 columns) and 128 (8 rows and 16 columns) contact points in two different sizes: 10mm diameter contacts with 15mm Inter-Electrode Distance (IED), and 5 mm diameter contacts with 15mm IED which is standard for HD EMG studies in research today [95 – 97]. It has dimensions of 12 cm x 25 cm based on the average forearm dimensions of the median male and female population [131]. The electrode array is made of out Flex PCB and has 128 contact points. The array is a double-layered flexible sheet. The first layer consists of the electrode contacts and the connections to the connector pin-out and the second layer is a crosshatched ground plane. Use of a crosshatched ground plane eliminates the presence of eddy currents which cause noise interference in the signals due to the induced magnetic fields. Each array is separated into 4 different 32 channel arrays. The design of the electrode array sheet allows each of the 4 sections to be cut out and placed on the arm separately for better conformity. Each array connects to a 32-channel amplifier board and ultimately leads to a processor that simultaneously processes all 128 channels of data. The Intan RHD2000 Evaluation System [128] was used with four different 32-channel amplifiers to acquire 128 channels of high - density monopolar signals.

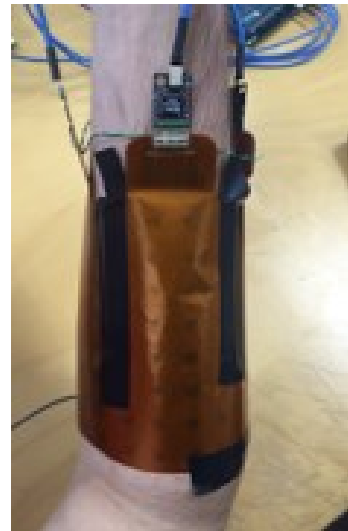
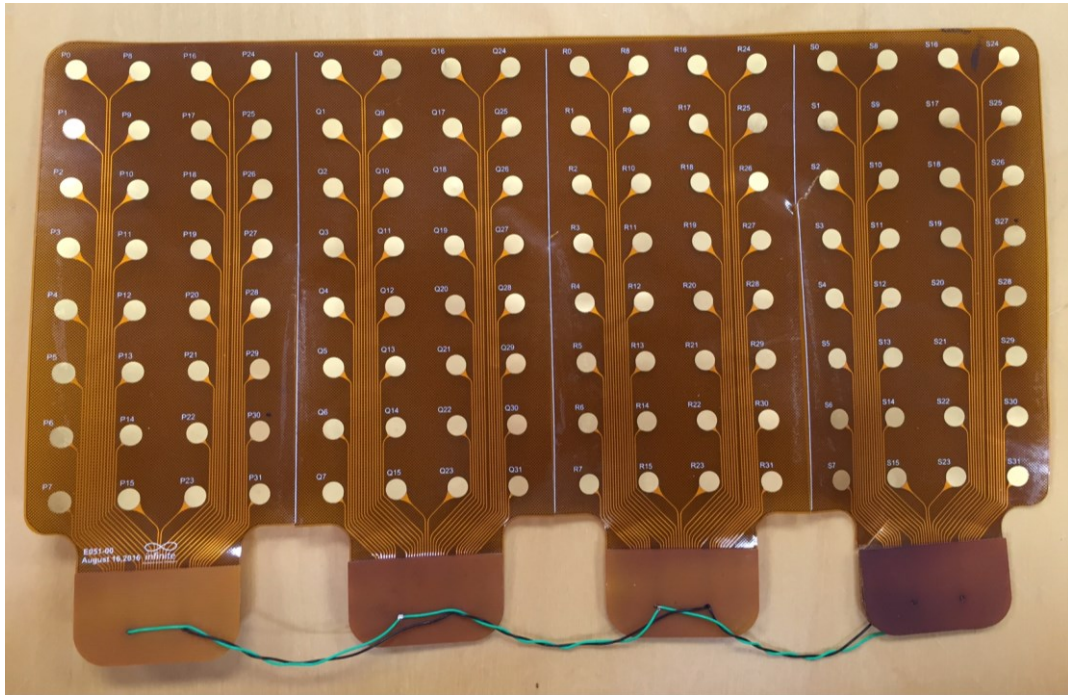


Figure 4.2. Hardware for HD EMG. The image on top shows a HD array used for HD EMG acquisition. The electrode array is made of out Flex PCB and has 128 contact points. Each array is separated into 4 different 32 channel arrays. Each array connects to a 32 channel amplifier board and ultimately leads to a processor that simultaneously processes all 128 channels of data. The figures on the bottom show the array being used on a trans-humeral amputee and on an able bodied individual.

4.2.2. Evaluation of the Electrode Array

4.2.2.1. Experimental Setup

The electrode array was attached to the forearm of an able bodied subject such that it was 5 centimeters distal from the elbow and wrapped around the forearm completely.

The ground and reference electrodes were connected to the epicondyles on the elbow for minimizing baseline noise. The subject performed Wrist Flexion, Wrist Extension and Hand Rest motions and 128 channel data was acquired for the same.

4.2.2.2. Signal Pre-processing

The gathered data were imported into MATLAB. The signals were band pass filtered between 30Hz and 500Hz by a 10th order Butterworth High-pass and Low-pass filter respectively. An Infinite Impulse Response (IIR) comb filter at 60 Hz was implemented to remove powerline noise as well as the resonant frequencies associated with the same. The data were reorganized to resemble the arrangement on the electrode array and an FFT was performed on each of the 32 or 128 channels of data (in two separate designs and experiments) to view the frequency spectrum and to ensure that noise was eliminated.

4.2.2.3. Fast Fourier Transform of the Monopolar Signals

The FFT of the signals from the HD EMG array, before and after filtering. Monopolar data like that of the HD EMG is very susceptible to motion artefact as well as to the

60 Hz powerline noise and its resonant frequencies. The same is evident in the Figure 4.3 below, the peaks in the FFT occur at multiples of 60 Hz. Following the implementation of an Infinite Impulse Response Comb Filter centered at 60 Hz, as well as implementation of the low pass and high pass filters as mentioned above, all noise interference is removed and the signal is used for further processing.

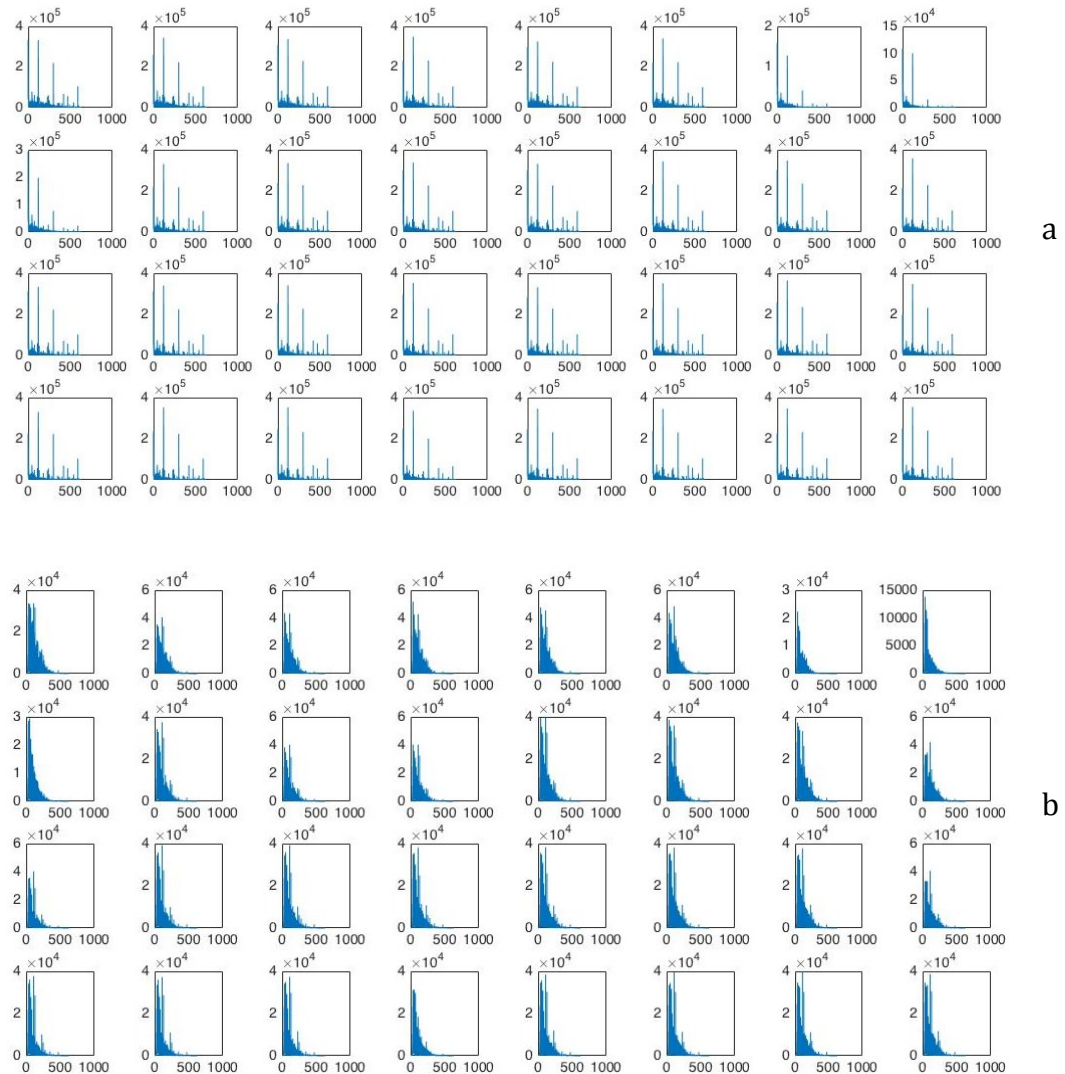


Figure 4.3: Fast Fourier Transform on the Monopolar Signals, before (a) and after (b) filtering.

4.3. HD EMG Muscle Activity Maps

As mentioned in the previous sections, HD EMG has traditionally been used to study the propagation of localized action potentials by representing the action potentials at each spot in a two-dimensional spatial image in which the color of each spot indicates the amount of activity [98 - 99]. The same principle can be applied to HD EMG maps for myoelectric control. Instead of viewing them as 128 channels of one-dimensional signal, the signal from each channel can be reduced to a point value reflecting the activity at the point and plotted as a two-dimensional image of muscle activity of the forearm. This can be done using time domain based feature extraction methods such as Root Mean Square (RMS) and Mean Absolute Value (MAV). These images can now be used for myoelectric control, thus converting a traditionally signal processing problem into an image processing one.

4.3.1. Creation of Muscle Activity Maps

4.3.1.1. Experimental Setup

The experimental setup was identical to that in Section 4.2.2.1.

4.3.1.2. Signal Preprocessing

The gathered data were imported into MATLAB. The signals were pre-processed based on the algorithm that has been outlined and verified in Section 4.2.2.2 and 4.2.2.3.

4.3.1.3. Creation of Muscle Activation Map

The amplifier channel data from the able-bodied data set were converted to Root Mean Square (RMS) as well Mean Absolute Values (MAV) following pre-processing. Both RMS and MAV are two different time domain based feature extraction methods based on the amplitude of the signal [100].

RMS: Root Mean Square value of a signal $x(t)$ is calculated as the square root of average of squared value of the signal in a given analysis time window with N samples. x_k is the k^{th} sample in this analysis window, Mathematically,

$$\text{RMS} = \sqrt{\frac{1}{N} \sum_{k=0}^{N-1} x_k^2} \quad (\text{Eq. 4.1})$$

MAV: This feature is the mean absolute value of signal x in an analysis time window with N samples. x_k is the k^{th} sample in this analysis window. This is also called normalized 1 norm of a signal or vector. Mathematically,

$$\text{MAV} = \frac{1}{N} \sum_{k=1}^N |x_k| \quad (\text{Eq. 4.2})$$

Studies have shown that the amplitude of the EMG corresponds to the intensity of the contraction; hence this is a good metric to look at the muscle activity [101]. This data set was then represented as an 4×8 matrix for a 32 channel system and as a 8×16 matrix for a 128 channel system respectively, corresponding to the electrode contact positions on the limb. The matrix was normalized by the maximum RMS or MAV

value across all channels. The same process was repeated for the test data set to generate a 4 x 8 or 8 x 16 matrix with the RMS or MAV values as the pixel at each ij^{th} position.

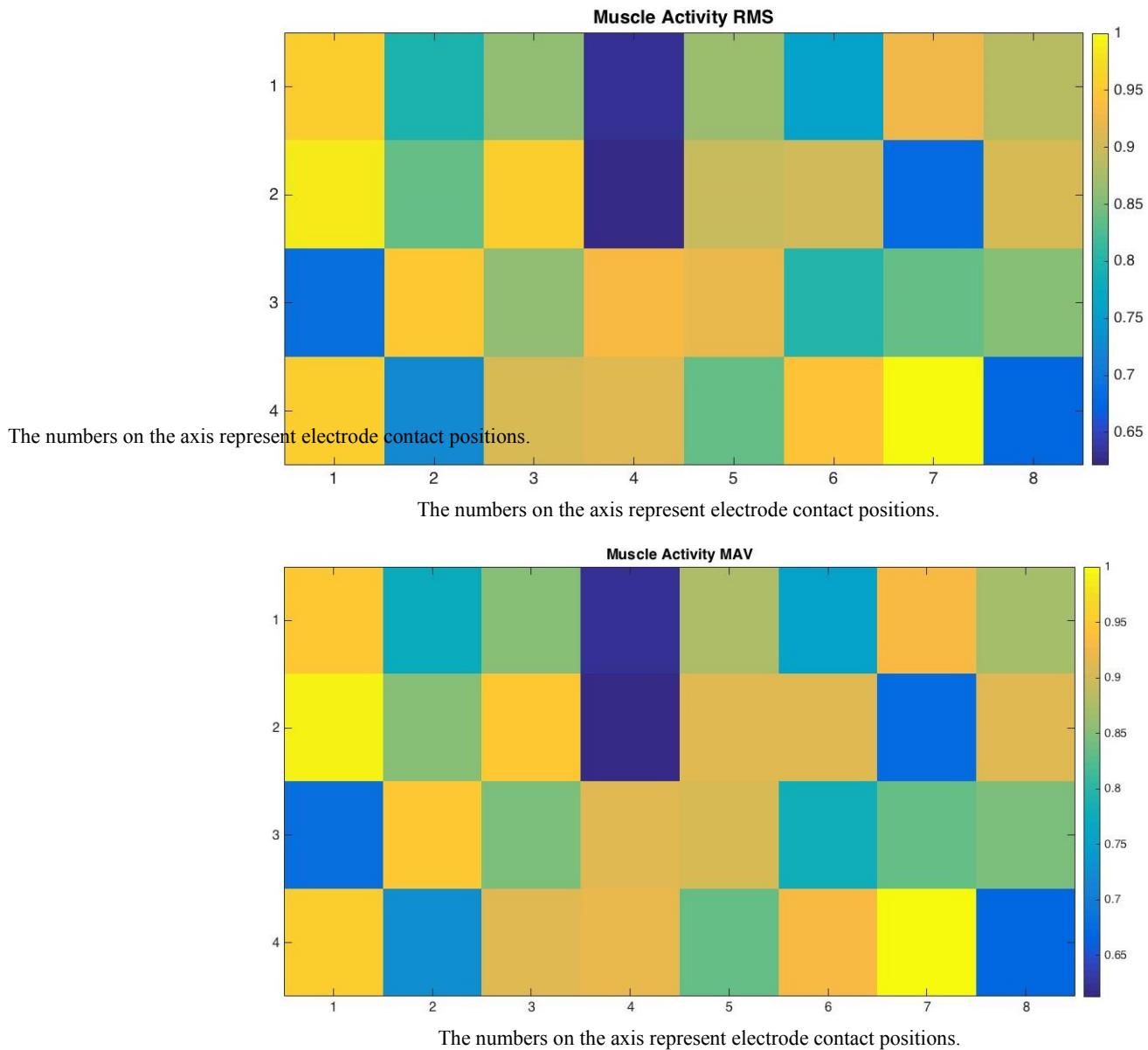


Figure 4.4. RMS (a) and MAV (b) Activity Maps. The above images show the activity maps by the application of two different time domain feature extraction techniques. We can see that both are almost identical, except for slight variations in areas that are intermediate to the extreme values.

The maps obtained using both RMS and MAV measures were almost identical, the variations occurred in regions intermediate to the maximum and minimum values.

(See Fig 4.4)

4.3.1.4. Removal of Noisy Channels

The baseline noise recording was used to identify noisy channels and to account for them in the subsequent processing. The RMS of the noise on all channels was calculated as well as the mean and standard deviation of the RMS values. Threshold was set to $\text{mean} \pm 2 \cdot \text{s.d.}$, and all channels having an RMS greater than this value were noted as noisy.

4.3.1.5. Muscle activity maps

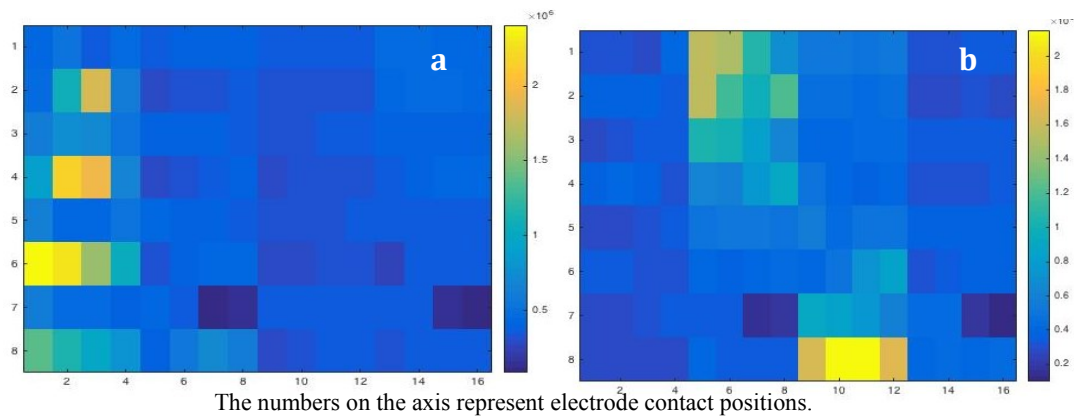
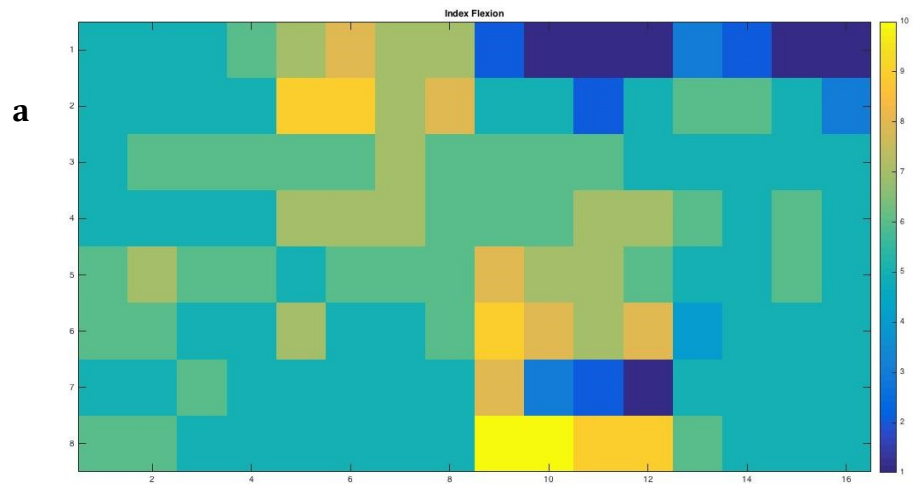
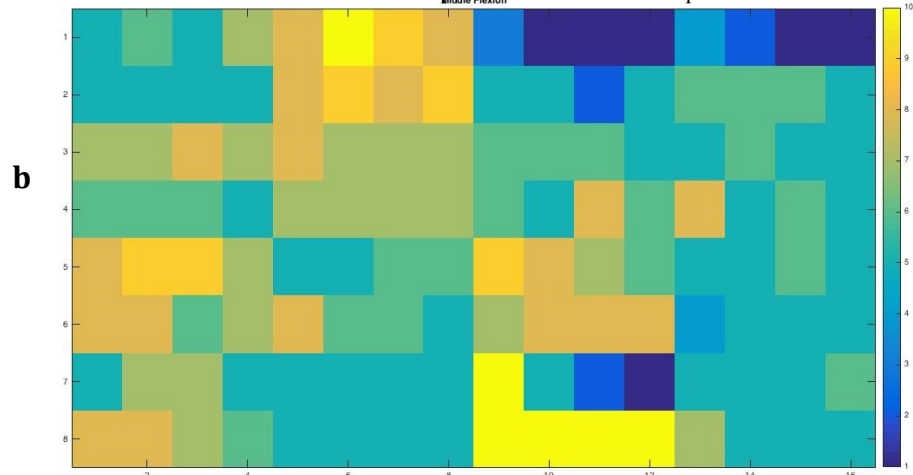


Figure 4.5. MAV Muscle Activity Maps for Wrist Flexion (a) and Wrist Extension (b) respectively (128 channels). The areas of activation are distinctly visible and are in antagonistic areas, anatomically identical to the placement of flexor and extensor muscles.

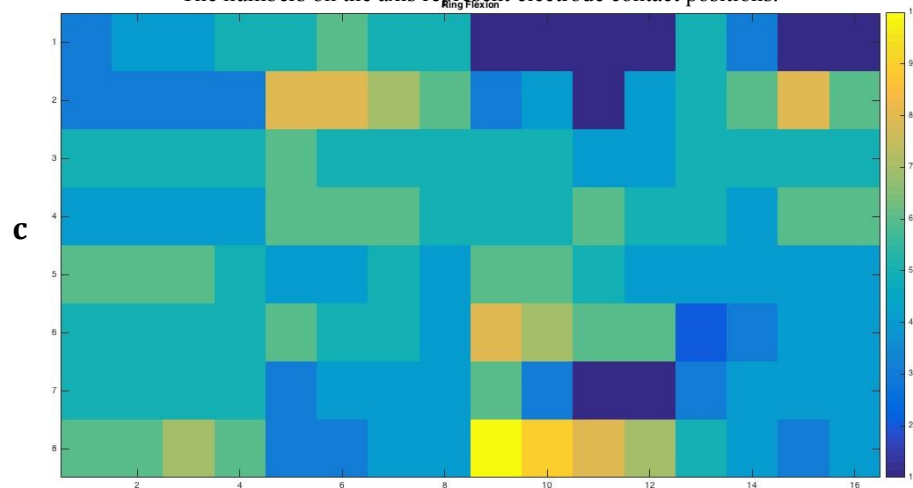
The obtained muscle activity maps based on the above algorithm were representative of the expected muscle activations for wrist flexion and extension. As in Figure 4.5, in wrist flexion, most of the activation observed was over the belly of the flexor muscle and minimal activation was observed over the extensor muscle group. Similarly, for extension, minimal activation as observed over the flexor muscle group and significant activation was observed over the extensor muscle group.



The numbers on the axis represent electrode contact positions.



The numbers on the axis represent electrode contact positions.



The numbers on the axis represent electrode contact positions.

Figure 4.6. Different finger flexion patterns, Index (a), Middle (b) and Ring (c). Visually, it is evident that the three finger flexion patterns obtained are very different from each other with distinct areas of activation. This could be used for fine motor control algorithms.

In addition to the traditional activation areas, additional activation areas could be identified for both flexion and extension. Activity maps for the respective finger flexion motions were also distinct from one another and in agreement with existing literature on the areas of muscle activation [102]. Some of these images are given in Figure 4.6.

The resolution between the muscle activity maps differed greatly between a 32 channel and 128 channel system as discussed in the next section.

4.3.1.5.1. Methods

An initial proof of concept of the system was implemented with a 32-channel system and the experiment was repeated again with a 128 channel system. We implemented a 128-channel system to overcome the resolution limitation of a 32-channel system. Data was gathered from three able bodied subjects and they performed Wrist Flexion, Wrist Extension and Hand Rest motions. Five trials were performed per movement.

In order to confirm repeatability of the movements, as well as to confirm the similarity in patterns between two movements, Mean Squared Error (MSE) was used to determine how closely related the two images were. MSE is a metric of image quality. It is applicable here since we are trying to quantify if the two images being studied are identical in terms of their data or if they differ then by how much. This is a normalized frobenius norm of the error matrix. Mathematically,

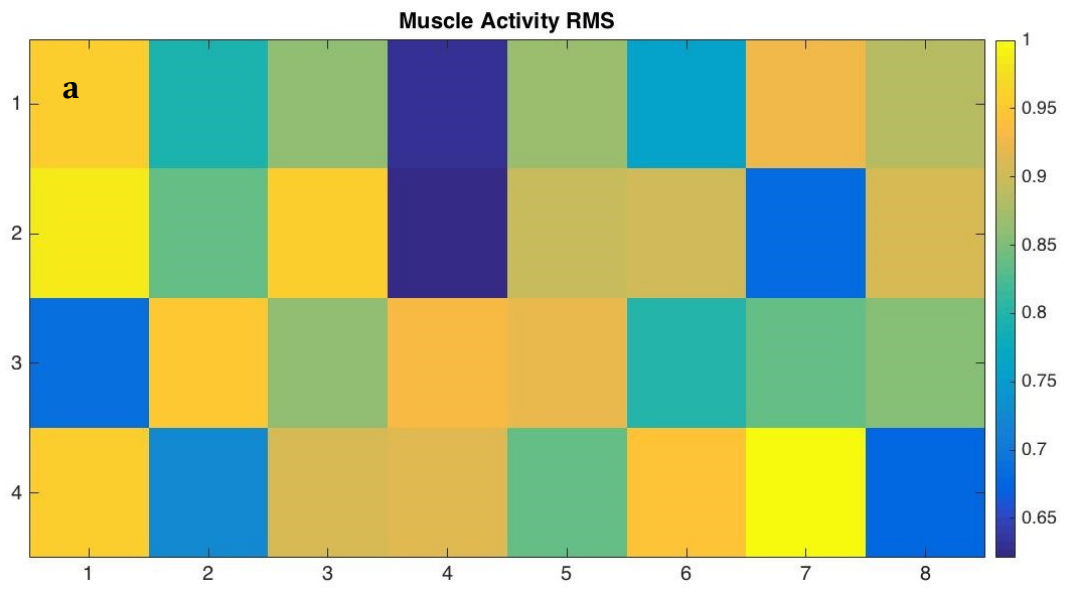
$$\text{MSE} = \frac{1}{MN} \sum_{n=1}^M \sum_{m=1}^N [g'(n, m) - g(n, m)]^2 \quad (\text{Eq. 4.3})$$

One problem with mean-squared error is that it depends strongly on the image intensity scaling. A mean-squared error of 100.0 for an 8-bit image (with pixel values in the range 0-255) looks dreadful; but a MSE of 100.0 for a 10-bit image (pixel values in [0,1023]) is barely noticeable [133]. However, since all our images are scaled between 0 – 255, we are unaffected by this problem.

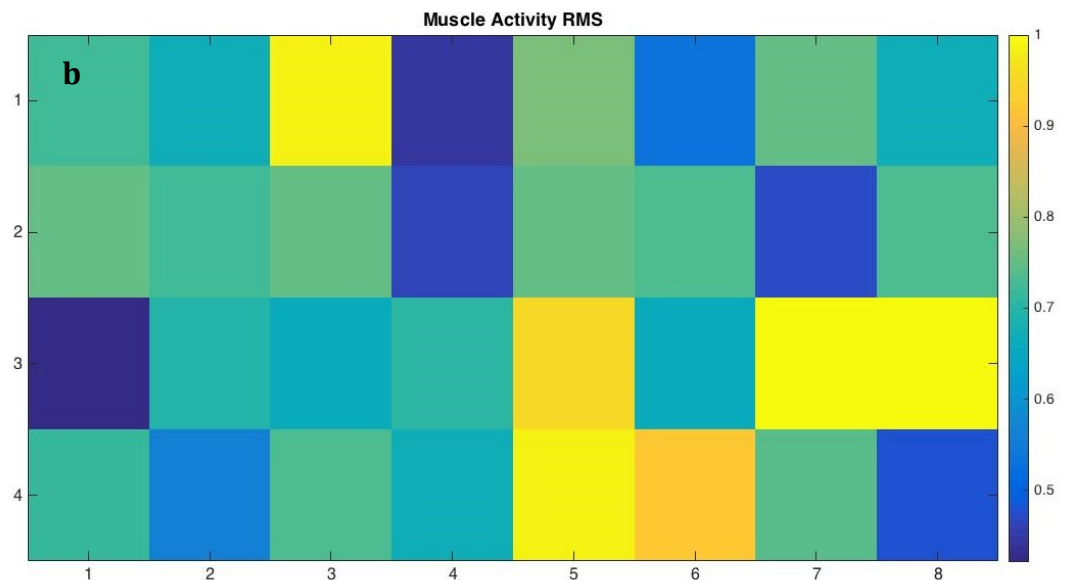
4.3.1.5.2. Results

4.3.1.5.2.1. 32 channel system versus 128 channel system

With a 32-channel resolution, the areas of muscle activation corresponding to wrist flexion and wrist extension tasks, respectively, are clearly identified (Fig. 4.7). Certain areas that show high levels of activity correspond to the flexor muscle and the extensor muscle. The 128-channel system provided greater resolution into the muscle as can be seen in the images seen in Fig. 4.8.

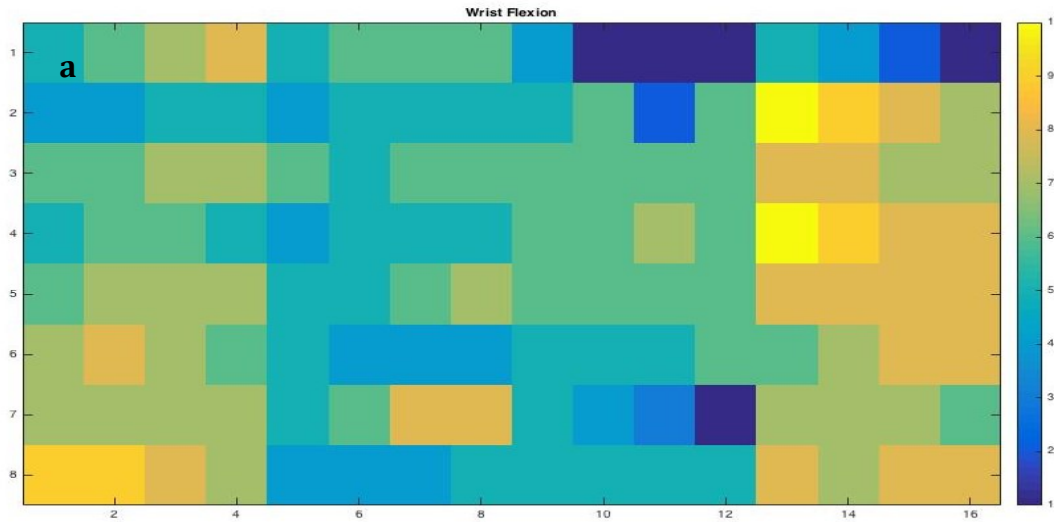


The numbers on the axis represent electrode contact positions.

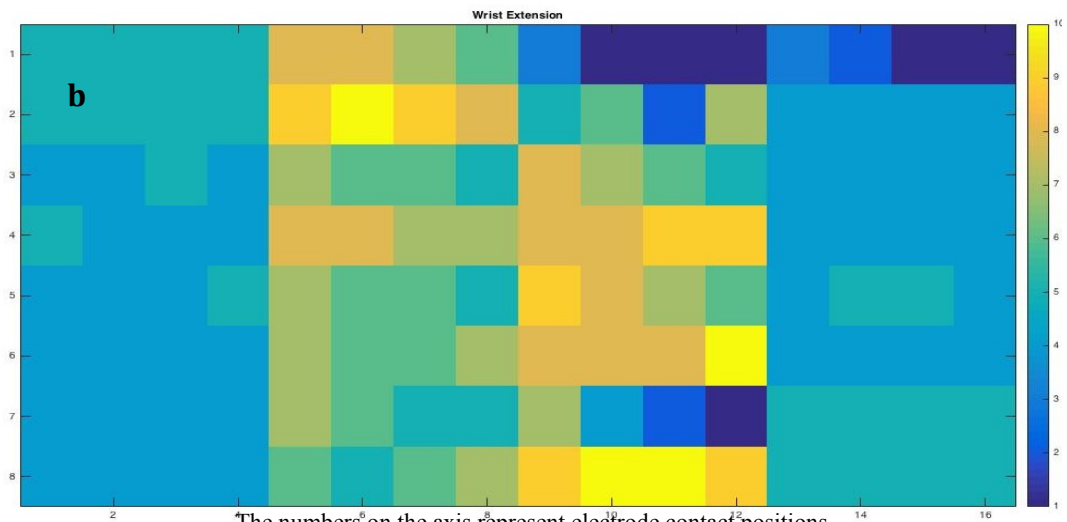


The numbers on the axis represent electrode contact positions.

Figure 4.7. 32 Channel HD EMG Maps. The images depict 32 channel based muscle activity patterns. The image on left shows an activity map for Wrist Flexion (a) and the one on the right shows Wrist Extension (b). As we can see, there is limited resolution on the muscle activity areas, limited distinction between the flexor and extensor muscles.



The numbers on the axis represent electrode contact positions.



The numbers on the axis represent electrode contact positions.

Figure 4.8. 128 Channel HD EMG Maps. The images depict 128 channel based muscle activity patterns. The image on top shows an activity map for Wrist Flexion (a) and the one on the bottom shows Wrist Extension (b). When compared to the 32 channel images, we can see greater distinction between regions as well as a better insight into localized muscle activity.

4.3.1.5.2.2. Repeatability of Muscle Activity Maps

The data from one subject is presented below in Table 4.1. The datasets A, B, C, D, E represent five different Wrist Flexion data sets acquired from a single subject with the electrode arrays placed on the forearm in the same position every single time.

Table 4.1. Mean Squared Error between 5 Wrist Flexion Muscle Activity Maps

Type of Motion	Trial Number	Dataset Combination	Mean Squared Error
Hand Flexion	1	A, B	0.0771
	2	A, C	0.1651
	3	A, D	0.1167
	4	A, E	0.0144
	5	B, C	0.065
	6	B, D	0.0441
	7	B, E	0.0499
	8	C, D	0.0066
	9	C, E	0.1515
	10	D, E	0.103
		AVERAGE	0.07934

The very low MSE indicates that the images are very minimally different from each other, in other words, they are repeatable. Thus the data acquisition hardware, as well as the algorithmic processing is working reliably and the muscle activity maps generated are usable for further studies.

4.3.1.5.2.3. Muscle alignment identification from muscle activity maps

The muscle activation patterns were mapped over an anatomically accurate image of the muscle distribution in the forearm and even it was observed that the areas of activation coincided with the major muscle belly groups involved in those particular movements.

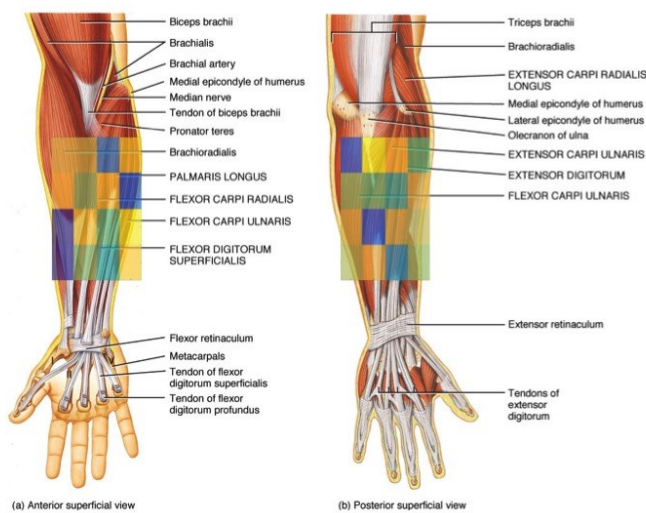
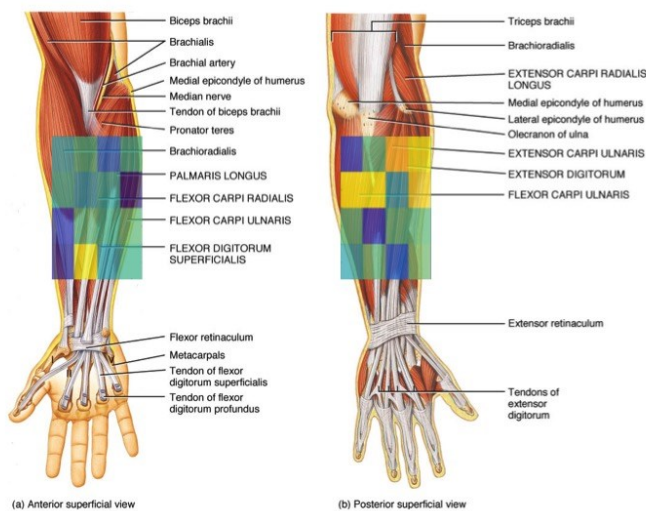


Figure 4.9. Muscle activity maps and forearm anatomy.

In the given figures on the side, the muscle activity maps are overlaid on the images of the forearm muscle anatomy.

Wrist Flexion



Wrist Extension

4.3.1.5.3. Discussion

4.3.1.5.3.1. 32-channel versus 128-channel system

The 32-channel system has several drawbacks. Lack of adequate resolution is evident. Even though the system provides very global EMG information, it is difficult to extract local, muscle-specific EMG information. In addition, the number of channels are not sufficient to generate distinction between different muscle activity patterns corresponding to different tasks or movements that use similar muscle anatomy. In order to get more detailed insight into the muscle activity patterns, scaling up to a 128 channels becomes essential.

With a 128-channel system, there was greater distinction between different muscle activation patterns to the extent that the signals can be used for proportional control as well as for fine motor control of the artificial electric hand as will be demonstrated in the next few sections.

4.3.1.5.3.2. Repeatability of Muscle Activity Maps

The average MSE for 10 different combinations of 5 datasets for hand flexion from a single subject is 0.07934. This low value indicates that the data acquired is repeatable in nature and hence can be used for further processing and analysis.

4.3.1.5.3.3. Muscle alignment identification from muscle activity maps

The muscle activity maps from both flexion and extension correlate well with the areas where the flexor and extensor muscle are on the forearm. It is possible that with additional research, we can use muscle activity maps to determine secondary muscle groups that are also used for a given hand motion.

4.4. Use of HD EMG in Myoelectric Prosthesis

4.4.1. Finger Identification and HD EMG Signal Acquisition for Proportional Control

4.4.1.1. Introduction

As seen from the previous sections, HD EMG maps give greater insight into muscle activation patterns for different hand motions. Moreover, it is possible to identify specific channels that provide the most distinct information for pattern recognition based control (Appendix, Section 6.1.1). These significant distinctions could potentially be used for discerning individual finger motions or a combination of finger motions. Moreover, the ability to study the temporal variation of a contraction may also allow for proportional control of the prosthesis.

4.4.1.2. Methods

As a proof of concept of this theory, we constructed HD EMG maps and ran them through a KL divergence algorithm (Appendix, Section 6.2) to determine if we could

algorithmically distinguish between rest, thumb flexion, index flexion and middle flexion. All motions were performed by an able bodied subject in three different trials.

4.4.1.3. Results

Upon taking the differential of the KL curves, we see that for each of the finger motion graphs, the curve representing the finger under consideration separated out from the remaining curves representing other finger motions very clearly. The point of separation occurs early in the motion and can be used not only to predict which finger is moving but the early onset allows the curve to be used for proportional control too.

The similarity between the different muscle movements is evident too, thumb flexion is very similar to the patterns for the hand in the rest position. Similarly, middle flexion uses very distinct muscle groups than the pattern/curve at rest and the same is evident in the separation of the pattern/curve from rest and the other fingers as well.

The KL curves are given in Figures 4.10 and 4.11.

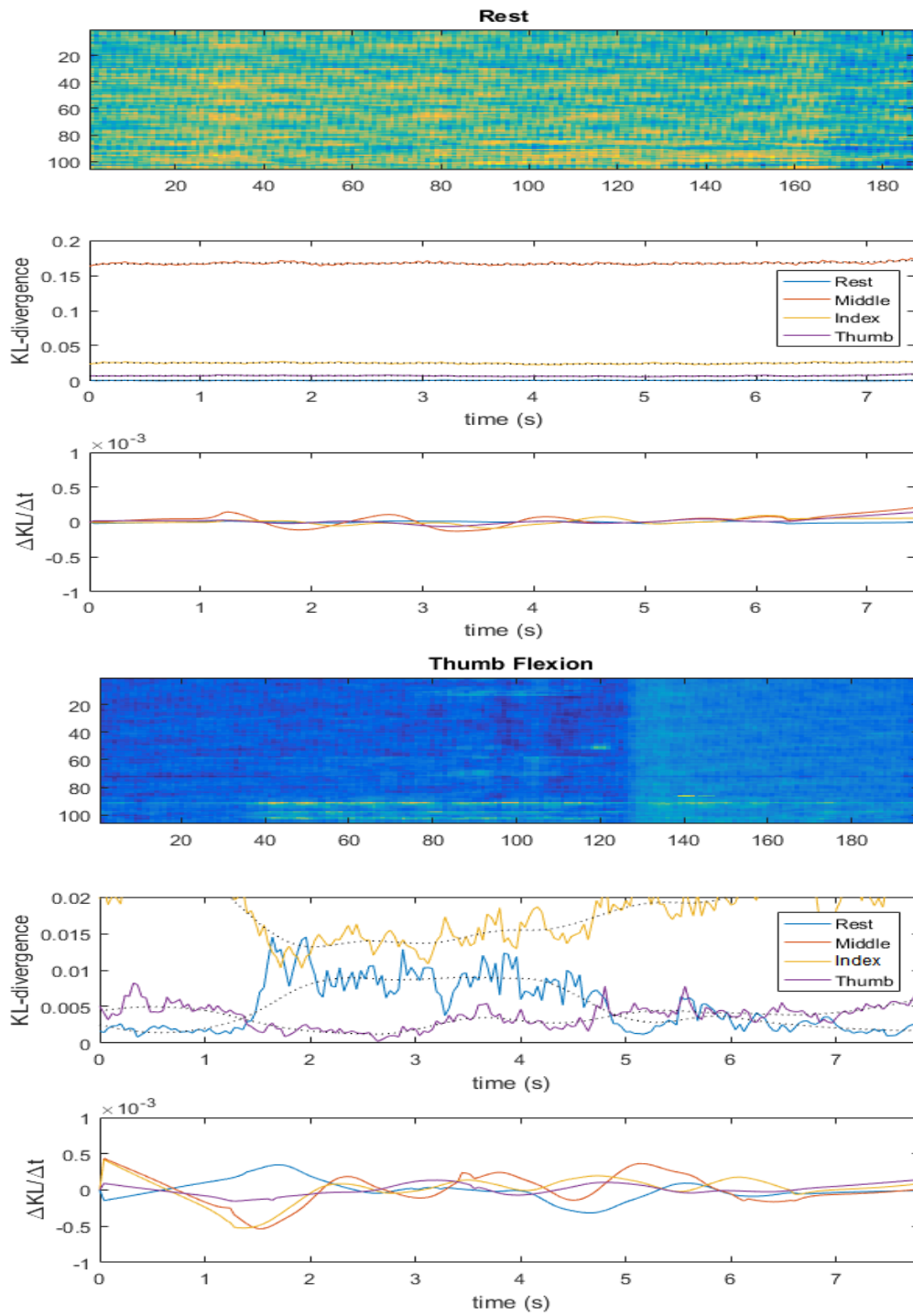


Figure 4.10. KL curves for hand at rest and for thumb flexion. In the above figures, we see that the KL curves separate out very neatly during thumb flexion. By looking at the differential of the divergence, we are able to determine the actual onset of the movement.

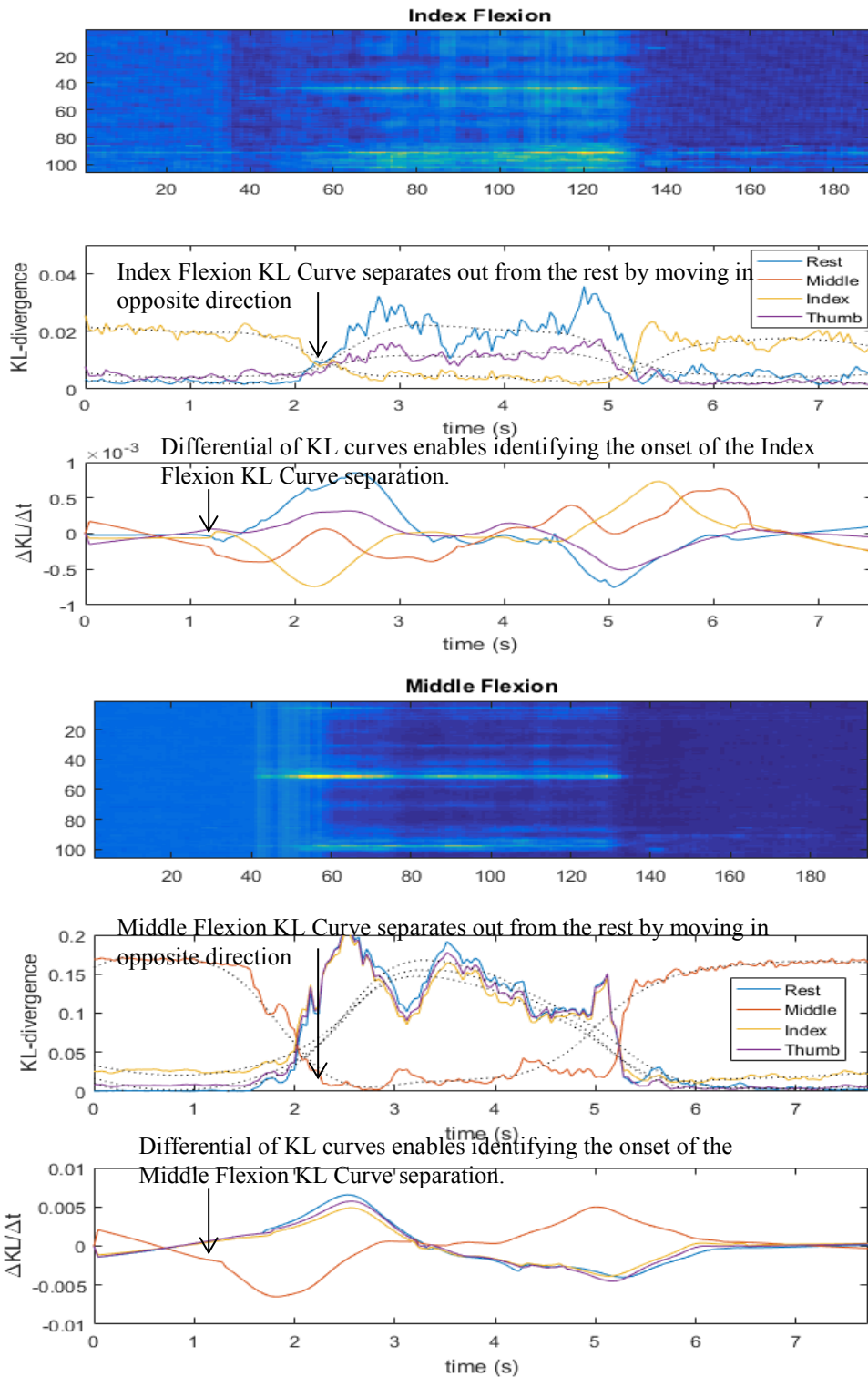


Figure 4.11. KL curves for index flexion and middle flexion. In the above figures, we see that the KL curves separate out very neatly for each of the movements thereby allowing us to identify which finger motion is being performed.

4.4.1.4. Discussion

Based on the data gathered and the K-L Divergence graphs given in Figure 4.10 and 4.11 not only are we able to determine which finger is being moved, we are also able to identify its onset early into the contraction. With greater research and evaluation on a larger dataset, the preliminary results in this section could be validated to become one of the first approaches in finger decoding and proportional control of prosthesis using HD EMG.

4.4.2. Time Varying Mapping of a Muscle Contraction from Onset to Decline

4.4.2.1. Introduction

The study of muscle activity is interesting and allows us to understand the nature of propagation of EMG signals from the surface of upper and lower limbs. This is important for multiple reasons. The direction of propagation of muscle signals helps in better alignment of EMG electrodes in a prosthesis. This is particularly important for amputees since post amputation, their muscle alignment and muscle activity can differ significantly from traditional anatomy. Study of muscle contractions can also facilitate better and more natural control of prosthesis by controlling an electric hand proportionally to the stage of the contraction itself.

4.4.2.2. Methods

We recorded 128-channel muscle activity from the entire forearm of an able bodied subject for a hand flexion from the beginning of the contraction to the end. The 128-channel signals acquired over a 10 second interval were windowed into 250 millisecond time intervals. Each windowed signal channel was converted into a muscle activity map by the protocol mentioned in section 4.3.1.3.

4.4.2.3. Results

Figures 4.12 – 4.14 show the images of the contraction evolving over time i.e. onset, maximum contraction and decline. We observe that when the muscle is at the maximum contraction, the activity maps alternate with high and low bursts of activity.

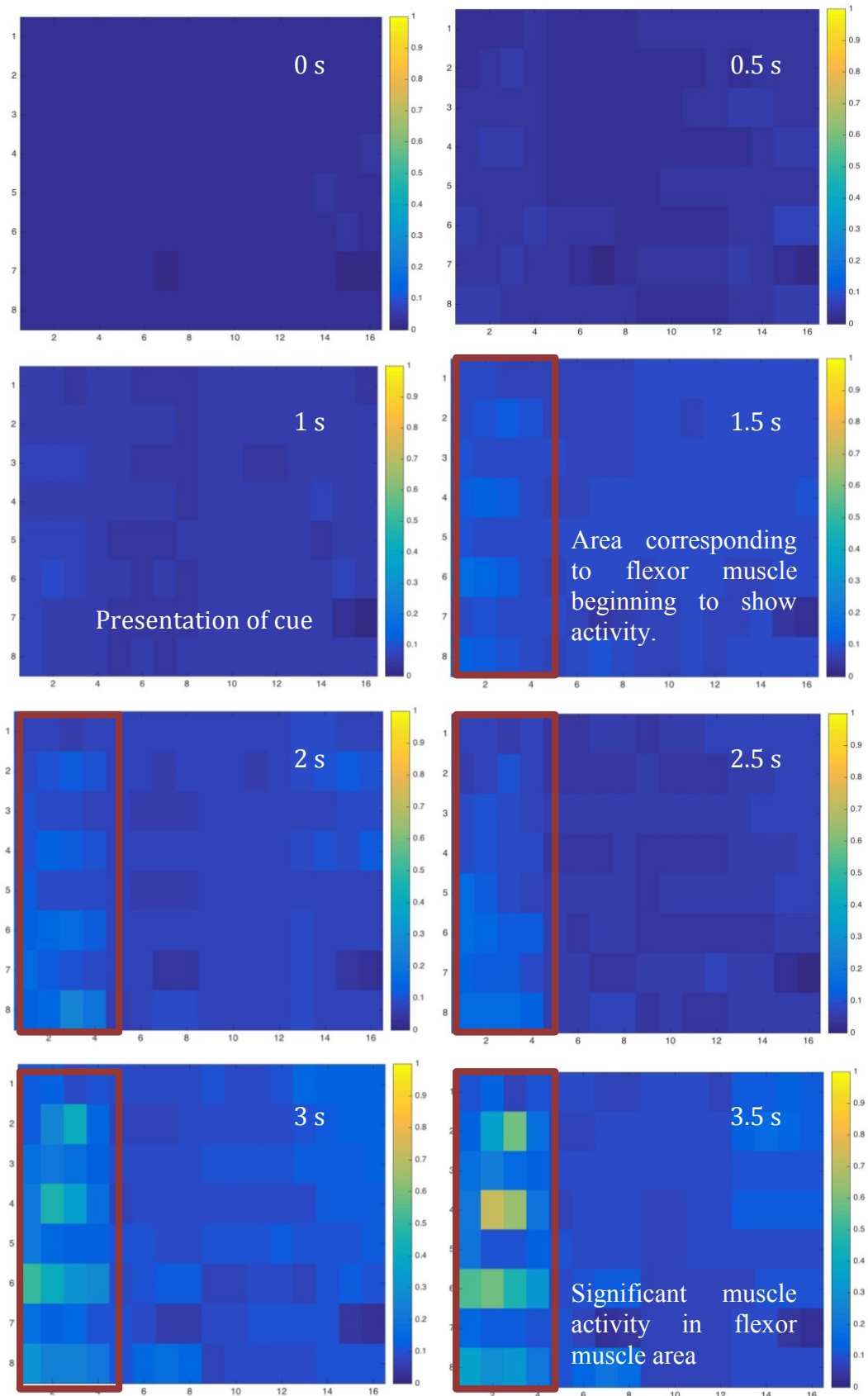


Figure 4.12. Onset of Contraction. The above maps show the onset of contraction in a flexor muscle during hand flexion. The onset of a contraction is fairly gradual, with muscle activity increasing over the bulk of the muscle over time. The cue was presented at 1 second.

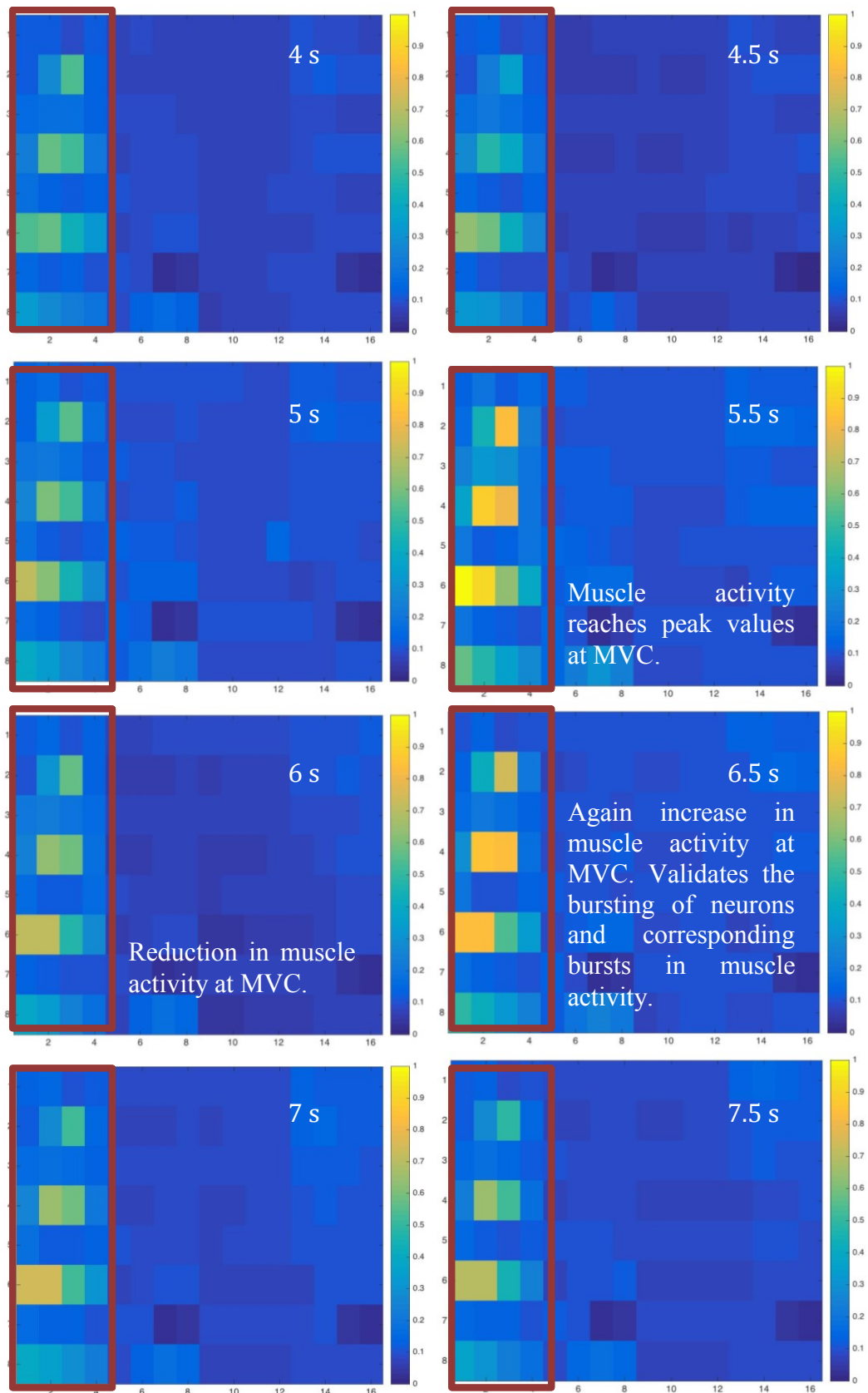


Figure 4.13. Peak Contraction. The above maps show the stable contraction period in a flexor muscle during hand flexion. The bursting of muscle activity is clearly visible it correlates with the traditional neuronal bursting at the neuromuscular junction as per literature.

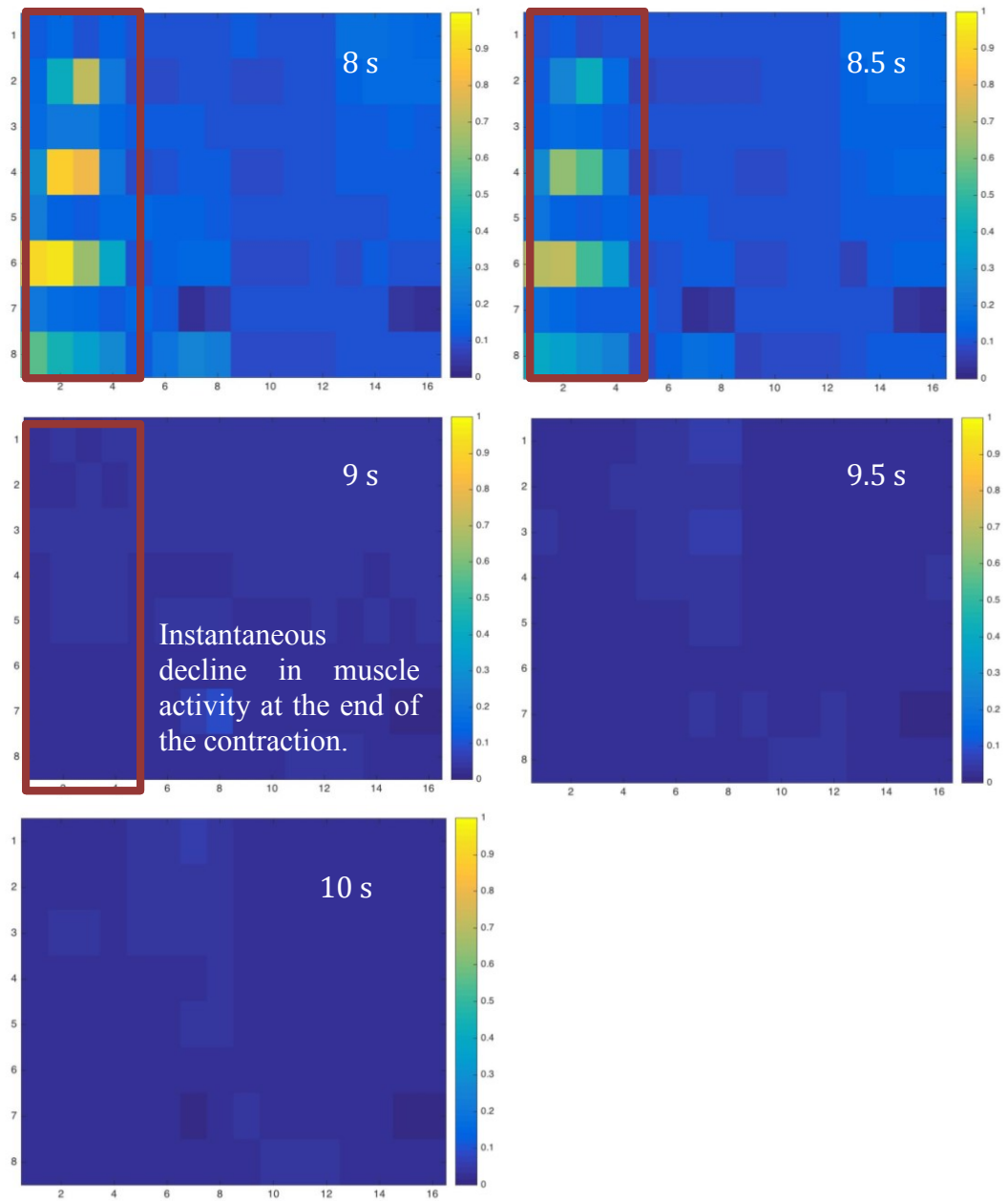


Figure 4.14. Decline of Contraction. The above maps show the decline of contraction in a flexor muscle during hand flexion. The decline is pretty quick; muscle activity reduces to almost negligible within a few seconds.

4.4.2.4. Discussion

The spatio-temporal maps also correspond to specific time frames in the contraction and give us an interesting insight into multiple aspects:

- a. The order of muscle activation for a given contraction
- b. The ability to predict which stage the contraction is in
- c. Using the above two, we should now be able to implement finer motor signal decoding and, subsequently, proportional control of the hand by algorithmically determining which fingers to move and by how much.

Moreover, we speculate that the bursting observed at maximum contraction may correlate with neuronal bursting at the neuromuscular junction and subsequent EMG bursting as reported in the literature [106].

The HD EMG signal acquisition and signal (and reconstructed image) processing approach should allow us to use image-processing techniques. Further, conducting time varying study of the muscle contraction activity maps should allow for video-graphical processing techniques as well for more developed myoelectric signal decoding, pattern recognition, and eventually control.

4.4.3. Automatic Liner Position Detection

4.4.3.1. Introduction

Preliminary studies reported in the previous sections establish future use of HD EMG as a more reliable, robust, location independent method for myoelectric signal acquisition and decoding. Such decoding should prove to be beneficial for achieving a more precise prosthesis control. However, for integrating HD EMG into a liner system that is usable for an amputee, a very important next step would be to determine the orientation of the electrode contacts, and thus by extension of the liner on an amputee's limb without regular re-calibration or training. The ability to do the same algorithmically can ensure that a liner based HD EMG system will make prosthesis control a very intuitive process for the amputee. The next section presents one way to algorithmically determine the position of the liner on a residual limb.

4.4.3.2. Methods

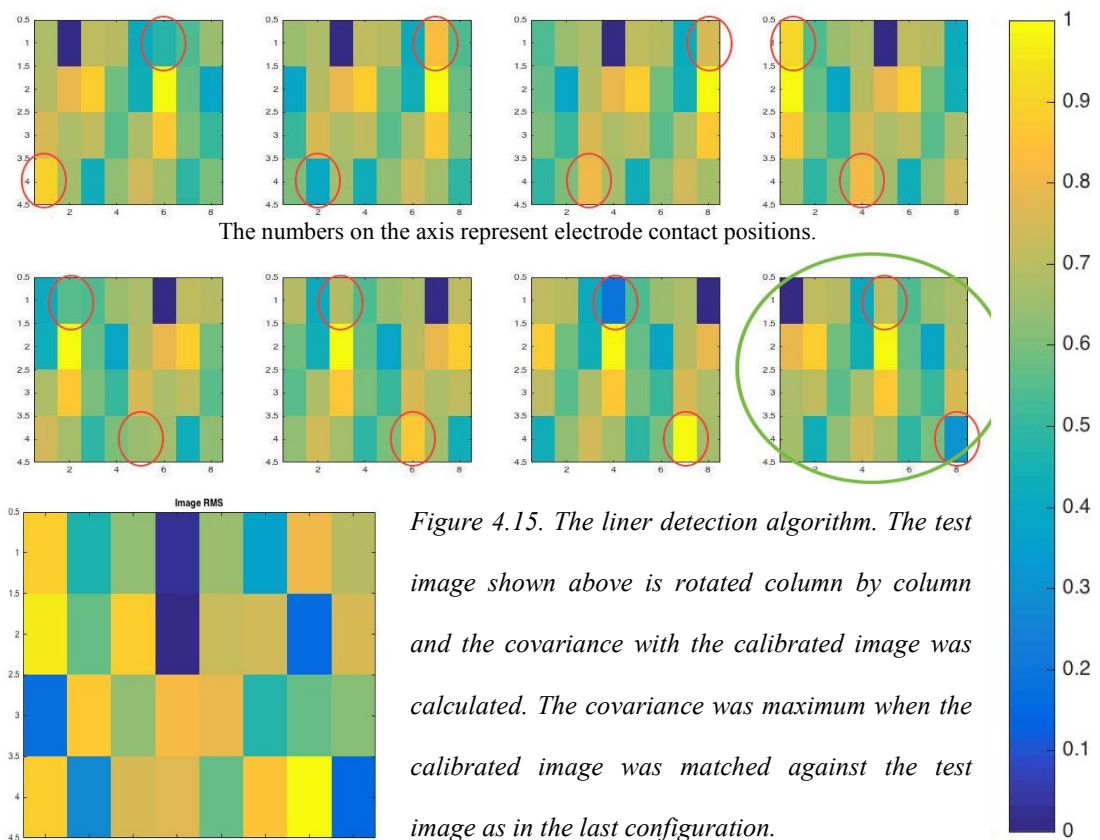
We collected an initial calibration dataset from an able bodied subject with the electrode array attached to the limb and positioned such that the electrode contact coincided with the belly of the flexor muscle and the proximal end of the HD array was 2 inches from the elbow. We recorded baseline noise signal of 5 seconds, followed by 5 seconds of the user performing Maximum Volume Contraction (MVC) for a specific hand motion such as Wrist Flexion.

We also gathered a test data set from the same subject by wearing the electrode array in a random position on the limb. We collected the same signals as highlighted above

with this orientation of the electrode array for the same hand motion i.e. Wrist Flexion.

4.4.3.3. Algorithm for Liner Position Detection

After creation of the calibrated image activation map and the test image activation map from the data sets gathered above, we warped the test map column wise towards the right. At each new position of the test map, we calculated the covariance between the calibrated image and the test image to obtain the degree of similarity. Figure 4.15 shows how the test image is warped column by column.



In order to account for the noisy channels, we replaced every noisy channel pixel with the corresponding pixel value from the calibrated image. The noisy channels were replaced with a new data set with every warp to ensure that the data in the noisy channel pixel matched the data in the calibrated image pixel that it would be compared with. The pixels encircled in red in Figure 4.15 represent the noisy channels that are replaced with the values from the calibrated image.

4.4.3.4. Results

The green encircled image represents the position of the test image that gave the highest covariance with the calibrated image, thus identifying the position of the electrode array with respect to the limb. The channels were re-numbered to match this configuration for further signal acquisition and processing and prosthetic control.

4.4.4. Electrode Site Location for Prosthesis Fitting

4.4.4.1. Introduction

Apart from use for prosthesis control, HD EMG has other very useful functions in the prosthesis realm especially in prosthesis fittings. Myosite location (Locations on the residual limb that provide high quality EMG signals) is one of the most important steps in the process of myoelectric prosthesis fitting. This is because identification of the best locations for electrode placement governs the quality of EMG signals and the subsequent performance of control algorithms [107 - 108]. The process requires precision, even for two-site based direct control systems that use antagonistic muscle

groups. The current industry standard is to manually palpate the residual limb while the patient performs a contraction to identify broad areas of muscle movement and then to use a differential electrode system for finer identification of myosites [109 - 110]. Shifting an electrode even by <1 cm over the muscle causes significant changes in sEMG amplitude subsequently affecting the quality of control [28, 111 - 112]. The time required as well as the reliability of this process is solely dependent on the skillset of the prosthetist, thus making it a highly specialized procedure.

New control strategies such as pattern recognition [113 - 117] use up to eight EMG sites for signal acquisition. In the case of above elbow amputation patients especially, all eight of these electrodes need to be placed in specific locations on the residual limb to maximize information content of each channel. With emerging control strategies such as pattern recognition which require multiple electrode sites, the problem of myosite identification is likely to become increasingly more challenging over traditional two-site direct control systems. Thus, there is a significant need to improve upon the traditional manual or empirical method of myosite location.

We have developed a novel flexible High-Density EMG array to “image” a patient’s residual limb prior to socket fabrication. This system generates muscle activity maps from 128 channels of simultaneously recorded monopolar EMG signals. The muscle activity maps provide a visual means of identifying all potential myosite locations for a given contraction. Moreover, by analyzing different muscle activity maps for different hand motions and contractions, it should be possible to determine the most unique combination of sites that provide differentiable patterns for control.

4.4.4.2 Methods

The HD EMG array was attached so as to cover the entire residual limb of a transhumeral amputee patient. The patient was asked to perform the eight different hand motions that were repeatable for him namely: Wrist Extension, Wrist Flexion, Hand Open, Hand Close, Pinky Flexion, Thumb Flexion, Pronation and Supination. 128 channels of monopolar signals were acquired and converted to muscle activity maps as per the algorithm highlighted in Section 4.3.1.3.

4.4.4.3. Results

Given below in Figure 4.16, are the images depicting six distinct motions that a transhumeral amputee performed. The muscle activity maps for each of the six motions were analyzed to determine a combination of eight locations that was distinct to each motion. A differential electrode was used at the eight spots identified from the HD EMG maps to determine their orientation for attachment within the prosthesis for optimum signals.

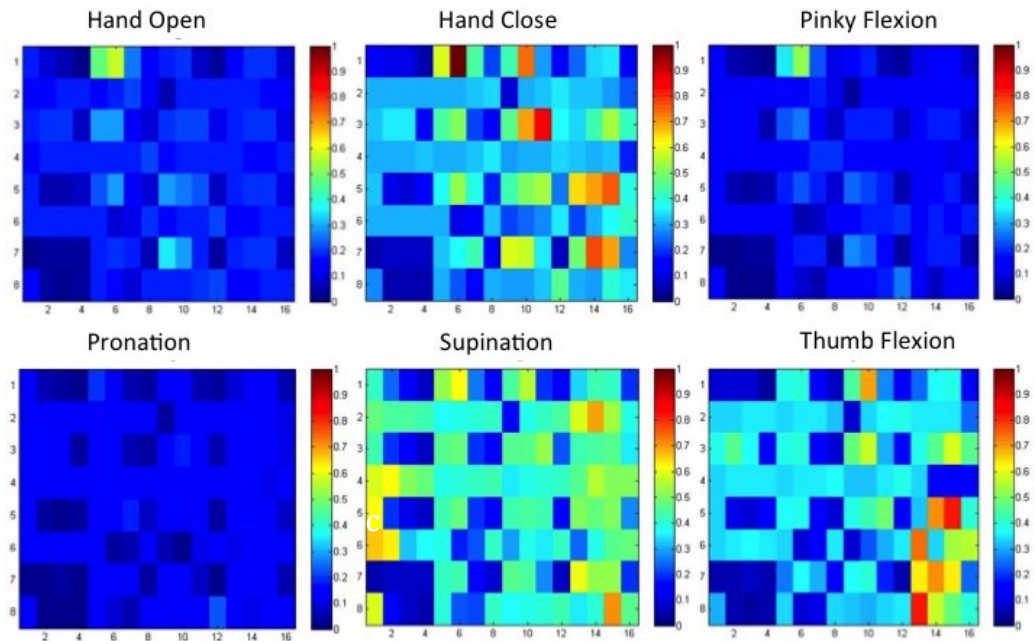


Figure 4.16. HD EMG maps for Myosite Location. Six distinct motions performed by an amputee subject to determine unique myosite locations for pattern recognition based control. The muscle activity maps for amputees will be highly variable based on the muscle arrangement following surgery and amputee. Muscle activity maps will be unique to each amputee.

4.4.4.4. Discussion

Use of this HD-EMG interface allowed for optimized identification of eight myosites for pattern recognition-based prosthesis fitting of a patient with a transhumeral amputation. Interestingly, in this case study, we identified unique EMG sites where there was little visually identifiable movement of the residual limb. Such sites would likely be missed by traditional myosite selection methods. Moreover, the time taken to identify all eight spots was fractional of the time taken when the myosites are located using traditional methods. Using the selected sites, the patient was subsequently successfully fit with a pattern recognition prosthesis. Thus, HD EMG is a valuable myosite visualization and identification tool that augments the prosthetists' skillset in myosite location.

4.5. Summary

This research paves the way for incorporating flexible electronics within a prosthetic liner. First, we developed thin flexible HD EMG array, and next we laid out the foundation of algorithms for image based EMG signal decoding for prosthetic control.

This has advantages due to multiple reasons:

1. A silicone liner fits the residual limb with better compression and doesn't move relative to the residual limb, allowing for better stability for the electrode skin interface.
2. It separates the electronics from the socket, which prevents problems like electrode lift off and electrode migration.
3. Use of HD EMG eliminates the need for location specificity of the electronics and makes prosthesis fittings a more generic process.
4. Eliminating location specificity and embedded electronics in a liner allows for use of a silicone liner with a myoelectric prosthesis. This enables fabrication of a socket with greater compression without significant damage to the residual limb.
5. It paves way for a new generation of robust, stable, more intuitive image controlled myoelectric prosthesis.

CHAPTER 5

5. Conclusion and Future Directions

Use of flexible electronics in conjunction with HD EMG is a novel approach that is yet to be explored for reliable myoelectric prosthesis control. We have established a number of relationships and parameters.

- * The Skin Electrode Complex Impedance and SNR relationship
- * Flexible electronics and HD EMG to be integrated with myoelectric prosthesis systems in numerous different ways.
- * Demonstration of fine motor control, proportional control, temporal study of a contraction as well as myosite localization using HD EMG

This chapter provides the summary and discussion.

5.1. Flexible Contacts

5.1.1. Flexible Electrodes in Socket for Myoelectric Prosthesis

On account of development of numerous different flexible conductive materials as well as due to a uniform method of characterizing them, there is an opportunity for redesign of current rigid electrodes that are embedded in a socket. By use of the flexible electrodes in a remote configuration such that the amplification is performed at a remote location, the size as well as the rigidity of traditional socket electronics can be eliminated.

Similarly, additional research in the realm of silicone encased flex PCB electrodes can now be pursued more easily with development of conductive silicones that conduct EMG signals with high SNR. Using SECI, the materials can be characterized more uniformly and the electrodes developed out of doped traditionally non-conductive materials will have stable and repeatable electrical characteristics.

5.1.2. Flexible Electrodes in Liner for Myoelectric Prosthesis

Replacement of rigid electronics in the socket with flexible contacts and electrodes is one important aspect of future EMG acquisition for prosthesis control. In addition, the more comprehensive solution is to incorporate the electrodes within the liner itself. Moreover, a key aspect of improved electronics for myoelectric signal acquisition for prosthesis control would include elimination of wired electronic components.

Development of encasing techniques and wireless data and power transfer methods would facilitate incorporation of wireless electronics within the liner itself and would eliminate the dependency on wired connections and the constraints due to them. Moreover, use of other flexible materials such as silk, elastic, PDMS and techniques such as screen-printing with conductive ink and traces can revolutionize wearable electronics for EMG acquisition and control of myoelectric prosthesis.

Flexible electrode contacts are the first step towards making prosthesis electronics completely flexible. Next generation thin film electronics and wireless data and power transmission technologies will augment the translation towards completely conformal electronics for the most stable and robust prosthesis control.

5.2. High Density EMG

5.2.1. HD EMG for Fine Motor Decoding and Signal Acquisition for Proportional Control

Based on the preliminary results generated in the previous chapter, it is evident that HD EMG muscle activity maps have the potential to be used for both individual finger control and proportional control for myoelectric prosthesis. With algorithms already in place to mitigate problems created by electrode shift, image based prosthesis control could become a reality and a more efficient means of control. Not only will users regain dexterity, it has a future potential for allowing multiple degrees of freedom using simple EMG signals.

Fine motor control and proportional control continue to remain a research problem, which requires a more optimized solution that can be implemented on fairly constrained processors for integration with actual myoelectric prosthesis. Channel optimization, image based processing and pattern recognition together can help in creating more intuitive prosthesis control systems.

5.2.2. HD EMG for Myoelectric Prosthesis Fitting

In the singular pattern recognition prosthesis fitting case study mentioned in the previous chapter, it is evident that HD EMG could become a very valuable tool in multi-site, prosthesis fitting. While the current implementation is by means of an offline system, a real-time system along with a visualization GUI tool would allow

the prosthetist to understand and correlate the array placement on the forearm with the muscle activity maps on the screen can make prosthesis fitting sessions more accurate and less time consuming. Moreover, the setup will allow for identification of the electrically best spots for signal acquisition, not only the ones that visibly move during a contraction.

In a further advanced implementation of the system, we could algorithmically determine the best combination of sites for electrode placement without any intervention from the prosthetist himself.

5.2.3. HD EMG in Socket for Myoelectric Prosthesis

While flexible electronics within the socket will significantly improve the stability of the skin electrode interface, use of HD EMG in a modular architecture will allow for greater robustness of the system by combining the benefits of a flexible remote system in a high-density configuration. Not only will this prevent electrode lift off and migration, it will eliminate the need for electrodes to be fabricated into the exact positions within a socket. Instead multiple arrays of remote monopolar electrodes could be attached to form a HD EMG configuration and provide a more advanced interface to myoelectric control.

This will lead to a significant shift in the current electronics design for upper limb prosthesis. Use of HD EMG will require a shift from traditional differential control to monopolar signal based control, for better noise removal as well as will allow the implementation of a very modular and modifiable system.

The control strategy will no longer be dependent on the electronics used for the signal acquisition and the user will have the ability to choose between different control strategies using the same electrode interface without having to undergo a completely new fabrication of their socket and prosthesis.

5.2.4. HD EMG in Liner for Myoelectric Prosthesis

Incorporation of HD EMG within a socket is one way of improving the current electrode interface to make it more universally compatible with different control schemes. However, in order to create a fool proof solution for prosthetic control, it is essential that the skin electrode interface be a very stable one. For this, the electronics would have to be independent of the socket so that socket movement does not interfere with the signal acquisition.

Thus, the most optimum solution for the hardware for signal acquisition would be to integrate the electronics within the silicone prosthetic liner itself, using the flexible silicone contacts as well as the HD EMG flex PCB array.

Moreover, further research would enable printing of the HD EMG array on materials such as textiles like silk as well as into thin film tattoos on the skin itself which is capable of wirelessly interfacing with the remaining processing electronics.

From an even futuristic point of view, these electronics could be implanted into the residual limb itself thus ensuring that they are always acquiring the best EMG signal

from the best spots and are no longer affected by changes in their external environment.

In the realm of electronics development for myoelectric control, we have made great strides in implementing innovative technologies to improve signal acquisition and processing. However, we have a long way to go before we can use electronics and algorithms to realistically replace a lost limb and truly achieve our goal of restoring complete limb control to an amputee.

6. Appendix

6.1. Ongoing Collaborative Research using the HD EMG developed as a part of this thesis

6. 1.1. Channel Subset Selection

HD EMG maps, open a new dimension of image based pattern recognition control of a myoelectric arm. The value of a signal source can be quantified based on its contribution to the recognition task at hand. When multiple signal sources are available, as is the case when decoding movement intentions from multichannel EMG, each of the channels can be ranked based on their respective contributions in terms of discrimination relevance [103]. By promoting channels of maximum relevance while reducing the influence of irrelevant or redundant channels, a much smaller channel subset emerges which is often equivalent or superior at performing the pattern recognition task [104 - 105]. Our HD EMG platform allows us to localize myoelectric channel sources which supply the most relevant task information for an individual human user. Due to this, the electrode location in the prosthesis no longer has to be customized for every individual. Instead, we can algorithmically determine the best subset of channels from 128 channels for signal acquisition for subsequent prosthesis control. Moreover, the ability to choose channels on the fly provides greater flexibility in choice of control strategy since the prosthesis hardware no longer has to be customized for it. Adding higher number of channels in the HD EMG format also has the potential to provide additional diagnostic insight into a person's

specific post-trauma innervated muscle anatomy and their potential ability to use myoelectrically controlled devices.

6.1.1.2. Methods

For an initial proof of concept, data from one able bodied subject was used. The subject was asked to perform different hand motions such as Wrist Flexion, Wrist Extension, Pronation, Supination, Hand Open and Hand Close. After using the HD EMG array to collect data, user-specific movement patterns can be established (Fig. 4.4).

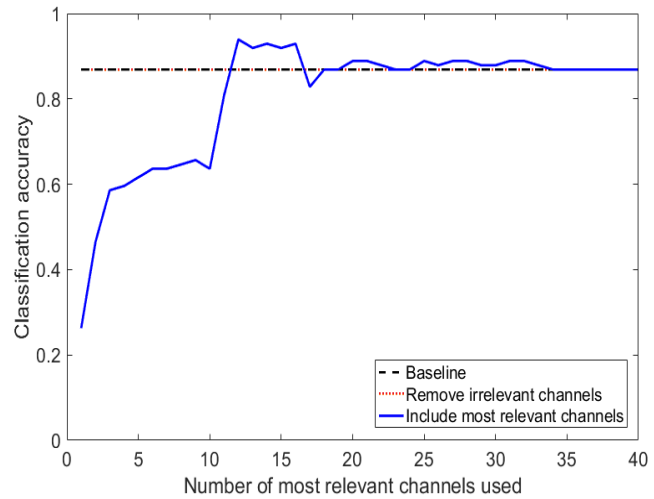


Figure 6.1. EMG pattern recognition performance based on feature relevancy. A reduced subject-specific optimal channel subset can be identified for movement decoding that is smaller than the baseline full channel set, and this subset may perform significantly better. Additionally, irrelevant and noise channels can be identified and removed with no penalty on performance.

6.1.1.3. Results

Physical observation of these patterns demonstrates that not all of the 128 channels are activated which, in itself, can tell us a great deal about the user's muscular anatomy. However, we can quantify the relative contribution of each channel to these movement patterns using separability criteria such as Bhattacharyya distance and mutual information [103-105] to make precise determinations about its degree of

influence. We rank the influence of all channels 3-ways: (i) identify *irrelevant* channels [105] which provide little to no information other than perhaps noise, (ii) identify *maximally relevant* channels critical to the pattern recognition objective, and (iii) identify *partially relevant* channels which are supplementary or redundant to varying degrees. We then choose to include or exclude certain of these channels based on their relative contributions.

6.1.1.4. Discussion

Determining such an optimal subset of signal channels is desirable in EMG pattern recognition for a number of reasons. First, limiting the amount of information to be actively processed improves the speed of real-time computation and processing. Second, it can be shown (Fig. 4.6.) that such a subset may improve the overall pattern recognition performance. From this 40 channel subset of the original 128 channels, the decoding accuracy is the highest when using only the twelve most informative channels. The improvement gained from the reduced channel set indicates that, not only are certain channels irrelevant to the pattern recognition task, but that some of them can actually be misleading. The influence of specific channels will vary from user to user, but identifying and discarding irrelevant or misleading channels for that user should make decoding their intended movements more robust.

6.2. K L Divergence Algorithm Theory [132]

To measure the difference between two probability distributions over the same variable x , a measure, called the Kullback-Leibler divergence, or simply, the KL divergence, has been popularly used in the data mining literature. The concept was originated in probability theory and information theory.

The KL divergence, which is closely related to relative entropy, information divergence, and information for discrimination, is a non-symmetric measure of the difference between two probability distributions $p(x)$ and $q(x)$. Specifically, the Kullback-Leibler (KL) divergence of $q(x)$ from $p(x)$, denoted $D_{KL}(p(x),q(x))$, is a measure of the information lost when $q(x)$ is used to approximate $p(x)$.

Let $p(x)$ and $q(x)$ are two probability distributions of a discrete random variable x . That is, both $p(x)$ and $q(x)$ sum up to 1, and $p(x) > 0$ and $q(x) > 0$ for any x in X . $D_{KL}(p(x),q(x))$ is defined in Equation (6.1).

$$D_{KL}(p(x)||q(x)) = \sum_{x \in X} p(x) \ln \frac{p(x)}{q(x)} \quad (\text{Eq. 6.1})$$

The KL divergence measures the expected number of extra bits required to code samples from $p(x)$ when using a code based on $q(x)$, rather than using a code based on $p(x)$. Typically $p(x)$ represents the “true” distribution of data, observations, or a precisely calculated theoretical distribution. The measure $q(x)$ typically represents a theory, model, description, or approximation of $p(x)$.

Although the KL divergence measures the “distance” between two distributions, it is not a distance measure. This is because that the KL divergence is not a metric

measure. It is not symmetric: the KL from $p(x)$ to $q(x)$ is generally not the same as the KL from $q(x)$ to $p(x)$. Furthermore, it need not satisfy triangular inequality. Nevertheless, $D_{KL}(P||Q)$ is a non-negative measure. $D_{KL}(P||Q) \geq 0$ and $D_{KL}(P||Q) = 0$ if and only if $P = Q$.

Notice that attention should be paid when computing the KL divergence. We know $\lim_{p \rightarrow 0} p \log p = 0$. However, when $p \neq 0$ but $q = 0$, $D_{KL}(p||q)$ is defined as ∞ . This means that if one event e is possible (i.e., $p(e) > 0$), and the other predicts it is absolutely impossible (i.e., $q(e) = 0$), then the two distributions are absolutely different. However, in practice, two distributions P and Q are derived from observations and sample counting, that is, from frequency distributions. It is unreasonable to predict in the derived probability distribution that an event is completely impossible since we must take into account the possibility of unseen events.

REFERENCES

- [1] S. Sudarsan, E. Chandra Sekaran, “Design and Development of EMG Controlled Prosthetics Limb”, *Procedia Engineering*, Volume 38, 2012, Pages 3547-3551,
- [2] G Purushothaman. “Myoelectric Control of Prosthetic Hands: State-of-the-Art Review.” *Medical Devices (Auckland, N.Z.)*, 2016: 247–255. PMC.
- [3] Carey SL, Lura DJ, Highsmith MJ; CP.; FAAOP. “Differences in myoelectric and body-powered upper-limb prostheses: Systematic literature review”. *J Rehabil Res Dev*. 2015 ;52(3):247-62.
- [4] A Searle and L Kirkup, “A direct comparison of wet, dry and insulating bioelectric recording electrodes”, *Physiological Measurement*, 2000, Volume 21, Issue 2, pp. 271
- [5] Link: http://jjengineering.info/EMG_AMPLITUDE.html
- [6] Padmadinata F Z, Veerhoek J J, Van Dijk G J A and Huijsing J H, 1990, *Microelectronic skin electrode Sensors Actuators*, 491–4
- [7] Taheri B, Knight R and Smith R, “A dry electrode for EEG recording” *Electroencephalography. Clin. Neurophysiol.* 1994, Volume 90, pp. 376–83
- [8] Liberating Technologies Inc.

[9] Smith, Lauren H., and Levi J. Hargrove. "Comparison of Surface and Intramuscular EMG Pattern Recognition for Simultaneous Wrist/hand Motion Classification." Conference proceedings: Annual International Conference of the IEEE Engineering in Medicine and Biology Society. IEEE Engineering in Medicine and Biology Society Conference, 2013, 4223–4226. PMC.

[10] Jayme S. Knutson, Gregory G. Naples, P. Hunter Peckham, Michael W. Keith, "Electrode fracture rates and occurrences of infection and granuloma associated with percutaneous intramuscular electrodes in upper-limb functional electrical stimulation applications", *Journal of Rehabilitation, Research and Development*, 2002, Vol. 39 No. 6, Pages 671-684

[11] Ningqi Luo; Jun Ding; Ni Zhao; Leung, B.H.K.; Poon, C.C.Y., "Mobile Health: Design of Flexible and Stretchable Electrophysiological Sensors for Wearable Healthcare Systems," in *Wearable and Implantable Body Sensor Networks (BSN)*, 2014, vol., no., pp.87-91

[12] Bergey G E, Squires R D and Sipple W C, "Electrocardiogram recording with pasteless electrodes". *IEEE Trans. Biomed. Eng.* 1971, Volume 18, pp. 206–11

[13] C. Pylatiuk, M. Müller-Riederer, A. Kargov, S. Schulz, O. Schill, M. Reischl and G. Bretthauer, "Comparison of Surface EMG Monitoring Electrodes for Long-term Use in Rehabilitation Device Control", *IEEE 11th International Conference on Rehabilitation Robotics Proc.*, 2009, June 23-26

[14] Masayuki Ohyama, Yutaka Tomita, Satoshi Honda, Hitoshi Uchida, Noriyoshi Matsuo, "Active Wireless Electrodes for Surface Electromyography", 18th Annual International Conference of the IEEE Engineering in Medicine and Biology Society, 1996, 1.7.2: Telemetry II

[15] Experimental Study of an EMG-Controlled 5-DOF Anthropomorphic Prosthetic Hand for Motion Restoration, Journal of Intelligent and Robotic Systems, Article, Jun 2014

[16] L. Hargrove, K. Englehart and B. Hudgins, "The effect of electrode displacements on pattern recognition based myoelectric control," 2006 International Conference of the IEEE Engineering in Medicine and Biology Society, New York, NY, 2006, pp. 2203-2206.

[17] Yu Mike Chi, Tzyy-Ping Jung and Gert Cauwenberghs, "Dry-Contact and Noncontact Biopotential Electrodes: Methodological Review", 2010, IEEE Reviews In Biomedical Engineering, Vol. 3

[18] Vidovic MM, Paredes LP, Han-Jeong Hwang, Amsüss S, Pahl J, Hahne JM, Graimann B, Farina D, Müller KR., "Covariate shift adaptation in EMG pattern recognition for prosthetic device control"., Conf Proc IEEE Eng Med Biol Soc. 2014, 4370-3

- [19] Sewell P., Noroozi S., Vinney J., & Andrews S. “Developments in the transtibial prosthetic socket fitting process: A review of past and present research.” *Prosthetics and Orthotics International*, 2000, 24(2), 97–107.
- [20] E. A. Biddiss & T. T. Chau, “Upper limb prosthesis use and abandonment: A survey of the last 25 years”. *Prosthetics and Orthotics International*, 2007, 31(3), 236–257.
- [21] S.H Roy, G De Luca, M.S. Cheng, A. Johansson, L.D. Gilmore, C.J De Luca, “Electro-mechanical stability of surface EMG sensors”, *Medical & Biological Engineering & Computing*, 2007, Volume 45, pp 447 – 457
- [22] M. R. Masters, R. J. Smith, A. B. Soares, and N. V. Thakor, “Towards better understanding and reducing the effect of limb position on myoelectric upper-limb prostheses,” *Conf. Proc. Annu. Int. Conf. IEEE Eng. Med. Biol. Soc. IEEE Eng. Med. Biol. Soc. Annu. Conf.*, vol. 2014, pp. 2577–2580, 2014.
- [23] L. G. Cohen, S. Bandinelli, T. W. Findley, and M. Hallett, “Motor Reorganization After Upper Limb Amputation In Man: A Study with Focal Magnetic Stimulation,” *Brain*, Feb. 1991, vol. 114, no. 1, pp. 615–627,
- [24] S. Roricht, B.-U. Meyer, L. Niehaus, and S. A. Brandt, “Long-term reorganization of motor cortex outputs after arm amputation,” *Neurology*, Jul. 1999, vol. 53, no. 1, p. 106,

- [25] Hanger Prosthetics and Orthotics and SIU HealthCare, SIU School of Medicine
- [26] Matthew R Masters, R. J. Beaulieu, R. J. Smith, A. B. Soares, R. R. Kaliki, and N. V. Thakor, "Aggregate Training Outperforms Location-Specific Training of Pattern Recognition-Based Myoelectric Prosthesis," *IEEE Trans. Neural Syst. Rehabil. Eng.*, in review 2015.
- [27] L. Hargrove, K. Englehart, and B. Hudgins, "The effect of electrode displacements on pattern recognition based myoelectric control," *Conf. Proc. Annu. Int. Conf. IEEE Eng. Med. Biol. Soc. IEEE Eng. Med. Biol. Soc. Conf.*, 2006, vol. 1, pp. 2203–2206.
- [28] A. J. Young, L. J. Hargrove and T. A. Kuiken, "The Effects of Electrode Size and Orientation on the Sensitivity of Myoelectric Pattern Recognition Systems to Electrode Shift," in *IEEE Transactions on Biomedical Engineering*, Sept. 2011, vol. 58, no. 9, pp. 2537-2544.
- [29] D. Tkach, H. Huang, and T. A. Kuiken, "Study of stability of time-domain features for electromyographic pattern recognition," *J. Neuroengineering Rehabil.*, 2010, vol. 7, p. 21.
- [30] L. Hargrove, K. Englehart, and B. Hudgins, "A training strategy to reduce classification degradation due to electrode displacements in pattern recognition based myoelectric control," *Biomed. Signal Process. Control*, Apr. 2008, vol. 3, no. 2, pp. 175–180,

- [26] A. Gruetzmann, S. Hansen, and J. Müller, “Novel dry electrodes for ECG monitoring,” *Physiol. Meas.*, 2007, vol. 28, no. 11, p. 1375,
- [32] A. C. Myers, H. Huang, and Y. Zhu, “Wearable silver nanowire dry electrodes for electrophysiological sensing,” *RSC Adv*, 2015, vol. 5, no. 15, pp. 11627–11632,
- [33] A. Cömert, M. Honkala, and J. Hyttinen, “Effect of pressure and padding on motion artifact of textile electrodes,” *Biomed. Eng. Online*, vol. 12, p. 26, 2013.
- [34] J. M. Miguelez, C. Lake, D. Conyers, and J. Zenie, “The Transradial Anatomically Contoured (TRAC) Interface: Design Principles and Methodology,” *JPO J. Prosthet. Orthot.*, 2003, vol. 15, no. 4,
- [36] C. Lake, “The Evolution of Upper Limb Prosthetic Socket Design,” *JPO J. Prosthet. Orthot.*, Jul. 2008, vol. 20, no. 3, pp. 85–92,
- [37] A. G. Hatfield and J. D. Morrison, “Polyurethane gel liner usage in the Oxford Prosthetic Service,” *Prosthet. Orthot. Int.*, Apr. 2001, vol. 25, no. 1, pp. 41–46,.
- [38] R. Emrich and K. Slater, “Comparative analysis of below-knee prosthetic socket liner materials,” *J. Med. Eng. Technol.*, Apr. 1998, vol. 22, no. 2, pp. 94–98.
- [39] O. Kristinsson, “The ICEROSS concept: a discussion of a philosophy,” *Prosthet. Orthot. Int.*, Apr. 1993, vol. 17, no. 1, pp. 49–55,

- [40] ArtLimb, Art of Prosthesis, Liners: Part3. Liner Care and General Tips
- [41] Kang, H., Jung, S., Jeong, S., Kim, G., & Lee, K. "Polymer-metal hybrid transparent electrodes for flexible electronics". Nature Communications, 2015, 6, 6503.
- [42] J. C. Agar, K. J. Lin, R. Zhang, J. Durden, K. S. Moon and C. P. Wong, "Novel PDMS(silicone)-in-PDMS(silicone): Low cost flexible electronics without metallization," 2010 Proceedings 60th Electronic Components and Technology Conference (ECTC), Las Vegas, NV, USA, 2010, pp. 1226-1230.
- [43] Guanglin Li, Yanjuan Geng, Dandan Tao, and Ping Zhou, "Performance of Electromyography Recorded Using Textile Electrodes in Classifying Arm Movements", 33rd Annual International Conference of the IEEE EMBS Boston, Massachusetts USA, August 30 - September 3, 2011
- [44] Bavani Balakrisnan, Aleksandar Nacev, Jeffrey M Burke, Abhijit Dasgupta and Elisabeth Smela, "Design of compliant meanders for applications in MEMS, actuators, and flexible electronics, Smart Materials and Structures", 2012, Volume 21, Issue 7, pp. 075033
- [45] M Stoppa, A Chiolerio, "Wearable Electronics and Smart Textiles: A Critical Review", Sensors 14 (7), 11957-11992

[46] T. Ramachandran, Chettiar Vigneswaran, “Design and Development of Copper Core Conductive Fabrics for Smart Textiles”, *Journal Of Industrial Textiles*, July 2009, 39(1):81-93,

[47] Farooq, M. Sazonov, E., Editor : Mukhopadhyay, C. Subhas, "Strain Sensors in Wearable Devices", *Wearable Electronics Sensors: For Safe and Healthy Living*, 2015, Springer International Publishing, pp. 221—239

[48] Giovanni Salvatore and Gerhard Tröster, “Chapter 3.3 - Flexible Electronics from Foils to Textiles: Materials, Devices, and Assembly, In *Wearable Sensors*”, edited by Edward Sazonov and Michael R. Neuman, Academic Press, Oxford, 2014, Pages 199-233

[49] E-Textiles For Wearability: Review On Electrical And Mechanical Properties, 2015, Link: http://www.textileworld.com/Articles/2010/June/Textile_News/

[50] S. Wagner and S. Bauer, “Materials for stretchable electronics,” *MRS Bull.* vol. 37, Mar. 2012, pp. 207–213

[51] M. Gonzalez, F. Axisa, M. Vanden Bulcke, D. Brosteaux, B. Vandeveld, and J. Vanfleteren, “Design of metal interconnects for stretchable electronic circuits,” *Microelectron. Reliab.*, vol. 48, Jun. 2008, pp. 825–832

[52] Gandhi, N.; Khe, C.; Chung, D.; Chi, Y.M.; Cauwenberghs, G., "Properties of Dry and Non-contact Electrodes for Wearable Physiological Sensors," in *Body Sensor*

Networks (BSN), 2011 International Conference on , May 2011, vol., no., pp.107-112, 23-25

[53] Anuj Dhawan, Tushar K. Ghosh, Abdelfattah M. Seyam and John Muth, "Development of Woven Fabric-based Electrical Circuits". MRS Proceedings, 2002, 736

[54] Tapomayukh Bhattacharjee, Advait Jain, Sarvagya Vaish, Marc D. Killpack, and Charles C. Kemp, "Tactile Sensing over Articulated Joints with Stretchable Sensors", World Haptics Conference (The 5th Joint EuroHaptics Conference and IEEE Haptics Symposium), 2013.

[55] Kazani, I.; Hertleer, C.; De Mey, G.; Schwarz, A.; Guxho, G.; Van Langenhove, L. Electrical Conductive Textiles Obtained by Screen Printing, *Fibres & Textiles in Eastern Europe* 2012, 20, 1(90) 57-63

[56] C.R. Cork, "Conductive fibres for electronic textiles: an overview", In *Electronic Textiles*, Editor Tilak Dias, Woodhead Publishing, Oxford, 2015, Pages 3-20

[57] Paul, G.M.; Fan Cao; Torah, R.; Kai Yang; Beeby, S.; Tudor, J., "A Smart Textile Based Facial EMG and EOG Computer Interface," in *Sensors Journal*, IEEE, Feb. 2014, vol.14, no.2, pp.393-400,

[58] Kannaian, T., Neelaveni, R., & Thilagavathi, G. Design and development of embroidered textile electrodes for continuous measurement of electrocardiogram signals. *Journal of Industrial Textiles*, 2012, 42(3), 303–318.

[59] Liang G, Guvanasen GS, Xi L, Tuthill C, Nichols TR, DeWeerth SP. “A PDMS based integrated stretchable microelectrode array (isMEA) for neural and muscular surface interfacing”. *IEEE Trans Biomed Circuits Sys*. 2013; 7(1):1-10.

[60] Greg U, “Ultrathin Electric 'Tattoo' Can Monitor Muscles and More”, *Live Science Tech*, 2016, Link: <http://www.livescience.com/55518-ultrathin-electric-tattoo-monitors-muscles.html>

[61] Ningqi Luo, Jun Ding, Ni Zhao, Leung, B.H.K., Poon, C.C.Y., "Mobile Health: Design of Flexible and Stretchable Electrophysiological Sensors for Wearable Healthcare Systems," in *Wearable and Implantable Body Sensor Networks (BSN)*, 2014, vol., no., pp.87-91,

[62] Mindo, National Chiao Tung University Brain Research Center, Taiwan

[63] Chen Y-H, de Beeck M.O., Vanderheyden L, “Soft, Comfortable Polymer Dry Electrodes for High Quality ECG and EEG Recording”. *Sensors (Basel, Switzerland)*. 2014

[64] Chin-Teng Lin, Lun-De Liao, Yu-Hang Liu, I-Jan Wang, Bor-Shyh Lin, Jyh-Yeong Chang, "Novel Dry Polymer Foam Electrodes for Long-Term EEG

Measurement," in Biomedical Engineering, IEEE Transactions on, May 2011, vol.58, no.5, pp.1200-1207

[65] Circuit Scribe

[66] Byoung J.K., Thomas H, Andreas F, Ji-Hoon L and Dae H.N., Joachim R.B., Werner B, In-Suk C, Young C. J., Patric A. G. and Oliver K., "Improving mechanical fatigue resistance by optimizing the nanoporous structure of inkjet-printed Ag electrodes for flexible devices", *Nanotechnology*, 2014, Volume 25, Issue 12, pp. 125706.

[67] Yu, Y., Yan, C. and Zheng, Z., "Polymer-Assisted Metal Deposition (PAMD): A Full-Solution Strategy for Flexible, Stretchable, Compressible, and Wearable Metal Conductors". *Adv. Mater.*, 2014, 26: 5508–5516.

[68] Enrique M. Spinelli, Miguel A. Mayosky, and Ramon Pallás-Areny, "A Practical Approach to Electrode-Skin Impedance Unbalance Measurement", *IEEE Transactions On Biomedical Engineering*, 2006, Volume. 53, No. 7

[69] Grimnes, S. "Impedance measurement of individual skin surface electrodes", *Med. Biol. Eng. Comput.* 1983, 21: 750.

[70] J. Rosell, J. Colominas, P. Riu, R. Pallas-Areny and J. G. Webster, "Skin impedance from 1 Hz to 1 MHz," in *IEEE Transactions on Biomedical Engineering*, Aug. 1988, vol. 35, no. 8, pp. 649-651, doi: 10.1109/10.4599

[71] Taji, B.; Shirmohammadi, S.; Groza, V., "Measuring skin-electrode impedance variation of conductive textile electrodes under pressure," in Instrumentation and Measurement Technology Conference (I2MTC), 2014 IEEE International , vol., no., pp.1083-1088

[72] Anthony Calabria, Understanding Lead Off Detection in ECG, Texas Instruments Application Report, 2015, SBAA196A

[73] The State of the Art on Sensors and Sensor Placement Procedures for Surface ElectroMyoGraphy: A proposal for sensor placement procedures, deliverable of the SENIAM project, eds. H.J. Hermens, B. Freriks, Roessingh Research and Development b.v., 1997, ISBN 90-75452-09-8.

[74] Dr. Scott Day, "Important Factors in Surface EMG Measurement ", Bortec Biomedical Report, 2013

[75] The ABC of EM: A Practical Introduction to Kinesiological Electromyography, Peter Konrad Version 1.4 March 2006, ISBN 0-9771622-1-4

[76] Gerald M Hefferman, Fan Zhang, Michael J Nunnery, He Huang, "Integration of surface electromyographic sensors with the transfemoral amputee socket: A comparison of four differing configurations", Prosthetics and Orthotics International, 201, Vol 39, Issue 2, pp. 166 – 173,

- [77] "Chapter 61: Upper and Lower Extremity Prosthetics", Physical Medicine and Rehabilitation: Principles and Practice, Volume 1, eds Joel A. DeLisa, Bruce M. Gans, Nicholas E. Walsh, Lippincott Williams & Wilkins, 2005
- [78] A. J. Young, L. J. Hargrove and T. A. Kuiken, "Improving Myoelectric Pattern Recognition Robustness to Electrode Shift by Changing Interelectrode Distance and Electrode Configuration," in IEEE Transactions on Biomedical Engineering, 2012, vol. 59, no. 3, pp. 645-652. doi: 10.1109/TBME.2011.2177662
- [79] T. Roland, W. Baumgartner, S. Amsuess and M. F. Russold, "Signal evaluation of capacitive EMG for upper limb prostheses control using an ultra-low-power microcontroller," 2016 IEEE EMBS Conference on Biomedical Engineering and Sciences (IECBES), Kuala Lumpur, 2016, pp. 317-320.
- [80] H. Fuket, "1 m-Thickness Ultra-Flexible and High Electrode-Density Surface Electromyogram Measurement Sheet With 2 V Organic Transistors for Prosthetic Hand Control," in IEEE Transactions on Biomedical Circuits and Systems, Dec. 2014, vol. 8, no. 6, pp. 824-833.
- [81] D. Tao, Haoshi Zhang, Zhenxing Wu and G. Li, "Real-time performance of textile electrodes in electromyogram pattern-recognition based prosthesis control," Proceedings of 2012 IEEE-EMBS International Conference on Biomedical and Health Informatics, Hong Kong, 2012, pp. 487-490.

[82] Y. Z. Wu, J. X. Sun, L. F. Li, Y. S. Ding and H. A. Xu, "Performance Evaluation of a Novel Cloth Electrode," 2010 4th International Conference on Bioinformatics and Biomedical Engineering, Chengdu, 2010, pp. 1-5.

[83] K. P. Hoffmann, R. Ruff and W. Poppendieck, "Long-Term Characterization of Electrode Materials for Surface Electrodes in Biopotential Recording," 2006 International Conference of the IEEE Engineering in Medicine and Biology Society, 2006, pp. 2239-2242.

[84] SS-24-25 Technical Datasheet, Silicone Solutions, Link: <http://siliconesolutions.com/media/pdf/SS-24-25TDS.pdf>

[85] SS-24-50 Technical Datasheet, Silicone Solutions, Link: <http://siliconesolutions.com/media/pdf/SS-24-50TDS.pdf>

[86] 5770 CF Technical Datasheet, Holland Shielding, Link: http://hollandshielding.com/content/Filemanager/PDF_5770%20series%20Conductiv e%20foam_January-25-2016-924am.pdf

[87] SS-2612 Technical Datasheet, Silicone Solutions, Link: <http://siliconesolutions.com/media/pdf/SS-2612TDS.pdf>

[88] C. C. Oliveira, J. Machado da Silva, I. G. Trindade and F. Martins, "Characterization of the electrode-skin impedance of textile electrodes," Design of

Circuits and Integrated Systems, Madrid, 2014, pp. 1-6.doi:
10.1109/DCIS.2014.7035526

[89] Alexandra-Maria Tautan, Vojkan Mihajlovic, Yun-Hsuan Chen, Bernard Grundlehner, Julien Penders and Wouter Serdijn, "Signal Quality in Dry Electrode EEG and the Relation to Skin-electrode Contact Impedance Magnitude", Proceedings of Biodevices, 2014, Vol. 1 - 978-989-758-013-0.

[90] Yun-Hsuan Chen, Maaïke Op de Beeck, Luc Vanderheyden, Evelien Carrette, Vojkan Mihajlović, Kris Vanstreels, Bernard Grundlehner, Stefanie Gadeyne, Paul Boon and Chris Van Hoof, "Soft, Comfortable Polymer Dry Electrodes for High Quality ECG and EEG Recording", Sensors 2014, 14, 23758-23780; doi:10.3390/s141223758

[91] Fernando Seoane, Juan Carlos Marquez, Javier Ferreira, Ruben Buendia and Kaj Lindecrantz, The Challenge of the Skin-Electrode Contact in Textile-enabled Electrical Bioimpedance, Measurements for Personalized Healthcare Monitoring Applications, Biomedical Engineering, Trends in Materials Science, Mr Anthony Laskovski (Ed.), InTech, 2014,

[92] H. Saadi and M. Attari, "Electrode-gel-skin interface characterization and modeling for surface biopotential recording: Impedance measurements and noise," 2013 2nd International Conference on Advances in Biomedical Engineering, Tripoli, 2013, pp. 49-52.

- [93] L. Beckmann, C. Neuhaus, G. Medrano, N. Jungbecker, M. Walter, T. Gries, S. Leonhardt, "Characterization of textile electrodes and conductors using standardized measurement setups", *Physiol. Meas.*, 2010, vol. 31, pp. 233,
- [94] Riaz Ahmed, Ken Reifsnider, "Study of Influence of Electrode Geometry on Impedance Spectroscopy" in *Int. J. Electrochem. Sci.*, 2011, 6,1159 – 1174
- [95] Monica Rojas-Martínez, Miguel A Mañanas, Joan F Alonso, "High-density surface EMG maps from upper-arm and forearm muscles", *Journal of NeuroEngineering and Rehabilitation*, 2012, 9:85 DOI: 10.1186/1743-0003-9-85
- [96] A. Boschmann and M. Platzner, "Towards robust HD EMG pattern recognition: Reducing electrode displacement effect using structural similarity," 2014 36th Annual International Conference of the IEEE Engineering in Medicine and Biology Society, Chicago, IL, 2014, pp. 4547-4550.
- [97] Lizhi Pan, Dingguo Zhang, Ning Jiang, Xinjun Sheng and Xiangyang Zhu, "Improving robustness against electrode shift of HD EMG for myoelectric control through common spatial patterns", *Journal of NeuroEngineering and Rehabilitation*, 2015, 12:110,
- [98] Stegeman Dick F., Kleine Bert U., Lapatki Bernd G., Van Dijk Johannes P., *High-density Surface EMG: Techniques and Applications at a Motor Unit Level*, *Biocybernetics and Biomedical Engineering*, 2012, Volume 32, Issue 3, Pages 3-27.

- [99] Hideo Nakamura, Yuto Konishi, Masaki Yoshida, "High-Density EMG Techniques in Neuromuscular Studies", IEEE EMBC Mini-Symposium
- [100] Tkach, Dennis, He Huang, and Todd A Kuiken. "Study of Stability of Time-Domain Features for Electromyographic Pattern Recognition." *Journal of NeuroEngineering and Rehabilitation*, 2010, 7: 21.
- [101] H Onishi, R Yagi, K Akasaka, K Momose, K Ihashi, Y Handa, "Relationship between EMG signals and force in human vastus lateralis muscle using multiple bipolar wire electrodes", *Journal of Electromyography and Kinesiology*, February 2000, Volume 10, Issue 1, Pages 59-67.
- [102] Gazzoni M, Celadon N, Mastrapasqua D, Paleari M, Margaria V, et al. "Quantifying Forearm Muscle Activity during Wrist and Finger Movements by Means of Multi-Channel Electromyography". *PLOS ONE*, 2014, 9(10): e109943.
- [103] H. Peng, F. Long, C. Ding, "Feature selection based on mutual information criteria of max-dependency, max-relevance, and min-redundancy," in *IEEE Transactions on Pattern Analysis and Machine Intelligence*, 2005, vol. 27, no. 8, pp. 1226-1238.
- [104] C.C. Reyes-Aldasoro, A. Bhalerao, "The Bhattacharyya space for feature selection and its application to texture segmentation," *Pattern Recognition*, 2006, vol. 39, no. 5, pp. 812-826,

[105] J. Han, S. W. Lee, Z. Bien, "Feature subset selection using separability index matrix," *Information Sciences*, Feb. 2013, vol. 223, pp. 102-118.

[106] Sanes, J.N. & Jennings, V.A. "Centrally programmed patterns of muscle activity in voluntary motor behavior of humans", *Exp Brain Res*, 1984, 54: 23. doi:10.1007/BF00235815

[107] C.J. De Luca "Surface Electromyography: Detection and Recording", Delsys Incorporated, 2002.

[108] Muhammad Zahak Jamal, *Signal Acquisition Using Surface EMG and Circuit Design Considerations for Robotic Prosthesis, Computational Intelligence in Electromyography Analysis - A Perspective on Current Applications and Future Challenges*, 2012, Dr. Ganesh R. Naik (Ed.), InTech,

[109] *Training Protocol for Therapists*, Touch Bionics, Part Number: MA01243, Issue No. 1, 2014

[110] Alicia J. Davis, MPA, CPO, FAAOP, Brian M. Kelly, DO, Mary Catherine Spires, PT, MD, "Chapter 2: Upper Extremity Amputation: Principles, Prosthetic Restoration and Rehabilitation", *Prosthetic Restoration and Rehabilitation of the Upper and Lower Extremity*, 2013, Demos Medical Publishing,

- [111] Hossein Ghapanchizadeh, Siti A Ahmad, Asnor Juraiza Ishak, Maged S. Al-quraishi, “Review of surface electrode placement for recording electromyography signals”. Biomedical Research, Special Issue. 2017.
- [112] Young AJ, Hargrove LJ, Kuiken TA. “Improving Myoelectric Pattern Recognition Robustness to Electrode Shift by Changing Interelectrode Distance and Electrode Configuration”. IEEE transactions on bio-medical engineering. 2012; 59(3):645-652.
- [113] Scheme, E., & Englehart, K. “Electromyogram pattern recognition for control of powered upper-limb prostheses: State of the art and challenges for clinical use”. J Rehabil Res Dev, 48. 2011.
- [114] Ajiboye AB, Weir RF. “A heuristic fuzzy logic approach to EMG pattern recognition for multifunctional prosthesis control”. IEEE Trans Neural Syst Rehabil Eng. 2005; 13:280–91.
- [115] Englehart K, Hudgins B. “A robust, real-time control scheme for multifunction myoelectric control”. IEEE Trans Biomed Eng. 2003; 50:848–54.
- [116] Chu JU, Moon I, Mun MS. “A real-time EMG pattern recognition system based on linear-nonlinear feature projection for a multifunction myoelectric hand”. IEEE Trans Biomed Eng. 2006; 53:2232–9.

- [117] Peleg D, Braiman E, Yom-Tov E, Inbar GF. "Classification of finger activation for use in a robotic prosthesis arm". *IEEE Trans Neural Syst Rehabil Eng.* 2002; 10:290–3.
- [118] Huang H, Zhou P, Li G, Kuiken TA. "An Analysis of EMG Electrode Configuration for Targeted Muscle Reinnervation Based Neural Machine Interface". *IEEE transactions on neural systems and rehabilitation engineering : a publication of the IEEE Engineering in Medicine and Biology Society.* 2008; 16(1):37-45.
- [119] Farina, D., Lorrain, T., Negro, F., & Jiang, N. "High-density EMG E-textile systems for the control of active prostheses BT". *Proc IEEE Int Conf Eng Med Biol Soc.* 2010
- [120] Merletti, R., Holobar, A., & Farina, D. "Analysis of motor units with high-density surface electromyography". *J Electromyogr Kinesiol*, 18. 2008,
- [121] Institute of Medicine (US) Committee on Military Nutrition Research; Carlson-Newberry SJ, Costello RB, editors. *Emerging Technologies for Nutrition Research: Potential for Assessing Military Performance Capability.* Washington (DC): National Academies Press (US); 1997. 7, Bioelectrical Impedance: A History, Research Issues, and Recent Consensus.
- [123] Cole, K. S. *Membranes, "Ions and Impulses: A Chapter of Classical Biophysics."* Berkeley, CA: Univ. of Calif. Press, 1972.

[124] Ørjan G. Martinsen, Sverre Grimnes, J.K. Nilsen, C. Tronstad, W. Jang, H. Kim and K. Shin, “Calibration of skin hydration measurements.” IFMBE Proceedings 2007, Volume 17, Part 6, 161-164

[125] Jaffrin MY, Fenech M, Moreno MV, Kieffer R. “Total body water measurement by a modification of the bioimpedance spectroscopy method.” Med. Biol. Eng. Comput. 2016; 44(10):873-82.

[126] S. Grimnes and Ø. G. Martinsen, Bioimpedance and Bioelectricity Basics

[127] Cal Stat® Plus Antiseptic Handrub with Enhanced Emollients, Steris Corporation, Link: <https://www.steris.com/products/hospital-hand-sanitizers/cal-stat-plus-antiseptic-handrub-with-enhanced-emollients>

[128] Intan Technologies LLC

[129] Infinite Biomedical Technologies LLC

[130] Mark Ison, Ivan Vujaklija, Bryan Whitsell, Dario Farina and Panagiotis Artemiadis, “High-Density Electromyography and Motor Skill Learning for Robust Long-Term Control of a 7-DoF Robot Arm.”, IEEE Trans Neural Syst Rehabil Eng. 2016, 24(4):424-33.

[131] Anthropometric Reference Data for Children and Adults: United States, 2007–2010, Centers for Disease Control and Prevention, Vital and Health Statistics, 2012, Series II, Number 252

[132] University of Illinois at Urbana-Champaign, School of Engineering, Introduction to Data Mining, K-L Divergence, Link: <http://web.engr.illinois.edu/~hanj/cs412/bk3/KL-divergence.pdf>

[133] Jasjit S. Suri, Advances in Diagnostic and Therapeutic Ultrasound Imaging, Artech House, 2008, Section 4.3, pp. 98

[134] P. Laferriere, E. D. Lemaire and A. D. C. Chan, "Surface Electromyographic Signals Using Dry Electrodes," in IEEE Transactions on Instrumentation and Measurement, 2011, vol. 60, no. 10, pp. 3259-3268

BIOGRAPHICAL SKETCH



Damini Agarwal received the Bachelor of Technology degree with a Major in Biomedical Engineering and a Minor in Computer Science from VIT University, Vellore, India in 2015. There, she graduated at the top of her class and was also awarded the Chancellor's Gold Medal for the Best Outgoing Student of the Class of 2015. In the same year, she received the TOEFL

India Scholarship as well as the Google Anita Borg Memorial Scholarship and enrolled in the M.S.E. Biomedical Engineering program at Johns Hopkins University,

Starting in June 2017, Damini will join Infinite Biomedical Technologies LLC as a Biomedical Engineer and will continue her work in developing electronics for upper limb myoelectric prosthesis.

The material in this thesis is based upon work supported by the National Institute of Health under Grant No. R44HD087065.

All Human Subjects Research performed for the data in this thesis is covered by the IRB Protocol No.: IRB00053158.